Preparation, structure, digestibility of starch spherulites with different morphologies and allomorphs

by

Jialiang Shi

B.S., Zhengzhou University of Light Industry, 2011
M.S., Kansas State University, 2016

AN ABSTRACT OF A DISSERTATION

submitted in partial fulfillment of the requirements for the degree

DOCTOR OF PHILOSOPHY

Department of Grain Science and Industry
College of Agriculture

KANSAS STATE UNIVERSITY
Manhattan, Kansas

2023

Abstract

Starch is the most important source of food energy, but information about the metabolic qualities of starchy foods is scarce. There is growing interest in understanding the relationships between digestion of starch and its effect on human health, particularly diet-related disorders such as obesity, diabetes, and cardiovascular disease. Our long-term goals are to understand how the structure, morphology and crystalline type affect the digestibility of starches, control the assembly of starch molecules for desired functional and nutritional properties, develop new starch-based ingredients and foods to improve human health, and design foods with controlled digestibility as well as desirable texture, quality, and shelf life. The specific objectives of this dissertation were to: (1) form spherulites with different allomorphs from debranched waxy potato starch; (2) produce starch spherulites with positive and negative birefringent signs from debranched high-amylose maize starch (longer chain length) and investigate the digestion mechanisms; (3) make products with an A-type crystalline structure from the debranched high-amylose maize starch by using high solid concentrations (> 25%) and heat-moisture treatment (HMT). Spherulites with a negative birefringent sign were formed from the debranched waxy potato starch (25% solids content), and the resistant content (RS) content was 74.1%. HMT changed the spherulites from B-type allomorph to A-type allomorph and reduced the RS content to 51.6%. However, due to their greater thermal stability, the RS of cooked spherulites was 33.1% while the RS content of cooked waxy potato starch was very low (1.9%). When the debranched high-amylose maize starch (25% solids content) was used, all the products exhibited a B-type allomorph, and the spherulites with positive birefringence showed high resistance to enzyme digestion. After HMT, the B-type allomorph was changed to A-type without significant effect on the morphology, and thermal stability increased. By increasing the solid content to 30-50%, products with A-type and C-type allomorphs were

formed by the debranched high-amylose maize starch at higher crystallization temperatures. The RS content of the spherulites with positive birefringent sign were approximately 90%, and HMT did not significantly change the RS content. Microscopic images revealed that α-amylase hydrolyzed the out layer of a spherulite, and the birefringence sign could still be observed after digestion. Overall, this study provides significant information on the digestibility of spherulite with different structures and helps to understand how the structure, morphology and crystalline type affect the digestibility of starches.

Preparation, structure, digestibility of starch spherulites with different morphologies and allomorphs

by

Jialiang Shi

B.S., Zhengzhou University of Light Industry, 2011
M.S., Kansas State University, 2016

A DISSERTATION

submitted in partial fulfillment of the requirements for the degree

DOCTOR OF PHILOSOPHY

Department of Grain Science and Industry
College of Agriculture

KANSAS STATE UNIVERSITY
Manhattan, Kansas

2023

Approved by:

Major Professor
Yong-Cheng Shi

Copyright

Abstract

Starch is the most important source of food energy, but information about the metabolic qualities of starchy foods is scarce. There is growing interest in understanding the relationships between digestion of starch and its effect on human health, particularly diet-related disorders such as obesity, diabetes, and cardiovascular disease. Our long-term goals are to understand how the structure, morphology and crystalline type affect the digestibility of starches, control the assembly of starch molecules for desired functional and nutritional properties, develop new starch-based ingredients and foods to improve human health, and design foods with controlled digestibility as well as desirable texture, quality, and shelf life. The specific objectives of this dissertation were to: (1) form spherulites with different allomorphs from debranched waxy potato starch; (2) produce starch spherulites with positive and negative birefringent signs from debranched high-amylose maize starch (longer chain length) and investigate the digestion mechanisms; (3) make products with an A-type crystalline structure from the debranched high-amylose maize starch by using high solid concentrations (> 25%) and heat-moisture treatment (HMT). Spherulites with a negative birefringent sign were formed from the debranched waxy potato starch (25% solids content), and the resistant content (RS) content was 74.1%. HMT changed the spherulites from B-type allomorph to A-type allomorph and reduced the RS content to 51.6%. However, due to their greater thermal stability, the RS of cooked spherulites was 33.1% while the RS content of cooked waxy potato starch was very low (1.9%). When the debranched high-amylose maize starch (25% solids content) was used, all the products exhibited a B-type allomorph, and the spherulites with positive birefringence showed high resistance to enzyme digestion. After HMT, the B-type allomorph was changed to A-type without significant effect on the morphology, and thermal stability increased. By increasing the solid content to 30-

50%, products with A-type and C-type allomorphs were formed by the debranched high-amylose maize starch at higher crystallization temperatures. The RS content of the spherulites with positive birefringent sign were approximately 90%, and HMT did not significantly change the RS content. Microscopic images revealed that α-amylase hydrolyzed the out layer of a spherulite, and the birefringence sign could still be observed after digestion. Overall, this study provides significant information on the digestibility of spherulite with different structures and helps to understand how the structure, morphology and crystalline type affect the digestibility of starches.

Table of Contents

List of Figures

List of Tables

Acknowledgements

The project was completed under the direction and guidance of Dr. Yong-Cheng Shi. He led me into starch research and gave me an opportunity to complete this dissertation and work with other outstanding researchers. I am very appreciative of Dr. Shi's advice and encouragement, especially when I have difficulties in my life and program.

Special thanks to Dr. Wang, Dr. Alavi, and Dr. Dogan for their time and effort in serving on the advisory committee.

I am very glad to meet my lab mates and friends in KSU. I also learned a lot from them, and they made my life in KSU more cherished.

Last but not least, I thank my parents in China. My father got his doctoral degree when I was in middle school, he is my role model. My mother always supports me, especially when I was in a very tough time. I cannot finish my program without them.

Chapter 1 - Starch spherulites formation, morphology, digestibility, and thermal properties – a review

Abstract

The formation of starch spherulites has been studied extensively using both native and modified starches. While the general principle of spherulite formation is the crystallization of amylose, the details of formation differ among studies, resulting in spherulites with different properties. In this chapter, the author reviewed previous research on starch materials, formation methods, and spherulite properties, highlighting that the heating temperatures and cooling rates used for spherulite formation are dependent on the characteristics of the materials. Spherulites with both positive and negative birefringence can be produced from different starches, or the same starch material by adding ethanol or changing crystallization temperatures. The morphology and structure of the spherulites are investigated using microscopy and X-ray diffraction, revealing spherulites have higher crystallinities and different crystalline structures (A-, B-, and V-type). As a crystallized material, spherulites show resistance to enzyme hydrolysis, with the enzyme mainly hydrolyzing the outer layer of the particles, making spherulites less digestible. Additionally, spherulites demonstrate higher thermal stability, influenced by the type of crystalline structure.

Introduction

Spherulites are spherical polycrystalline aggregates filled with highly anisometric crystallites (Shtukenberg et al., 2012). The history of spherulites dates back to 1837 when circular crystals were formed by borax, which were later called spherulites (Crist & Schultz,

2016). Organic and inorganic materials have been studied for spherulite formation. Crist and Schultz (2016) summarized the conditions for spherulite formation as a large degree of undercooling ΔT (the difference between the melting point and the crystallization temperature), indicating the process of transforming from a disordered to an organized structure. Based on the material's status before spherulite formation, the conditions for spherulite formation were classified as growth from melt, growth from solid, and growth from solutions or gels (Shtukenberg et al., 2012). Starch has been used in previous studies to produce spherulites. Melting and crystallization were carried out in a liquid medium, such as water and ethanol solution (Cai & Shi, 2013; Creek et al., 2006; Fanta et al., 2002, 2006, 2008; Helbert et al., 1993; Kiatponglarp et al., 2016; Ma et al., 2011; Nordmark, 2002; Shi et al., 2021; Singh et al., 2010; Ziegler, 2020; Ziegler et al., 2003, 2005).

Starch generally contains two types of polymers: amylose and amylopectin. Amylose is an essentially linear molecule containing mostly α-1,4-glycosidic bonds, and amylopectin contains α-1,4-glycosidic bonds and about 5% α-1,6-glycosidic bonds, indicating a large number of branches (Hizukuri et al., 2006). Normal starch contains approximately 20-30% amylose. Waxy starch contains less amylose, such as waxy maize starch with an amylose content of lower than 1%. High-amylose starches always contain an apparent amylose higher than 50% (Jane, 2009). Starch molecules form two crystalline types: A-type and B-type. A-type crystalline is observed in most cereal starches, while B-type is observed in root, tuber, and amylose-rich cereal starches. A mixture of A- and B-type is called C-type, which is observed in legume starches (Bogracheva et al., 1998; Pérez et al., 2013). These crystals are radially arranged from the center of a starch granule, and an amorphous area exists between

two crystal layers, resulting in a crystallinity that varies from 15% to 45% (Waigh et al., 1996; Pérez et al., 2013).

When starch is heated in sufficient water, the crystalline structure is destroyed, and the molecules are diffused in the water. This process is called gelatinization. After gelatinization, cooling could result in crystallization of starch molecules, which is termed retrogradation. Spherulites form during crystallization (retrogradation) and show Maltese crosses. According to Shtukenberg et al. (2012), the Maltese crosses indicated the crystals have the same crystallographic orientation. After inserting a waveplate, the Maltese cross showed two patterns which were classified as positive and negative birefringence signs (Crist & Schultz, 2016; Haudin, 1986; Shi et al., 2021; Shtukenberg et al., 2012). An equation, $\Delta n=n1 - n2$, was used to define the positive and negative pattern, where n1 is the arbitrarily the optical axis radiating from the center, and n2 is perpendicular to n1 (Haudin, 1986; Shi et al., 2021; Shtukenberg et al., 2012). By applying polarized light and a waveplate, the positive Maltese crosses showed blue quadrants occupying the North East and South West quadrants. So, the negative spherulites showed the blue quadrants on the opposite position, which indicated the orientation of crystals was perpendicular to that of positive spherulites (Kobayashi et al., 2000; Shi et al., 2021). Due to the radially arranged crystals, positive Maltese crosses were observed in native starch granules (Figure 1.1). By using native starches as a reference, starch spherulites could show positive and negative Maltese crosses (Cai & Shi, 2013; Creek et al., 2006; Fanta et al., 2002, 2013; Kiatponglarp et al., 2016; Ma et al., 2011; Nordmark, 2002; Ring et al., 1987; Shi et al., 2021; Ziegler, 2020). The

schematic diagram of positive and negative spherulites were also proposed in previous studies (Figure 1.2) (Cai & Shi, 2013; Crist & Schultz, 2016; Shi et al., 2021).

As a crystallized material, starch spherulites formation is influenced by the crystallization temperature, degree of polymerization (DP), solid concentration, and solvent (Buléon et al., 2007; Cai et al., 2010; Cai & Shi, 2010, 2014; Gidley & Bulpin, 1987; Helbert et al., 1993; Jane, 2004; Shi et al., 2018). To archive a high temperature to gelatinize starch and control the crystallization temperature, a differential scanning calorimeter (DSC) was used to produce spherulites (Bhosale & Ziegler, 2010; Creek et al., 2006; Kiatponglarp et al., 2016; Ma et al., 2011; Nordmark, 2002; Nordmark & Ziegler, 2002; Singh et al., 2010; Ziegler et al., 2003, 2005). The advantage of using DSC was precise temperature control. However, the amount of produced spherulites was limited due to the size of DSC pans. Other devices, such as pressure vessels, parr reactor, and jet cookers, were also used and the amount of produced spherulites could be increased for some measurements (Cai & Shi, 2013; Fanta et al., 2006; Fanta et al., 2002, 2008, 2013; Felker et al., 2013; Shi et al., 2021; Ziegler, 2020). But the crystallization temperature and cooling rate were less controllable.

Starch spherulites formation were also influenced by the amylopectin content and the starch source (Ma et al., 2011; Ziegler et al., 2003). When native starch was used, the degree of polymerization and amylose content were mainly different due to the variety of starch. To manipulate the amylose content, leached amylose or debranching amylopectin were used. Since debranching also produced short amylose, this method and acid hydrolysis were used to alter the chain length (Cai et al., 2010; Cai & Shi, 2013, 2010; Creek et al., 2006; Helbert et al., 1993; Kiatponglarp et al., 2016; Shi et al., 2021; Ziegler, 2020; Ziegler et al., 2003).

By reviewing the previous studies, the following questions are raised: what starches formed spherulites; what conditions were required to form spherulites; and how to measure the spherulites properties? By answering these three questions, this paper could support the studies on formation of spherulites with different birefringence properties and different crystalline structures. The technologies used to analyze spherulites will also be provided, so that supporting information could be offered for the application of starch spherulites.

Starches used to form spherulites

Native starch

Starch is a widely available material found in many plants. According to Ziegler et al. (2003), various starches had different abilities to form spherulites. The order of spherulite formation ability was: waxy maize starch < normal maize starch < high-amylose maize starch < normal potato starch < mung bean starch. Waxy maize starch did not form spherulites, while mung bean starch formed high-quality spherulites. Among the three types of maize starch, the amylose content was found to be critical for spherulite formation. This was studied by mixing amylose and amylopectin at different ratios (Ma et al., 2011). Ma et al. (2011) reported that when potato amylose was used, spherulites were not formed if the amylose content was below 20%, while for corn amylose, the required amylose content was 33%. The difference of these two required amylose contents indicated chain length of linear molecules also plays an important role in spherulite formation. Leached amylose from native starch granules can form spherulites with clear Maltese crosses and uniform size (Creek et al., 2006; Ziegler, 2020). Ziegler (2020) reported that the chain length of leached normal corn amylose

was 642 DP, and Ring et al. (1987) used amylose of DP 22 to produce spherulites. Commercially available materials are limited by chain length, and there is insufficient information about spherulites formed by molecules of different chain lengths. To obtain molecules with more diverse chain lengths, native starch can be modified using acid and enzymes (Cai & Shi, 2013; Helbert et al., 1993; Kiatponglarp et al., 2016; Shi et al., 2021; Ziegler, 2020; Ziegler et al., 2003).

Acid and enzyme hydrolysis

Both acid and enzymes can be used to hydrolyze starch molecules and reduce their degree of polymerization. Ziegler et al. (2003) employed acid to modify corn starch and observed that hydrolysis mainly occurred at the branching points. After the acid hydrolysis of corn starch, the ability of spherulites formation increased to the level of normal potato starch. In 2020, Ziegler used acid to treat leached amylose (DP 642), producing shorter linear molecules (DP 120) that successfully formed spherulites with a uniform size and a fine texture. Similarly, Helbert et al. (1993) used acid to treat potato amylose, which produced short molecules (DP 15) that formed spherulites.

Acid is able to hydrolyze starch molecules, but the hydrolysis is less controllable (Chen et al., 2018). Enzymatic modification is an alternative method for altering the degree of polymerization (DP) of starch molecules, as enzymes can hydrolyze specific linkages. Shang et al. (2018) combined α-amylase, amyloglucosidase, and acid hydrolysis to treat corn starch and produce materials with different DP values. However, the spherulites did not show clear Maltese crosses, possibly due to the uneven and imperfect crystallization of short and

branched chains. To produce linear molecules of different chain length, previous studies used debranching enzymes such as pullulanase and isoamylase for spherulite formation (Cai & Shi, 2013; Kiatponglarp et al., 2016; Shi et al., 2021).

Pullulanase hydrolyzes the amylopectin from the outer branches, while isoamylase hydrolyzes α-1,6 linkages from the outer and inner branches (Hizukuri et al., 2006; Manners & Matheson, 1981; Yokobayashi et al., 1973). The hydrolysis rate of isoamylase is 7 times higher than that of pullulanase (Robyt, 2009). Shi et al. (2018) used pullulanase to debranch waxy maize starch, resulting in a highly reduced amylopectin content and an average DP lower than 20.4. Although a few α-1,6 linkages were detected, the debranched material formed spherulites (Shi et al., 2021). Isoamylase was also used by Shi et al. (2018) to debranch waxy maize starch, and no branches were observed. This result was consistent with other studies using isoamylase (Cai et al., 2010; Cai & Shi, 2010), and the resulting debranched materials successfully formed spherulites (Cai & Shi, 2013; Kiatponglarp et al., 2016). Kiatponglarp et al. (2016) used isoamylase to debranch normal rice starch and waxy rice starch. Debranched normal rice starch contained longer molecules (DP 775) and formed positive spherulites. However, debranched waxy rice starch did not contain the long chain molecules, and the resulting morphology was different.

Octenyl succinic (OS) starch

OS starch is a modified starch prepared by treating native starch with octenyl succinic anhydride (OSA). This modification imparts amphiphilic properties to the OS starch, making it suitable for use as an emulsifier (Bai & Shi, 2011; Sweedman et al., 2013). Wang (2017)

employed a combination of debranching and OSA modification to form spherulites. Firstly, waxy maize and waxy potato starches were debranched to form spherulites. The resulting spherulites were then treated with sodium hydroxide solution and OSA to produce OS spherulites, which were capable of stabilizing Pickering emulsion for 2 months. However, microscopy images did not reveal Maltese crosses, suggesting that the samples were not true spherulites.

Additives

In the previous paragraphs, spherulites were produced by starch. However, other molecules can also participate in spherulites formation as shown in several studies (Fanta et al., 2006; Fanta et al., 2008; Felker et al., 2013; Helbert et al., 1993; Ring et al., 1987; Liu et al., 2021). Fanta et al. (2002) reported that starch containing native lipid can form spherulites as amylose-lipid complex. Subsequent studies added fatty acids such as palmitic and oleic acid to form spherulites (Fanta et al., 2006; Fanta et al., 2008; Felker et al., 2013). Ethanol solution was another additive but added after heating when starch molecules did not crystallize. Previous studies showed effects of adding ethanol on the spherulites morphology and crystalline structure (Ring et al., 1987; Helbert et al., 1993; Shi et al., 2021). Except the organic material, inorganic ingredients also formed spherulites with starch. In a recent study, Liu et al. (2021) used nanosilica and cassava starch to produce spherulites containing V-type and A-type crystals. However, the birefringence morphology was not clear enough to determine the spherulites formation. Another study (Luo et al., 2019) reported spherulites formed by debranched waxy maize starch and iron oxide nanoparticles. The birefringence

morphology was not reported too, but the samples showed magnetic properties, and then further formed immunomagnetic material with protein.

Conditions of starch spherulites formation

Heating temperature

After complete gelatinization, individual molecules were dispersed in water so that spherulites could be produced. DSC measurements by Ai and Jane (2018) showed that most native starch could be gelatinized at temperatures lower than 100°C, except high-amylose maize starch which required a conclusion temperature (T_c) higher than 110°C. When native starch was debranched, its T_c increased to over 130°C as linear molecules crystallized during debranching (Cai et al., 2010; Cai & Shi, 2010; Shi et al., 2018).

For spherulite formation, fully gelatinized starch was mostly obtained by heating to 170~190°C (Bhosale & Ziegler, 2010; Cai & Shi, 2013; Creek et al., 2006; Kiatponglarp et al., 2016; Ma et al., 2011; Nordmark & Ziegler, 2002a, b; Singh et al., 2010; Ziegler, 2020; Ziegler et al., 2003, 2005). Although some studies have heated starch to 140°C to form spherulites, four important points need to be noted: (1) the solid concentration was 4%; (2) the cooling rate was slow; (3) an amylose-lipid complex was formed; and (4) the yields were lower than 12% (Bhosale & Ziegler, 2010; Fanta et al., 2006, 2008, 2013; Felker et al., 2013). If the molecules were shorter, spherulites could be formed by heating to 120°C or in a boiling water bath (Helbert et al., 1993; Ring et al., 1987).

According to Vesterinen et al. (2001), a heating temperature higher than 150°C was necessary for native high-amylose starch. Guenet (1996) suggested that sufficient heating

offered chain flexibility which could support chain folding, necessary for spherulite formation (Ziegler et al., 2003). However, short-chain molecules such as acid-treated starch could form spherulites without chain folding (Kobayashi et al., 2000). Heating degradation, especially for materials of higher molecular weight or more branched molecules, is another factor that can influence spherulite formation at high temperatures (Nordmark & Ziegler, 2002b; Ziegler et al., 2003).

Cooling condition

As described above, the spherulites formation involves crystallization during cooling, and previous studies (Cai & Shi, 2013; Creek et al., 2006; Fanta et al., 2008, 2013; Felker et al., 2013; Kiatponglarp et al., 2016; Shi et al., 2021; Nordmark & Ziegler, 2002; Ziegler et al., 2005) have investigated the impact of cooling rate and crystallization temperature. From these studies, it can be concluded that the cooling rate has a varying influence on different materials. For instance, Ziegler et al. (2005) investigated the effect of cooling rates between 1°C/min and 250°C/min on the spherulites formation of mung bean starch. They found that an increase in cooling rate from 1°C/min to 50°C/min led to an increase in the mean particle size. Similarly, Nordmark and Ziegler (2002a) studied the impact of different cooling rates on high-amylose maize starch and observed that no spherulites were produced at cooling rates of 0.1°C/min and 1°C/min. In contrast, spherulites were observed in normal maize starch when the cooling rate was faster than 2.5°C/min, and the particle size was influenced by the cooling rate (Creek et al., 2006). However, when leached amylose from normal maize starch was

used for spherulites formation, the cooling rate had a minimal effect on particle size (Creek et al., 2006).

DSC is capable of heating samples to high temperatures and controlling the cooling rate with precision ranging from 1°C/min to 250°C/min. However, the amount of produced spherulites was limited. Other pressure containers were used to increase spherulite production, and cooling was mostly carried out using cooling water or air, although the cooling rate was less controllable in these cases (Cai & Shi, 2013; Shi et al., 2021; Ziegler, 2020). Slow cooling rates were used in some studies, whereby samples were firstly cooled to a relatively high temperature (95°C or 78°C) and then slowly cooled to a lower temperature for spherulite formation (Fanta et al., 2008, 2013; Felker et al., 2013; Helbert et al., 1993). When spherulites were formed at a slow cooling rate, starch molecules may crystallize gradually at different temperatures. Two steps of cooling could be considered as a very slow cooling with spherulite formation at two temperatures (Shi et al., 2021). For instance, debranched waxy maize starch crystallized at 50°C, then further crystallized at 4°C, resulting in positive spherulites with A-type crystalline structure (Shi et al., 2021). In contrast, spherulites formed by directly cooling to 4°C exhibited negative Maltese crosses and B-type crystalline structure. When debranched waxy maize starch crystallized at 50°C without further cooling, A-type crystallites were formed, but the Maltese crosses were less apparent (Cai and Shi, 2013). These studies indicated the effects of crystallization temperatures. Meanwhile, the material should be considered when determining the crystallization temperature for spherulite formation as observed by Ziegler et al. (2005) who used DSC and

mung bean starch to investigate crystallization temperatures. The birefringence indicated spherulites were formed at temperatures from 40°C to 60°C.

Solid concentration

The formation of spherulites is influenced by solid concentration in two ways: higher solid content may require a higher temperature to melt the starch completely and increasing solid concentration supports the formation of A-type crystalline structure. Ring et al. (1986) used short amylose (DP 22) and solid concentrations of 5-20%, and reported a lower solid content required a longer precipitation time. Nordmark and Ziegler (2002a) investigated the effect of solid concentration on high-amylose maize starch, ranging from 5% to 30%. Lower solid concentration resulted in less uniform particle size but more regular shape. When solid concentration was 30%, spherulites were observed in clusters with impinged particles. Ziegler et al. (2003) studied the impact of solid concentration on potato starch and acid-treated starch, ranging from 5% to 30%. Acid-treated starch formed spherulites at all concentrations, while potato starch did not. However, solid concentration was not investigated extensively, and it was generally below 30% (Bhosale & Ziegler, 2010; Cai & Shi, 2013; Creek et al., 2006; Fanta et al., 2002, 2006, 2008, 2013; Helbert et al., 1993; Kiatponglarp et al., 2016; Ma et al., 2011; Nordmark & Ziegler, 2002b; Singh et al., 2010; Ziegler, 2020; Ziegler et al., 2005). In previous studies, spherulites of A-type crystalline structure were not observed even when the solid concentration was as high as 25% or 30% (Cai & Shi, 2013; Kiatponglarp et al., 2016; Shi et al., 2021).

Analysis of spherulites properties

Morphology

As previously mentioned, spherulites display Maltese crosses under polarized light, making light microscopy a common technique to measure spherulite formation. Since light microscopy used a small amount of samples, this technique could be applied to spherulites formed by a DSC or using low solid concentrations. A summary of spherulites birefringence signs was in Table 1.1. Except the positive and negative Maltese crosses, previous works also reported another type of spherulite showing an "X" shape, formed by amylose-lipid complex (Fanta et al., 2002, 2006, 2008, 2013; Felker et al., 2013). A few studies used a wave plate and reported the type of birefringence. Kiatponglarp et al. (2016) used a wave plate and found that debranched normal rice starch formed positive spherulites, while debranched waxy rice starch formed "X" shape spherulites rotated 45° from the positive spherulites. In another study (Shi et al., 2021), debranched waxy maize starch formed negative spherulites and some "X" shape spherulites. The molecular size results indicated that long chains support positive spherulite formation. However, when mixed with ethanol during spherulite formation or when two-step crystallization was applied, debranched waxy maize starch also formed positive spherulites (Shi et al., 2021).

Electron microscopy can provide more detailed morphology of spherulites with a small amount of samples. Two types of electron microscopy have been used in previous studies: scanning electron microscopy (SEM) and transmission electron microscopy (TEM). SEM has been used to examine the surface of spherulites, and four morphologies have been

reported. Fanta et al. (2002) identified three types: spherical particles with a coarse surface, disc-shaped spherulites, and torus-shaped spherulites. The torus-shaped spherulites were also observed by Felker et al. (2013). The spherical type was large and could be formed by different native starches. The disc-shaped spherulites and torus-shaped spherulites were smaller. The disc-shaped spherulites were observed in samples formed by normal maize starch, while the torus-shaped spherulites were formed by high-amylose maize starch or normal rice starch. The fourth type was spherical particles of stacking lamellae (Singh et al., 2010). When spherulites were fractured, the internal structure could be observed by SEM, and the studies revealed radial organization (Helbert et al., 1993; Ma et al., 2011; Fanta et al., 2002). Compared to SEM, TEM requires sectioning of the samples to observe the internal structure of spherulites. Ma et al. (2011) detected holes when amylopectin was present. The center of the spherulites was more crystallized, while amorphous material may exist in the outer side. Electron diffractogram could focus on a few crystals of a specific area and show the crystal structure. Helbert et al. (1993) used this technique to reveal that the direction of crystals was radial from the center. Atomic force microscopy (AFM) is similar to TEM in that it uses cross-sectional samples to examine the internal morphology, and blocks were clearly observed when amylose of DP 120 formed spherulites (Ziegler, 2020).

Crystalline structure

Wide-angle X-ray diffraction (WAXD) is a widely used technique for analyzing the crystalline structure within spherulites. Previous studies have shown the diffraction patterns obtained from WAXD reveal the presence of different crystalline structures within the

spherulites (Table 1.1). Lipid acid can crystallize with amylose as single helices of a V-type crystalline structure (Fanta et al., 2008, 2013; Felker et al., 2013), while ethanol causes amylose to form A-type crystallites (Helbert et al., 1993; Shi et al., 2021). As mentioned earlier, Shi et al. (2021) produced A-type spherulites by crystallization at 50°C followed by further crystallization at 4°C. The results suggest that the crystalline type of spherulites can be determined during the early crystallization phase, even if no clear birefringence sign is observed at 50°C.

Small-angle X-ray diffraction (SAXD) was less used, but details on the crystals were offered by applying this technique (Kiatponglarp et al., 2016). The thickness of crystalline and amorphous lamellae were 7.4 nm and 6 nm, respectively.

Digestibility

Starch spherulites, as crystallized materials, exhibit resistance to enzyme digestion. The digestibility of spherulites has been investigated using two methods: AOAC 2002.02 and Englyst's method (Bhosale & Ziegler, 2010; Cai & Shi, 2013; Kiatponglarp et al., 2016; Shi et al., 2021; Ziegler, 2020). Bhosale & Ziegler (2010) formed spherulites by heating to 180°C and 140°C and used the AOAC 2002.02 method to hydrolyze them. The resistant starch (RS) contents of samples formed at 180°C and 140°C were 28% and 39%, respectively. However, the sample formed at 140°C was not spherulites. Ziegler (2020) and Kiatponglarp et al. (2016) also used the AOAC 2002.02 method with modifications such as extending digestion time and reducing sample amount. Ziegler (2020) used amylose of DP 120 and DP 642 to produce spherulites, and the RS contents measured by the AOAC 2002.02 method were

61.7% and 36.6%, respectively. After extending the digestion time from 16 h to 48 h, there was no clear change in the morphology of digested samples observed under a light microscope. By using SEM, pitting was observed only on the surface of spherulites, and the out-layers were peeled off. After 16 h of digestion, the residue was collected and digested by the AOAC 2002.02 method, and the RS content of digested spherulites (DP 642) was nearly doubled. Kiatponglarp et al. (2016) used debranched normal rice starch and debranched waxy rice starch to produce spherulites and studied the digestibility by using multiple digestion times between 0 h and 24 h. The spherulites formed by debranched waxy rice starch were less digestible and showed clear negative birefringence after 24 h, while the positive spherulites formed by debranched normal rice starch were more digestible, and the birefringence was blurred. Englyst's method (Cai et al., 2010; Sang & Seib, 2006) was also used to study the digestibility of spherulites, and multiple digestion times were applied to plot the digestion curve (Cai and Shi, 2013; Shi et al., 2021). The RS content of spherulites was found to be higher than 70%, and the A-type crystalline spherulites were more resistant to enzyme hydrolysis (Cai & Shi, 2013). Shi et al. (2021) also observed the morphology of positive and negative spherulites during digestion. The birefringence signs of both types of spherulites were observed after digestion, but morphology changes were more influenced by the formation temperatures. The digested residue was applied to the Englyst's method by Cai and Shi (2013), and the residue showed high resistance to enzyme digestion, and the digestion curve became straighter.

Thermal properties

Previous studies have utilized differential scanning calorimetry (DSC) to measure the thermal properties of spherulites (Bhosale & Ziegler, 2010; Cai & Shi, 2013; Fanta et al., 2002; Kiatponglarp et al., 2016; Shi et al., 2021; Ziegler, 2020). The thermograms showed distinct peaks depending on the type of spherulite formed. For instance, when amylose and lipid acid formed spherulites, two or three peaks were observed. The amorphous amylose-lipid complex exhibited a peak at 90-100°C, while the crystalline amylose-lipid complex, which had V-type crystalline structure, displayed a peak at 100-120°C. B-type crystallinity, on the other hand, exhibited a peak at 130-140°C. Using the enthalpy, the amount of complexed lipid acid was calculated (Bhosale & Ziegler, 2010). Fanta et al. (2002) produced V-type spherulites and observed two peaks at around 100°C and 115°C, suggesting that the two temperatures resulted from V-type crystallites with varying H-bond distances. The melting peaks of B-type crystalline spherulites varied among different studies (Cai & Shi, 2013; Kiatponglarp et al., 2016; Shi et al., 2021; Ziegler, 2020). For instance, spherulites of amylose with degree of polymerization (DP) 120 and DP 642 exhibited melting peaks at 97.6°C and 116.1°C, respectively. After digestion, due to a higher crystallinity of the spherulite residue, the melting peaks increased to 107°C and 122°C, respectively. When debranched normal rice starch, debranched waxy rice starch, and debranched waxy maize starch were utilized to form B-type crystalline spherulites, the melting peaks were observed between 81.1°C and 91.8°C. The chain length of amylose showed positive correlation to the melting temperature, but spherulites of debranched normal rice starch showed a lower melting temperature, which was attributed to lower structural homogeneity (Kiatponglarp et

al. 2016). The thermal properties of A-type crystalline spherulites were less frequently reported. A-type crystalline structure was formed by debranched waxy maize starch through crystallization at 50°C, and the melting peak was observed at approximately 115°C, while the conclusion temperature increased to approximately 140°C (Cai & Shi, 2013; Shi et al., 2021).

Conclusion

Previous studies have shown that the amylose content plays a crucial role in the formation of spherulites. The required amylose content altered with different chain length of amylose. Starch materials are heated to high temperatures and then the spherulites are formed during cooling. When lipid is added to form spherulites, the heating temperature can be reduced to 140°C, but the yield is low. When native or modified starch is used, the heating temperature is typically around 180°C. If short amylose is used, the heating temperature can be lowered to 120°C. Thermal conditions have a significant impact on the formation of spherulites, affecting both the birefringence properties and the crystallization properties. Fast cooling is recommended for spherulite formation when using only starch, while slow cooling is preferred when using lipid acid or ethanol. The additive and cooling rate influence the birefringence properties and crystalline structure. Additionally, the crystallization temperature is another factor affecting the birefringence sign and crystalline structure. As a crystallized material, the solid concentration also plays a role in determining the crystalline structure, but this aspect has not been extensively studied, since the solid content was always lower than 30%.

Birefringence properties can be studied using polarized light microscopy with a waveplate, while scanning electron microscopy, transmission electron microscopy, and atomic force microscopy can provide more detailed information on spherulite morphology and internal structure. Spherulites are classified as positive or negative based on their birefringence. Negative spherulites are produced from debranched waxy starches, while positive spherulites are formed from long-chain amylose, debranched waxy starches with added ethanol, or two stages of crystallization. In addition, the addition of lipids to form spherulites can result in the observation of rotated Maltese crosses.

The crystalline structure was investigated using X-ray diffraction, which showed that cooling starch material to a low temperature produced B-type crystalline spherulites. V-type crystalline structure indicated the formation of amylose-lipid complex, while A-type crystalline spherulites were produced by short chain amylose with adding ethanol or crystallization at a high temperature. Small angle X-ray scattering could provide more details on the crystalline structure, but it was used less frequently in previous studies. Spherulites, as a crystallized starch material, were also found to be resistant to enzyme digestion. Based on the digestion curve and morphology of digested spherulites, high resistant starch contents were reported, and the enzyme hydrolysis mostly occurred on the surface of the particles. As a result, the digested samples still showed birefringence sign, and their digestibility was lower compared to the undigested spherulites. After crystallization, the thermal properties of spherulites differed from those of native starches, with increased melting peaks. The thermal stability of V-type and A-type spherulites was also higher than that of B-type spherulites.

Spherulites mimic both granular morphology and the crystalline types of native starches. Therefore, they are good model systems to study the enzymatic hydrolysis of starch crystallites and provide great insight on enzyme digestion of starch. The increased RS content and thermal stability of spherulites indicate the potential application as a new starch-based ingredient and food to improve human health, and design foods with controlled digestibility as well as desirable texture, quality, and shelf life. However, the birefringence sign of spherulites was less reported, and spherulites with A-type crystalline structure was less produced. Although different starch materials have been used to form spherulites, there is a lack of molecules with chain length between DP 30 and DP 120. As the results, the following studies focus on three objectives: (1) to produce spherulites with A-type crystalline structure from debranched waxy potato starch; (2) to produce spherulites with positive and negative birefringence signs from debranched high-amylose maize starch; (3) to produce spherulites with A-type crystalline structure from debranched high-amylose maize starch. The thermal properties and digestibility are also investigated.

References:

Ai, Y., & Jane, J. (2018). Chapter 3—Understanding Starch Structure and Functionality. In M. Sjöö & L. Nilsson (Eds.), *Starch in Food (Second Edition)* (pp. 151–178). Woodhead Publishing. https://doi.org/10.1016/B978-0-08-100868-3.00003-2

Bai, Y., & Shi, Y.-C. (2011). Structure and preparation of octenyl succinic esters of granular starch, microporous starch and soluble maltodextrin. *Carbohydrate Polymers*, *83*(2), 520–527. https://doi.org/10.1016/j.carbpol.2010.08.012

Bhosale, R. G., & Ziegler, G. R. (2010). Preparation of spherulites from amylose–palmitic acid complexes. *Carbohydrate Polymers*, *80*(1), 53–64. https://doi.org/10.1016/j.carbpol.2009.10.069

Bogracheva, T. Ya., Morris, V. J., Ring, S. G., & Hedley, C. L. (1998). The granular structure of C-type pea starch and its role in gelatinization. *Biopolymers*, *45*(4), 323–332. https://doi.org/10.1002/(SICI)1097-0282(19980405)45:4<323::AID-BIP6>3.0.CO;2-N

Buléon, A., Véronèse, G., & Putaux, J.-L. (2007). Self-Association and Crystallization of Amylose. *Australian Journal of Chemistry*, *60*(10), 706–718. https://doi.org/10.1071/CH07168

Cai, L., & Shi, Y.-C. (2010). Structure and digestibility of crystalline short-chain amylose from debranched waxy wheat, waxy maize, and waxy potato starches. *Carbohydrate Polymers*, *79*(4), 1117–1123. https://doi.org/10.1016/j.carbpol.2009.10.057

Cai, L., & Shi, Y.-C. (2013). Self-Assembly of Short Linear Chains to A- and B-Type Starch Spherulites and Their Enzymatic Digestibility. *Journal of Agricultural and Food Chemistry*, *61*, 10787–10797.

Cai, L., & Shi, Y.-C. (2014). Preparation, structure, and digestibility of crystalline A- and B-type aggregates from debranched waxy starches. *Carbohydrate Polymers*, *105*, 341–350. https://doi.org/10.1016/j.carbpol.2014.01.075

Cai, L., Shi, Y.-C., Rong, L., & Hsiao, B. S. (2010). Debranching and crystallization of waxy maize starch in relation to enzyme digestibility. *Carbohydrate Polymers*, *81*(2), 385–393. https://doi.org/10.1016/j.carbpol.2010.02.036

Chen, Y.-F., Kaur, L., & Singh, J. (2018). Chemical modification of starch. In M. Sjoo & L. Nilsson (Eds.), *Starch in food structure, function and applications* (2nd ed., pp. 283–324). Woodhead.

Creek, J. A., Ziegler, G. R., & Runt, J. (2006). Amylose Crystallization from Concentrated Aqueous Solution. *Biomacromolecules*, *7*(3), 761–770. https://doi.org/10.1021/bm050766x

Crist, B., & Schultz, J. M. (2016). Polymer spherulites: A critical review. *Progress in Polymer Science*, *56*, 1–63. https://doi.org/10.1016/j.progpolymsci.2015.11.006

Fanta, G. F., Felker, F. C., & Shogren, R. L. (2002). Formation of crystalline aggregates in slowly-cooled starch solutions prepared by steam jet cooking. *Carbohydrate Polymers*, *48*(2), 161–170. https://doi.org/10.1016/S0144-8617(01)00230-2

Fanta, G. F., Felker, F. C., Shogren, R. L., & Salch, J. H. (2008). Preparation of spherulites from jet cooked mixtures of high amylose starch and fatty acids. Effect of preparative conditions on spherulite morphology and yield. *Carbohydrate Polymers*, *71*(2), 253–262. https://doi.org/10.1016/j.carbpol.2007.05.034

Fanta, G. F., Kenar, J. A., & Felker, F. C. (2013). Preparation and properties of amylose complexes prepared from hexadecylamine and its hydrochloride salt. *Carbohydrate Polymers*, *98*(1), 555–561. https://doi.org/10.1016/j.carbpol.2013.06.028

Fanta, G., Felker, F., Shogren, R., & Salch, J. (2006). Effect of fatty acid structure on the morphology of spherulites formed from jet cooked mixtures of fatty acids and defatted cornstarch☆. *Carbohydrate Polymers*, *66*(1), 60–70. https://doi.org/10.1016/j.carbpol.2006.02.017

Felker, F. C., Kenar, J. A., Fanta, G. F., & Biswas, A. (2013). Comparison of microwave processing and excess steam jet cooking for spherulite production from amylose-fatty acid inclusion complexes. *Starch - Stärke*, *65*(9–10), 864–874. https://doi.org/10.1002/star.201200218

Gidley, M. J., & Bulpin, P. V. (1987). Crystallisation of malto-oligosaccharides as models of the crystalline forms of starch: Minimum chain-length requirement for the formation of double helices. *Carbohydrate Research*, *161*(2), 291–300. https://doi.org/10.1016/S0008-6215(00)90086-7

Guenet, J.-M. (1996). Factors influencing gelation versus crystallization in cooling polymer solutions. *Trends in Polymer Science*, *4*, 6–11.

Helbert, W., Chanzy, H., Planchot, V., Buléon, A., & Colonna, P. (1993). Morphological and structural features of amylose spherocrystals of A-type. *International Journal of Biological Macromolecules*, *15*(3), 183–187. https://doi.org/10.1016/0141-8130(93)90021-D

Hizukuri, S., Abe, J., & Hanashiro, I. (2006). Starch: Analytical aspects. In *Carbohydrates in food* (2nd ed, pp. 305–391). Taylor & Francis Group.

Jane, J. (2009). Chapter 6—Structural Features of Starch Granules II. In J. BeMiller & R. Whistler (Eds.), *Starch (Third Edition)* (pp. 193–236). Academic Press. https://doi.org/10.1016/B978-0-12-746275-2.00006-9

Jane, J.-L. (Ed.). (2004). Starch: Structure and Properties. In *Chemical and functional properties of food saccharides* (Tomasik, Tomasik, pp. 81–100). CRC Press.

Kiatponglarp, W., Rugmai, S., Rolland-Sabaté, A., Buléon, A., & Tongta, S. (2016). Spherulitic self-assembly of debranched starch from aqueous solution and its effect on enzyme digestibility. *Food Hydrocolloids*, *55*, 235–243. https://doi.org/10.1016/j.foodhyd.2015.11.027

Kobayashi, S., Hobson, L. J., Sakamoto, J., Kimura, S., Sugiyama, J., Imai, T., & Itoh, T. (2000). Formation and Structure of Artificial Cellulose Spherulites via Enzymatic Polymerization. *Biomacromolecules*, *1*(2), 168–173. https://doi.org/10.1021/bm990010w

Liu, Y.-X., Liang, Z.-S., Liang, J.-N., & Liao, L.-Y. (2021). Effect of different surface properties of nanosilica on retrogradation behavior and structures of thermoplastic cassava starch. *Journal of Polymer Research*, *28*(5), 147. https://doi.org/10.1007/s10965-021-02507-z

Luo, K., Park, K.-H., Lee, D.-H., Hong, C.-E., Song, Y.-W., Yoo, S.-H., & Kim, Y.-R. (2019). Self-assembly kinetics of debranched short-chain glucans from waxy maize starch to form spherical microparticles and its applications. *Colloids and Surfaces B: Biointerfaces*, *176*, 352–359. https://doi.org/10.1016/j.colsurfb.2019.01.002

Ma, U. V. L., Floros, J. D., & Ziegler, G. R. (2011). Effect of starch fractions on spherulite formation and microstructure. *Carbohydrate Polymers*, *83*(4), 1757–1765. https://doi.org/10.1016/j.carbpol.2010.10.041

Manners, D. J., & Matheson, N. K. (1981). The fine structure of amylopectin. *Carbohydrate Research*, *90*(1), 99–110. https://doi.org/10.1016/S0008-6215(00)85616-5

Sweedman, M. C., Tizzotti, M. J., Schäfer, C., & Gilbert, R. G. (2013). Structure and physicochemical properties of octenyl succinic anhydride modified starches: A review. Carbohydrate Polymers, 92(1), 905–920.

Nordmark, T. S., & Ziegler, G. R. (2002a). Structural features of non-granular spherulitic maize starch. *Carbohydrate Research*, *337*(16), 1467–1475. https://doi.org/10.1016/S0008-6215(02)00192-1

Nordmark, T., & Ziegler, G. (2002b). Spherulitic crystallization of gelatinized maize starch and its fractions. *Carbohydrate Polymers*, *49*(4), 439–448. https://doi.org/10.1016/S0144-8617(01)00353-8

Pérez, S., Baldwin, P. M., & Gallant, D. J. (2013). Structural Features of Starch Granules I. In *Resistant starch: Sources, applications and health benefits* (Yong-Cheng Shi, Clodualdo C. Maningat, Yong-Cheng Shi, Clodualdo C. Maningat, pp. 149–192). John Wiley & Sons, Ltd.

Ring, S. G., Miles, M. J., Morris, V. J., Turner, R., & Colonna, P. (1987). Spherulitic crystallization of short chain amylose. *International Journal of Biological Macromolecules*, *9*(3), 158–160. https://doi.org/10.1016/0141-8130(87)90044-4

Robyt, J. F. (2009). Chapter 7—Enzymes and Their Action on Starch. In J. BeMiller & R. Whistler (Eds.), *Starch (Third Edition)* (pp. 237–292). Academic Press. https://doi.org/10.1016/B978-0-12-746275-2.00007-0

Shang, Y., Chao, C., Yu, J., Copeland, L., Wang, S., & Wang, S. (2018). Starch Spherulites Prepared by a Combination of Enzymatic and Acid Hydrolysis of Normal Corn Starch. *Journal of Agricultural and Food Chemistry*, *66*(25), 6357–6363. https://doi.org/10.1021/acs.jafc.8b01370

Shi, J., Sweedman, M. C., & Shi, Y.-C. (2018). Structural changes and digestibility of waxy maize starch debranched by different levels of pullulanase. *Carbohydrate Polymers*, *194*, 350–356. https://doi.org/10.1016/j.carbpol.2018.04.053

Shi, J., Sweedman, M. C., & Shi, Y.-C. (2021). Structure, birefringence and digestibility of spherulites produced from debranched waxy maize starch. *International Journal of Biological Macromolecules*, *183*, 1486–1494. https://doi.org/10.1016/j.ijbiomac.2021.05.127

Shtukenberg, A. G., Punin, Y. O., Gunn, E., & Kahr, B. (2012). Spherulites. *Chemical Reviews*, *112*(3), 1805–1838. https://doi.org/10.1021/cr200297f

Singh, J., Lelane, C., Stewart, R. B., & Singh, H. (2010). Formation of starch spherulites: Role of amylose content and thermal events. *Food Chemistry*, *121*(4), 980–989. https://doi.org/10.1016/j.foodchem.2010.01.032

Vesterinen, E., Suortti, T., & Autio, K. (2001). Effects of Preparation Temperature on Gelation Properties and Molecular Structure of High-Amylose Maize Starch. *Cereal Chemistry Journal*, *78*(4), 442–446. https://doi.org/10.1094/CCHEM.2001.78.4.442

Waigh, T. A., Jenkins, P. J., & Donald, A. M. (1996). Quantification of water in carbohydrate lamellae using SANS. *Faraday Discussions*, *103*, 325. https://doi.org/10.1039/fd9960300325

Wang, C., Fu, X., Tang, C.-H., Huang, Q., & Zhang, B. (2017). Octenylsuccinate starch spherulites as a stabilizer for Pickering emulsions. *Food Chemistry*, *227*, 298–304. https://doi.org/10.1016/j.foodchem.2017.01.092

Yokobayashi, K., Akai, H., Sugimoto, T., Hirao, M., Sugimoto, K., & Harada, T. (1973). Comparison of the kinetic parameters of Pseudomonas isoamylase and Aerobacter pollulanase. *Biochimica et Biophysica Acta (BBA) - Enzymology*, *293*(1), 197–202. https://doi.org/10.1016/0005-2744(73)90391-4

Ziegler, G. R. (2020). Enzyme-Resistant Starch Spherulites. *Starch - Stärke*, *72*(7–8), 1900217. https://doi.org/10.1002/star.201900217

Ziegler, G. R., Creek, J. A., & Runt, J. (2005). Spherulitic Crystallization in Starch as a Model for Starch Granule Initiation. *Biomacromolecules*, *6*(3), 1547–1554. https://doi.org/10.1021/bm049214p

Ziegler, G. R., Nordmark, T. S., & Woodling, S. E. (2003). Spherulitic crystallization of starch: Influence of botanical origin and extent of thermal treatment. *Food Hydrocolloids*, *17*(4), 487–494. https://doi.org/10.1016/S0268-005X(03)00020-1

Table 1.1 Summary of birefringence sign of spherulites and their crystalline type.

Birefringence sign	Publication	Crystalline structure
Positive	Shi et al., 2021	A-type and B-type
	Kiatponglarp et al., 2016	B-type
Negative	Shi et al., 2021	B-type
"X" shape	Fanta et al., 2002, 2013	V-type
	Shi et al., 2021	B-type
	Kiatponglarp et al., 2016	B-type
Maltese crosses were observed, but the type was not identified	Cai and Shi, 2013	B-type
	Bhosale and Ziegler, 2010	Mixture of B- and V-type
	Creek et al., 2013	B-type
	Ma et al., 2011	Not measured
	Nordmark and Ziegler, 2002a	Not measured
	Nordmark and Ziegler, 2002b	B-type
	Singh et al., 2010	Mixture of B- and V-type
	Ziegler et al., 2003	Not measured
	Ziegler et al., 2005	B-type
	Ziegler, 2020	B-type

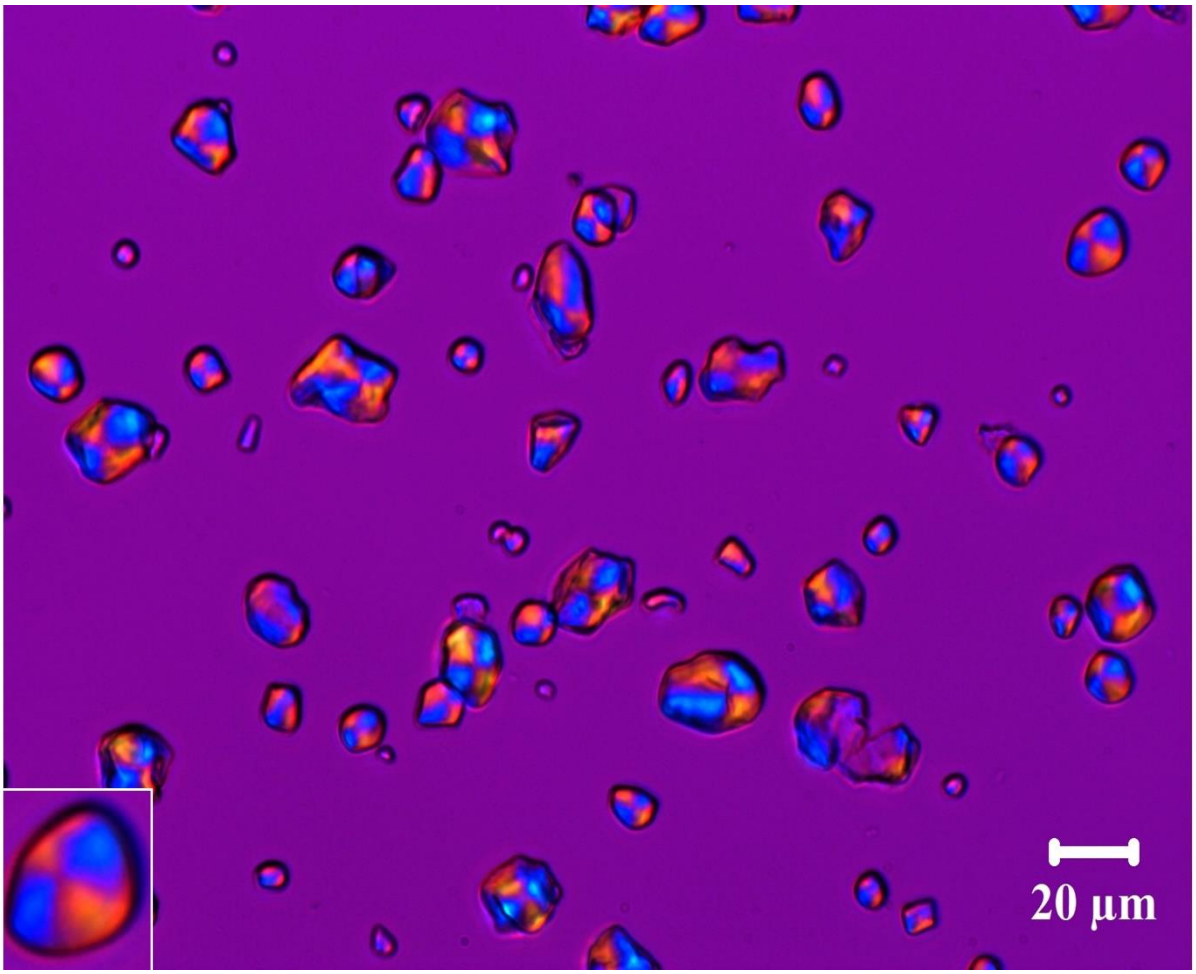

Figure 1.1 Microscopy image of native waxy maize starch granules observed under a polarized light combined with a waveplate (Shi et al., 2021).

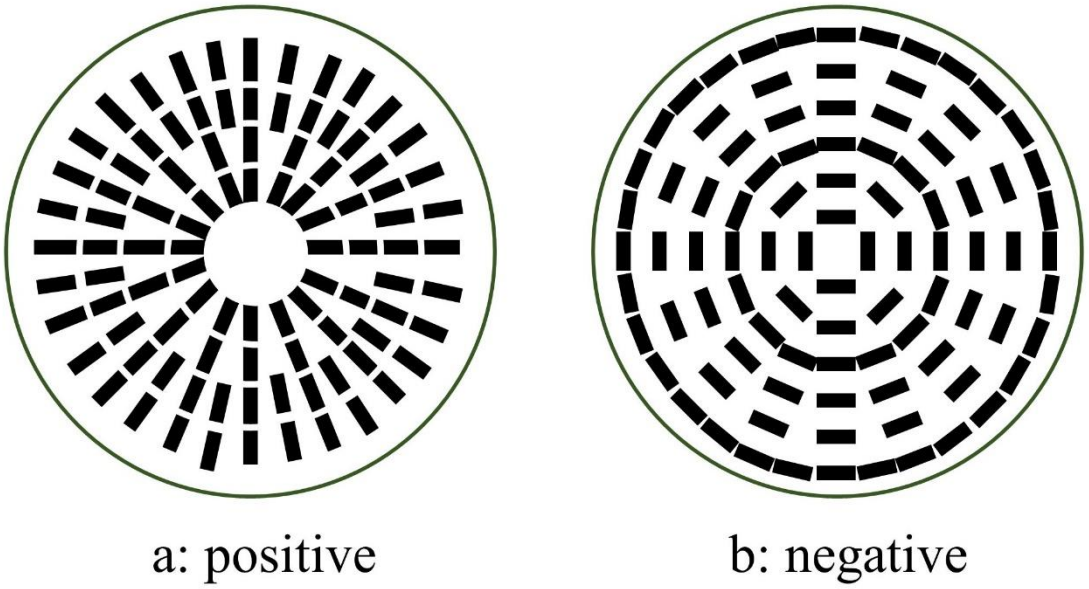

Figure 1.2 The schematic diagram of positive and negative spherulites proposed by Shi et al. (2021).

Chapter 2 - Spherulites with A-type and B-type allomorphs produced from debranched waxy potato starch

Abstract

Waxy potato starch has a longer average chain length than waxy maize starch. The objectives of this study were to examine factors affecting the formation of spherulites from debranched waxy potato starch (DBWPS) and study their structure and digestibility. At a crystallization temperature of 25°C, spherulites with B-type allomorph and negative birefringence were produced from the DBWPS, while higher crystallization temperatures were used to alter the crystalline structure. However, raising the crystallization temperature did not result in the production of A-type spherulites. The B-type spherulites formed at 25°C were subjected to heat-moisture treatment (HMT). At 140°C, spherulites with A-type allomorph were produced with negative birefringence. Compared to native waxy potato starch, the spherulites generated in this study had a lower resistant starch (RS) content, except when the crystallization temperature was set at 50°C, 70°C, and 90°C, where the RS content was approximately 78%, and not significantly different from the RS content of waxy potato starch. Following crystallization, the spherulites also had higher melting temperatures and a greater degree of crystallinity. The degree of crystallinity was decreased by HMT, but the melting temperature was further increased.

Keywords

Crystalline structure, heat-moisture, spherulites, digestion, thermal stability

Introduction

Spherulites, which are crystallized materials that display Maltese crosses, can be formed using various starches (Cai & Shi, 2013; Creek et al., 2006; Crist & Schultz, 2016; Kiatponglarp et al., 2016; Ma et al., 2011; Nordmark & Ziegler, 2002; Shi et al., 2021; Singh et al., 2010; Ziegler et al., 2003, 2005; Ziegler, 2020). Ziegler et al. (2003) applied different native starches to form spherulites and discovered the importance of amylose content in their formation. Amylose chain length is another factor that affects spherulite formation (Ma et al., 2011). When the linear molecules were shorter than potato amylose, the required amylose content for spherulites formation was increased from 20% to 33% (Ma et al., 2011). Although spherulites were observed in materials with amylose chain lengths of DP 120 and DP 642, the DP 642 amylose formed spherulites with rough surfaces and inconsistent sizes.

Previous studies have demonstrated that debranching amylopectin can increase the level of linear molecules, with pullulanase and isoamylase being common debranching enzymes used for this purpose (Cai et al., 2010; Cai & Shi, 2010, 2013, 2014; Kiatponglarp et al., 2016; Shi et al., 2018, 2021; Shi & Gao, 2011). Spherulites have been produced from debranched waxy rice, normal rice, and waxy maize starches using microscopy and cross-polarized light, with Maltese crosses observed in these spherulites (Cai & Shi, 2013; Kiatponglarp et al., 2016; Shi et al., 2021).

During the process of starch crystallization, spherulites can be classified based on their crystalline structure, which depends on the way starch molecules crystallize into double helices. A-type and B-type crystalline structures are formed, with A-type being favored by high crystallization temperatures, high solid concentrations, and short molecule chain lengths

(Cai & Shi, 2013; Helbert et al., 1993; Ring et al., 1987; Buléon et al., 2007; Gidley & Bulpin, 1987). Previous studies have shown that B-type spherulites can be formed by high-amylose maize starch, acid-treated starch, and debranched starch (Ziegler, 2020; Fanta et al., 2002; Kiatponglarp et al., 2016; Cai & Shi, 2013; Shi et al., 2021). Moreover, in our previous studies, by increasing the crystallization temperature, we were able to obtain A-type spherulites from debranched waxy maize starch (Cai & Shi, 2013; Shi et al., 2021).

After reviewing previous studies (Cai & Shi, 2013; Creek et al., 2006; Crist & Schultz, 2016; Kiatponglarp et al., 2016; Ma et al., 2011; Nordmark & Ziegler, 2002; Shi et al., 2021; Singh et al., 2010; Ziegler et al., 2003, 2005; Ziegler, 2020), it has been found that the chain length of amylose influences spherulite formation. The chain length is determined by the variety of starch, and the presence of amylopectin in native starch inhibits spherulite formation. Previous studies used debranched waxy maize starch to produce spherulites (Cai & Shi, 2013; Shi et al., 2021). However, there is a lack of research using materials with a chain length between debranched waxy maize starch and high amylose starch.

To address this gap, debranched waxy potato was used in this study to form spherulites. Since longer linear molecules were used, it is hypothesized that the formation of A-type crystallites would require a higher crystallization temperature. The highest crystallization temperature used in this study was 120°C to prevent significant heating degradation. It is anticipated that B-type spherulites could form at a lower temperature of 25°C. To convert the B-type crystalline structure to A-type, hydrothermal treatment (HTT) was applied. By increasing the crystallization temperature or applying HTT, A-type spherulites could be formed. This study aims to provide more details about spherulite

formation and crystalline structure changes by investigating the formation of A-type spherulites. The study also aims to investigate the RS content and thermal properties, as well as the digestibility and thermal properties of the spherulites for their potential applications. The results of this study would offer information on the application of spherulites.

Materials and Methods

Materials

Waxy potato starch (Eliane) was obtained from Avebe (Veendam, The Netherlands). The amylose content was less than 1% (reported by Avebe), the ash content was 0.2% as measured by the AACC method 08-03.01. Isoamylase (77 IAU/ml) was from Weissbiotech (Ascheberg, Germany). The enzyme activity of isoamylase was defined as the amount of enzyme required to increase 0.01 in absorbance at 600 nm per min under an assay condition (Ara et al., 1993; Li et al., 2016). Other chemicals were analytical grade.

Debranching

Waxy potato starch (25 g) was suspended in 75 ml of water in a pressure jar and heated at 120°C for 60 min in an oven. When the mixture was cooled to 50°C, isoamylase (0.25 g) was added. Then the mixture was incubated at 50°C for 24 h with stirring. One debranched sample was crystallized at 25°C for 24 h, and then collected by centrifuge and drying in an air oven (40°C). The other debranched materials were processed by the procedure below to produce crystallized product.

Spherulites formation

After debranching, the debranched starch and water mixture (20 g) was transferred to an aluminum bottle and heated in a pressure reactor to 180°C (Cai & Shi, et al., 2013; Shi et al., 2021). When the temperature was 180°C, the pressure reactor was cooled by water to 100°C and then opened. The sample was cooled to 25, 50, 70, and 90 °C, respectively. After 24 h, the samples cooled to 50°C, 70°C, and 90°C were further cooled to 25°C for another 24 h. Another sample was cooled to 120°C after heating, and the sample was maintained at 120°C in the pressure reactor for 4 h, then the sample was further cooled to 25°C and crystallized for 24 h. The crystallized materials were filtered and dried in an oven at 40°C for 24 h. The soluble carbohydrate content was measured by a portable refractometer (Fisher Scientific Inc., Pittsburgh, PA, USA). The yields of spherulites formed were calculated by the difference of the soluble carbohydrate content and solid concentration used.

Heat-moisture treatment (HMT)

The spherulite (20 g) formed at 25°C was weighted into a pressure tube. Water was added in the tube to adjust the water content to 20% or 25%. The tube was sealed and placed at ambient for 24 h for equilibrium. Then the tube was heated at 120 or 140°C for 4 h and followed by cooling to 40°C. All samples were dried in an oven overnight at 40°C for 24 h.

Gel permeation chromatography (GPC)

A PL-GPC 220 (Polymer Laboratories, Inc., Amherst, MA, USA) was used to measure molecular size distribution (Vilaplana & Gilbert, 2010; Shi et al., 2018, 2021). A dried sample was dissolved in dimethyl sulfoxide (DMSO) containing lithium bromide (0.5% w/w)

(Vilaplana & Gilbert, 2010), and the solid concentration was 1 mg/ml. Fully dissolving was archived by heating the mixture at a high temperature (80~ 100°C) with stirring. The dissolved sample was filtered by a 2 μm filter at 25°C. Three Phenogel columns (Phenomenex, Inc., Torrance, CA, USA) were used to separate molecules by their size (Cai et al., 2010). Then the molecular size was converted to the degree of polymerization (DP) by a method described by Li et al. (2020).

X-ray diffraction (XRD)

A wide-angle X-ray diffraction (PANalytical, Almelo, The Netherlands) was used to determine the type of crystalline structure and calculate the degree of crystallinity. A theta-compensating slit, and a diffracted beam monochromator were applied. Samples were scanned at 35 kV and 20 mA, the bragg angle was from 3°(2θ) to 35°(2θ). The Origin 9.0 software was used to plot the XRD graph and measured the amorphous area which was used to calculate the relative degree of crystallinity (Chakraborty et al., 2021; Komiya & Nara, 1986). The moisture of the samples was equilibrated in a humidity chamber to 17%.

Light microscopy

Dried spherulites (10 mg) were mixed in 50% glycerol solution (1 ml) by gently stirring on a vortex. A drop of the sample was deposited on a glass microscope slide with a coverslip. A light microscopy (Olympus BX51TF, Olympus optical Co. Ltd., Shijuku-ku, Tokyo, Jap) was used to observe the samples, and the images were captured by a SPOT 18.2 Color Mosaic camera (Diagnostic Instruments Inc., Sterling Heights, MI, USA). A waveplate

(Olympus optical Co. Ltd., Shijuku-ku, Tokyo, Japan) was inserted to observe the birefringence properties.

Differential scanning calorimetry (DSC)

Spherites were loaded in a DSC pan, then distilled water was dropped on the sample. The dry weight of spherulites was 8 ~ 10 mg. The amount of water, including the weight of added water and the moisture content of spherites, was twice the dry weight of the solid. The DSC pan was sealed and heated in a DSC (DSC 25, TA Instruments, New Castle, DE, USA). The scanning was from 10°C to 160°C at 10°C/min. The software TRIOS (TA 223 Instruments, New Castle, DE, USA) was used to record and analyze data, the onset, peak, conclusion temperatures (T_o, T_p, and T_c, respectively) and enthalpy (ΔH) were calculated from the DSC thermogram.

Digestibility

The digestibility of the waxy potato starch and the spherulites was determined by a modified Englyst method as described in previous studies (Sang & Seib, 2006; Shi et al., 2021). A digestion curve was plotted by measuring the digested starch after 20, 40, 60, 80, 120, and 240 min of hydrolysis (Shi et al., 2021). The digested starch (4 ml) was transferred into 66% ethanol solution (20 ml), and then applied to the glucose content determination. Resistant starch (RS) content was calculated based on the amount of digested starch after 120 min of hydrolysis.

In another test, waxy potato starch and spherulites were cooked in a boiling water bath with shaking for 1 h before adding α-amylase and amyloglucosidase. After cooking, the

samples were cooled to 37°C and the enzymes were added immediately. The rest procedure was same to the modified Englyst method.

Statistical analysis

Statical analysis was processed by Minitab 17 Statistical Software Program (Minitab Inc. State College PA, USA). All experiments were duplicated, the mean value and standard deviation were reported.

Results and Discussion

Yields of spherulites formed at different crystallization temperatures

The yield of the crystallized products was found to be 87.7% when the crystallization temperature was 25°C. However, when the debranched waxy potato starch was crystallized at higher temperatures (50~120°C) and then further crystallized at 25°C, the yields increased to approximately 91~92% (Table 2.1). The yield of spherulites formed at 25°C were used to plot a yield curve. The yield increased rapidly to approximately 55% within the first two hours, after which the increase rate slowed down, and the yield gradually increased from 75% to 88% after eight hours of cooling (Figure 2.1).

Moat previous studies using DSC to produce spherulites did not report yield (Bhosale & Ziegler, 2010; Creek et al., 2006; Kiatponglarp et al., 2016; Ma et al., 2011; Nordmark & Ziegler, 2002; Ziegler et al., 2003). Our earlier studies using pressure tubes produced spherulites with yields higher than 80% at low crystallization temperatures (Cai & Shi, 2013; Shi et al., 2021). Temperature was found to have a significant influence on yield. In our previous study, spherulites made from debranched waxy maize had a yield of 82.2% at

a crystallization temperature of 4°C, which decreased to 44.5% at 50°C. However, a further crystallization step at 4°C increased the yield to 86.5% (Shi et al., 2021). In this study, a yield of 87.7% was achieved, which was higher than that obtained from debranched waxy maize. The two-step crystallization process was also found to increase the yields which became 91.0% - 92.3% (Table 2.1).

Gel permeation chromatography (GPC)

The molecular size distribution of the debranched waxy potato starch and spherulites is shown in Figure 2.2. Debranched waxy potato had two peaks at approximately DP 15 and DP 40 (Figure 2.2). During spherulite formation at temperatures below 120°C, the two peaks of debranched waxy potato were observed. However, at a crystallization temperature of 120°C, the area of peak at DP 40 was reduced, and the area of peak at DP 15 increased, with most molecules smaller than DP 300. After heat-moisture treatment (HMT) of samples crystallized at 25°C, the peak DP 40 was also reduced, and the DP distribution was affected by the heating temperature. At 120°C, a few molecules were larger than DP 300, and the moisture content had no effect on the DP distribution. However, at 140°C, molecules degraded to smaller than DP 200, and higher moisture content caused a greater reduction in molecular size (Figure 2.2).

Figure 2.2 shows that the difference in molecular size distribution was similar when DP was greater than 100. However, the difference of two peaks at DP 15 and DP 40 were noticeable. Shi et al. (2021) reported that at higher crystallization temperatures resulted smaller molecules crystallize first. With further crystallization at a lower temperature, longer

molecules also crystallized due to the longer crystallization time. The proportion of the area of peaks at DP 15 and DP 40 was the smallest when the crystallization temperature was 90°C. At a crystallization temperature of 120°C, the heating caused molecular degradation, resulting in shorter molecule lengths.

After HMT, degradation was also observed. Especially, when the heating temperature was 140°C, a higher moisture content enhanced the heating degradation. But when the temperature was lower to 120°C, the moisture content showed less influence on the heating degradation.

X-ray diffraction (XRD)

The X-ray diffraction patterns of waxy potato starch and the spherulites formed are shown in Figure 2.3. The B-type crystalline structure of native waxy potato starch was observed as indicated by the presence of peaks at 5, 17, 22, and 24 °2θ. Upon crystallization to form spherulites at different temperatures, the peaks became sharper and new peaks appeared at 14, 15, and 20 °2θ (Figure 2.3). The degree of crystallinity of native waxy potato starch was initially 39.1%, which increased to 63.9% upon crystallization at 25°C. Crystallization at higher temperatures of 50°C and 70°C, followed by a final crystallization at 25°C, resulted in increased degrees of crystallinity of 67.1% and 68.8%, respectively. However, when the crystallization temperatures were further increased to 90°C and 120°C, the degree of crystallinity decreased to 64.5% and 58.7%, respectively (Table 2.1).

After crystallization at 25°C, the sample was subjected to HMT, and the resulting crystalline structure changed to A-type at 140°C. At the HMT temperature of 120°C, the

crystalline type remained unchanged, but the peaks were less defined as shown in Figure 2.3. The degree of crystallinity decreased after the HMT. A higher moisture content (25%) resulting in a higher crystallinity of 54.2% at 120°C. In contrast, a lower moisture content (20%) yielded a degree of crystallinity of 50.4%. When the temperature was increased to 140°C, the degree of crystallinity was not affected by the moisture content as presented in Table 2.1.

In our previous study, we found that debranched waxy maize starch sample, which was crystallized at 50°C and then further crystallized at 4°C, showed a high degree of crystallinity (Shi et al., 2021). Additionally, debranched waxy maize starch formed an A-type crystalline structure when crystallized at 50°C (Cai & Shi, 2013; Shi et al., 2021). However, debranched waxy potato starch did not form A-type crystallites when crystallized at temperatures ranging from 50-120°C. This was likely because the chain length of debranched waxy potato starch was longer than that of debranched waxy maize starch (Figure 2.2), and the longer chain length of debranched favors the formation of B-type crystalline structure (Helbert et al., 1993; Ring et al., 1987; Buléon et al., 2007; Gidley & Bulpin, 1987). In this study,

Two-step crystallization increased the crystallinity of debranched waxy potato starch (Figure 2.3). But when the crystallization temperature was 120°C, heating degradation reduced the chain length, and consequently reduced crystallinity. The heating degradation can also explain the lower crystallinity observed when the HMT was used, which was also reported previously (Yang et al., 2016; Chakraborty et al., 2021).

Nishiyama et al. (2010) reported that when potato amylopectin was heated to 120°C, the HMT samples had A-type crystalline structure. Heating provided energy for the B-type crystallites to expand and release water molecules, allowing the helices to be repacked and form an A-type crystalline structure (Perez et al., 1990). In this study, the sample had a crystallinity of 63.9%, which was higher than that of native starch. Therefore, a higher HTT temperature of 140°C was required to induce a crystalline structure transition. A higher moisture content may increase the mobility of the molecules, which can support the repacking of the helices and increase crystallinity. Consequently, when the moisture content was 25% and the HTT temperature was 120°C, the crystallinity was higher.

Morphology

The morphology of spherulites was observed by a light microscopy and is shown in Figure 2.4. Native waxy potato starch granules exhibit various sizes under light microscopy, with oval and round shapes being observed. The long axis of oval granules was around 40 μm, while some granules have a diameter of about 10 μm. Under polarized light, these starch granules exhibited a clear Maltese cross, and a positive birefringence was observed when a waveplate is inserted. When debranched waxy potato starch crystallized to form spherulites, negative birefringence was observed, and the morphology was influenced by the crystallization temperature. Spherical particles of uniform size, approximately 8 μm in diameter, were observed when the spherulites crystallized at 25°C. At 90°C, the morphology was similar to that at 25°C. Large particles, approximately 20 μm in diameter, were observed when the crystallization temperature was 50°C and 70°C. These large particles aggregate,

making the Maltese cross less clear under polarized light, although negative birefringence was still observed with the insertion of a waveplate. When the crystallization temperature was 120°C, large particles are still observed, but their diameter was slightly smaller than 20 μm. The samples crystallized at 25°C were used for the HMT, and their morphology remained unchanged, except for the sample treated at 140°C with a moisture content of 25%, which showed more particle aggregates (Figure 2.4).

In our previous study (Shi et al., 2021), we also observed the formation of negative spherulites by debranched waxy maize starch at 25°C, with a particle size similar to that of the debranched waxy potato starch samples at 25°C. At 50°C or 70°C, the molecules crystallized to form small particles, which increased in size upon further crystallization at a low temperature, as we also observed in our previous study (Shi et al., 2021). At 90°C and 120°C, the heating degradation was more significant and influenced the morphology. HMT could repack the double helices without changing the orientation, so the birefringence was not affected. However, when the temperature was 140°C and the moisture content was 25%, most of the molecules were degraded (Figure 2.2), resulting in more aggregates being observed.

Thermal properties of waxy potato starch, debranched waxy potato starch and spherulites

Thermal properties of waxy potato starch and its debranched and crystallized forms are shown in Table 2.2. The onset gelatinization temperature for waxy potato starch was 60.2°C, with complete melting occurring at 97.5°C and an enthalpy of gelatinization of 20.6 J/g. The

onset and peak melting temperatures increased after debranching and crystallization. The spherulites crystallized at 90°C and then 25°C had the highest peak temperature was 93.5°C, other spherulites had peak temperatures ranging from 85.7°C to 89.7°C. The conclusion temperature for the spherulites crystallized at different temperatures ranged from 107.1°C to 108.5°C. The highest enthalpy required to melt the crystallized material was approximately 36 J/g at crystallization temperatures of 25°C and 120°C, the enthalpy value of spherulites crystallized at other temperatures ranging from 21.5 J/g to 26.6 J/g.

The thermal properties were significantly altered after HMT. The onset temperatures increased from 63.8°C to above 72°C, and the peak temperature was over 90°C after HMT. A higher temperature or moisture content during HMT resulted in even higher onset and peak temperatures. When HMT was performed at 140°C and 25% water, the highest onset and peak temperatures were recorded (83.4°C and 97.7°C, respectively), and a second peak at 125.2°C was observed. Additionally, a higher HMT temperature resulted in a higher conclusion temperature. At 120°C, a higher moisture content increased the conclusion temperature from 106.3°C to 116.5°C. However, at 140°C, a higher moisture content decreased the conclusion temperature from 155.3°C to 138.9°C. The enthalpy of HMT samples ranged from 22.1 J/g to 27.5 J/g, with the highest enthalpy observed at a temperature of 120°C and a moisture content of 25%.

The changes in onset temperature were found to be consistent with the molecular size distribution. However, this pattern was not observed in the HMT samples, as the re-packing of the helices during HMT may have influenced the thermal properties. The re-packing of helices was more pronounced at higher moisture content and temperature, particularly at

140°C, where the crystalline structure changed from B-type to A-type. The conclusion temperatures of the HMT samples treated at 140°C were significantly higher than those of other samples. Nonetheless, the higher degradation observed at 140°C and a moisture content of 25% resulted in a lower conclusion temperature.

Digestibility of waxy potato starch, and spherulites

The initial resistant starch (RS) content in native waxy potato starch was 80.4%. However, when the debranched waxy potato starch crystallized at different temperatures, the RS content was found to decrease (Table 2.1). The RS content did not decrease significantly when samples were crystallized at 50°C, 70°C, and 90°C, remaining at approximately 78%. However, at a crystallization temperature of 25°C, the RS content decreased to 74.1%. The lowest RS content of 66.9% was observed when samples were crystallized at 120°C.

When the moisture content was 20%, two HMT samples contained approximately 67% RS and were barely affected by the HMT temperature. However, when the moisture content was increased to 25%, the RS content showed more variation with HMT temperature. Specifically, the RS content increased to 75.3% when the temperature was 120°C, but decreased to 51.6% when the temperature was 140°C.

Although the RS contents of spherulites were lower than that of waxy potato starch, spherulites had higher melting temperature. As a result, waxy potato starch, the spherulites formed at 25°C and spherulites of HMT were cooked for 1h, and then applied to the enzyme hydrolysis. Table 2.3 showed the RS contents of cooked samples. The RS content was drastically reduced to 1.9%. The spherulites formed at 25°C had 7.4% RS. After HMT, the

RS contents were increased. Both temperature and moisture content of HMT showed positive correlation to the RS contents. When the HMT temperature was 140°C, and moisture content was 25%, the RS content was the highest (33.1%).

The digestion curves of spherulites were plotted by measuring the amount of digested starch at different hydrolysis times (Figure 2.5). The influence of crystallization temperature on the RS content was evident in the digestion curve. Samples crystallized at 50°C, 70°C, and 90°C showed lower digestibility and higher RS content. The digestion curves also reflected the RS contents observed in the HMT samples (Table 2.1). In addition to indicating the RS content, the digestion curves revealed an increase in digestion rate between 60 and 80 minutes.

The RS content of spherulites varied depending on the crystallization temperature, with the highest content observed at 50°C, 70°C, and 90°C, where the crystallinity was relatively higher compared to other temperatures (Table 2.1). The type-3 RS formed by crystallization is known to be influenced by crystallinity (Topping et al., 2003; Hasjim et al., 2013; Shi et al., 2018, 2021). The RS content of HMT samples also correlated with their degree of crystallinity, except for those treated at 140°C and 25% water (Table 2.1). HMT caused re-packing of helices, where high temperature provided energy but also caused degradation, resulting in a high degree of crystallinity but low RS content in the samples.

However, a higher melting peak influenced the RS contents when samples were cooked. Waxy potato starch had a melting peak at the lowest temperature (Table 2.2), cooking resulted in the loss of crystalline structure, and the RS content was the lowest (Table 2.3). Spherulites formed at 25°C showed a higher melting temperature, the RS content after cooking was also

higher. After HMT, the thermal stability was further improved, and showed less reduction in RS content after cooking. A-type spherulites were more thermal stable, so the RS contents were also higher, although they showed lower RS contents before cooking.

Previous studies have shown that resistant starch can be formed by debranched waxy maize and waxy potato starches (Cai & Shi, 2014; Shi et al., 2018). However, digestion curves did not show an increased digestion rate when RS was formed after debranching. On the other hand, when spherulites were formed, a noticeable increase in digestion rate was observed (Shi et al., 2021). This increase can be attributed to the larger particle size of the spherulites, which produced small fragments during digestion, but still maintained their Maltese cross structure. These fragments were more digestible, while the intact particles with the Maltese cross structure remained resistant to enzyme digestion. Therefore, the production of fragments led to an increased digestion rate.

Conclusions

After debranching, waxy potato starch was used to form spherulites at different crystallization temperatures. The resulting spherulites all showed negative birefringence, and the molecular size distribution, thermal properties, and crystallinity varied depending on the crystallization temperature. Compared to native waxy potato starch, the melting temperatures and crystallinity were increased, but significant degradation was observed when the temperature was 120°C. The formation of spherulites did not lead to a higher RS content, but the RS content was not significantly reduced when the temperature was 50°C, 70°C, or 90°C, which were the three crystallization temperatures that resulted in the highest degree of crystallinity. All samples formed B-type crystallites regardless of the crystallization temperature. When HMT was applied,

negative birefringence was still observed, but the crystalline structure changed to A-type at 140°C. The degree of crystallinity was reduced to approximately 50% after HMT, and the RS content was also reduced. However, the melting temperature significantly increased. As a result, the highest RS content of HMT samples after cooking was 33.1%, but the RS content of waxy potato starch was reduced to 1.9%.

References

Ara, K., Saeki, K., & Ito, S. (1993). Purification and characterization of an alkaline isoamylase from an alkalophilic strain of Bacillus. In *Microbiology,* (Vol. 139, Issue 4, pp. 781–786). Microbiology Society.

Buléon, A., Véronèse, G., & Putaux, J.-L. (2007). Self-Association and Crystallization of Amylose. *Australian Journal of Chemistry*, *60*(10), 706.

Cai, L., & Shi, Y. C. (2013). Self-Assembly of Short Linear Chains to A- and B-Type Starch spherulites and Their Enzymatic Digestibility. *Journal of Agricultural and Food Chemistry*, *61*, 10787–10797.

Cai, L., & Shi, Y.-C. (2010). Structure and digestibility of crystalline short-chain amylose from debranched waxy wheat, waxy maize, and waxy potato starches. *Carbohydrate Polymers*, *79*(4), 1117–1123.

Cai, L., & Shi, Y.-C. (2014). Preparation, structure, and digestibility of crystalline A- and B-type aggregates from debranched waxy starches. *Carbohydrate Polymers*, *105*, 341–350.

Cai, L., Shi, Y.-C., Rong, L., & Hsiao, B. S. (2010). Debranching and crystallization of waxy maize starch in relation to enzyme digestibility. *Carbohydrate Polymers*, *81*(2), 385–393.

Chakraborty, I., Govindaraju, I., Rongpipi, S., Mahato, K. K., & Mazumder, N. (2021). Effects of Hydrothermal Treatments on Physicochemical Properties and In Vitro Digestion of Starch. *Food Biophysics*, *16*(4), 544–554.

Creek, J. A., Ziegler, G. R., & Runt, J. (2006). Amylose Crystallization from Concentrated Aqueous Solution. *Biomacromolecules*, *7*(3), 761–770.

Crist, B., & Schultz, J. M. (2016). Polymer spherulites: A critical review. *Progress in Polymer Science*, *56*, 1–63.

Fanta, G. F., Felker, F. C., & Shogren, R. L. (2002). Formation of crystalline aggregates in slowly-cooled starch solutions prepared by steam jet cooking. *Carbohydrate Polymers*, *48*(2), 161–170.

Fanta, G. F., Felker, F. C., Shogren, R. L., & Salch, J. H. (2008). Preparation of spherulites from jet cooked mixtures of high amylose starch and fatty acids. Effect of preparative conditions on spherulite morphology and yield. *Carbohydrate Polymers*, *71*(2), 253–262.

Fanta, G. F., Kenar, J. A., & Felker, F. C. (2013). Preparation and properties of amylose complexes prepared from hexadecylamine and its hydrochloride salt. *Carbohydrate Polymers*, *98*(1), 555–561.

Fanta, G., Felker, F., Shogren, R., & Salch, J. (2006). Effect of fatty acid structure on the morphology of spherulites formed from jet cooked mixtures of fatty acids and defatted cornstarch☆. *Carbohydrate Polymers*, *66*(1), 60–70.

Gidley, M. J., & Bulpin, P. V. (1987). Crystallisation of malto-oligosaccharides as models of the 365 crystalline forms of starch: Minimum chain-length requirement for the formation of 366 double helices. *Carbohydrate Polymers*, *161*, 291–300.

Hasjim, J., Ai, Y., & Jane, J. (2013). Novel Applications of Amylose-Lipid Complex as Resistant Starch Type 5. In Yong Cheng Shi and Clodualdo C. Maningat (eds.) *Resistant Starch: S ources, Applications and Health Benefits*. First Edition, pp. 79–94. Southern Gate, Chichester, West Sussex, UK: John Wiley & Sons, Ltd.

Haudin, J. M. (1986). *Optical studies of polymer morphology. In optical properties of polymers*. Elsevier Applied Science Publishers.

Helbert, W., Chanzy, H., Planchot, V., Buléon, A., & Colonna, P. (1993). Morphological and structural features of amylose spherocrystals of A-type. *International Journal of Biological Macromolecules*, *15*(3), 183–187.

Kiatponglarp, W., Rugmai, S., Rolland-Sabaté, A., Buléon, A., & Tongta, S. (2016). Spherulitic self-assembly of debranched starch from aqueous solution and its effect on enzyme digestibility. *Food Hydrocolloids*, *55*, 235–243.

Komiya, T., & Nara, S. (1986). Changes in crystallinity and gelatinization phenomena of potato 386 starch by acid treatment. *Starch - Stärke*, *38*, 9–13.

Li, Q., Li, C., Li, E., Gilbert, R. G., & Xu, B. (2020). A molecular explanation of wheat starch physicochemical properties related to noodle eating quality. *Food Hydrocolloids*, *108*, 106035.

Lin, Q., Facon, M., Putaux, J.-L., Dinges, J. R., Wattebled, F., D'Hulst, C., Hennen-Bierwagen, T. A., & Myers, A. M. (2013). Function of isoamylase-type starch debranching enzymes ISA1 and ISA2 in the *Zea mays* leaf. *New Phytologist*, *200*(4), 1009–1021.

Lopez-Rubio, A., Flanagan, B. M., Gilbert, E. P., & Gidley, M. J. (2008). A novel approach for calculating starch crystallinity and its correlation with double helix content: A combined XRD and NMR study. *Biopolymers*, *89*(9), 761–768.

Ma, U. V. L., Floros, J. D., & Ziegler, G. R. (2011). Effect of starch fractions on spherulite formation and microstructure. *Carbohydrate Polymers*, *83*(4), 1757–1765.

Nishiyama, Y., Putaux, J., Montesanti, N., Hazemann, J.-L., & Rochas, C. (2010). B→A Allomorphic Transition in Native Starch and Amylose Spherocrystals Monitored by In Situ Synchrotron X-ray Diffraction. *Biomacromolecules*, *11*(1), 76–87.

Nordmark, T., & Ziegler, G. R. (2002). Spherulitic crystallization of gelatinized maize starch and its fractions. *Carbohydrate Polymers*, *49*(4), 439–448.

Perez, S., Imberty, A., & Scaringe, R. P. (1993). *Computer modeling of carbohydrate molecules* (French, A. D., Brady, J. W.). American Chemical Society. Washington, DC

Ring, S. G., Miles, M. J., Morris, V. J., Turner, R., & Colonna, P. (1987). Spherulitic crystallization of short chain amylose. *International Journal of Biological Macromolecules*, *9*(3), 158–160.

Shi, J., Sweedman, M. C., & Shi, Y.-C. (2018). Structural changes and digestibility of waxy maize starch debranched by different levels of pullulanase. *Carbohydrate Polymers*, *194*, 350–356.

Shi, J., Sweedman, M. C., & Shi, Y.-C. (2021). Structure, birefringence and digestibility of spherulites produced from debranched waxy maize starch. *International Journal of Biological Macromolecules*, *183*, 1486–1494.

Shi, M., & Gao, Q. (2011). Physicochemical properties, structure and in vitro digestion of resistant starch from waxy rice starch. *Carbohydrate Polymers*, *84*(3), 1151–1157.

Singh, J., Lelane, C., Stewart, R. B., & Singh, H. (2010). Formation of starch spherulites: Role of amylose content and thermal events. *Food Chemistry*, *121*(4), 980–989.

Topping, D. L., Fukushima, M., & Bird, A. R. (2003). Resistant starch as a prebiotic and synbiotic: State of the art. *Proceedings of the Nutrition Society*, *62*(1), 171-176.

Vilaplana, F., & Gilbert, R. G. (2010). Characterization of branched polysaccharides using multiple-detection size separation techniques: Liquid Chromatography. *Journal of Separation Science*, *33*(22), 3537–3554.

Yang, J., Xie, F., Wen, W., Chen, L., Shang, X., & Liu, P. (2016). Understanding the structural features of high-amylose maize starch through hydrothermal treatment. *International Journal of Biological Macromolecules*, *84*, 268–274.

Ziegler, G. R. (2020). Enzyme-Resistant Starch Spherulites. *Starch - Stärke*, *72*(7–8), 1900217.

Ziegler, G. R., Creek, J. A., & Runt, J. (2005). Spherulitic Crystallization in Starch as a Model for Starch Granule Initiation. *Biomacromolecules*, *6*(3), 1547–1554.

Ziegler, G. R., Nordmark, T. S., & Woodling, S. E. (2003). Spherulitic crystallization of starch: Influence of botanical origin and extent of thermal treatment. *Food Hydrocolloids*, *17*(4), 487–494.

Table 2.1 Properties of waxy potato starch (WPS), spherulites crystallized at different temperatures from debranched WPS, and heat-moisture treated spherulite crystallized at 25°C.

Formation temperature (°C)		Yields (%)	Type of crystalline structure	Degree of crystallinity (%)	Type of birefringence	Resistant starch content (%)
Waxy potato starch		\	B	39.7±0.1^{f}	positive	80.4±0.5^{a}
25		87.7±0.1^{b}	B	63.9±1.1^{b}	negative	74.1±0.3^{c}
50-25		91.5±0.5^{a}	B	67.1±1.0^{a}	negative	78.4±0.0^{b}
70-25		92.0±0.3^{a}	B	68.8±0.4^{a}	negative	78.2±0.2^{b}
90-25		92.3±0.5^{a}	B	64.5±0.9^{b}	negative	78.1±0.4^{b}
120-25		91.0±0.9^{a}	B	58.7±0.4^{c}	negative	66.9±0.4^{e}
HMT conditions						
Temperature (°C)	Moisture content (%)					
120	20	\	B	50.4±1.3^{e}	negative	67.8±1.1^{e}
	25	\	B	54.2±0.2^{d}	negative	75.3±0.0^{d}
140	20	\	A	49.7±0.6^{e}	negative	67.2±0.2^{e}
	25	\	A	50.6±0.5^{e}	negative	51.6±0.5^{f}

Values bearing the same small letter superscript(s) do not significantly differ at $p < 0.05$.

Table 2.2 Thermal properties of waxy potato starch (WPS), spherulites crystallized at different temperatures from debranched WPS, and heat-moisture treated spherulite crystallized at 25°C.

Temperature (°C)		To (°C)	Tp (°C)	Tc (°C)	ΔH (J/g)
Waxy potato starch		60.2±0.4^{f}	71.8±0.2^{g}	97.5±0.5^{e}	20.6±0.2^{f}
25		63.8±0.2^{e}	88.2±0.2^{ef}	108.4±0.5^{d}	36.4±0.6^{a}
50-25		66.6±0.7^{d}	89.7±0.2^{de}	108.5±0.2^{d}	23.6±0.6^{bc}
70-25		65.3±0.3^{de}	85.7±0.7^{f}	107.1±0.3^{d}	21.5±0.2^{c}
90-25		65.6±0.9^{de}	93.5±0.9^{bc}	107.7±0.4^{d}	26.6±1.1^{bc}
120-25		59.4±0.8^{f}	86.8±1.1^{ef}	107.4±0.0^{d}	35.9±0.9^{a}
HMT conditions					
Temperature (°C)	Moisture content (%)				
120	20	72.0±0.5^{c}	90.0±0.6^{cde}	106.3±1.0^{d}	22.1±1.0^{e}
	25	75.7±0.3^{b}	92.2±0.4^{bcd}	116.5±0.5^{c}	27.5±0.7^{b}
140	20	76.9±1.0^{b}	95.4±0.6^{ab}	155.3±0.4^{a}	26.6±0.2^{bc}
	25	83.4±0.1^{a}	97.7±0.7^{a} (125.2±0.5)	138.9±0.3^{b}	22.6±0.6^{bc}

Values bearing the same small letter superscript(s) do not significantly differ at $p < 0.05$.

Table 2.3 Resistant starch (RS) content of waxy potato starch (WPS), spherulites crystallized 25°C from debranched WPS, and heat-moisture treated spherulite crystallized at 25°C. All samples were cooked in a boiling water bath for 1 h before adding the mixture of α-amylase and amyloglucosidase.

Sample		RS
Waxy potato starch		1.9±0.2[f]
Spherulites		7.4±0.2[e]
HMT conditions		
Temperature (°C)	Moisture content (%)	
120	20	11.2±0.7[d]
	25	23.8±0.3[c]
140	20	28.9±0.6[b]
	25	33.1±0.9[a]

Values within columns bearing the same small letter superscript(s) do not significantly differ at $p < 0.05$.

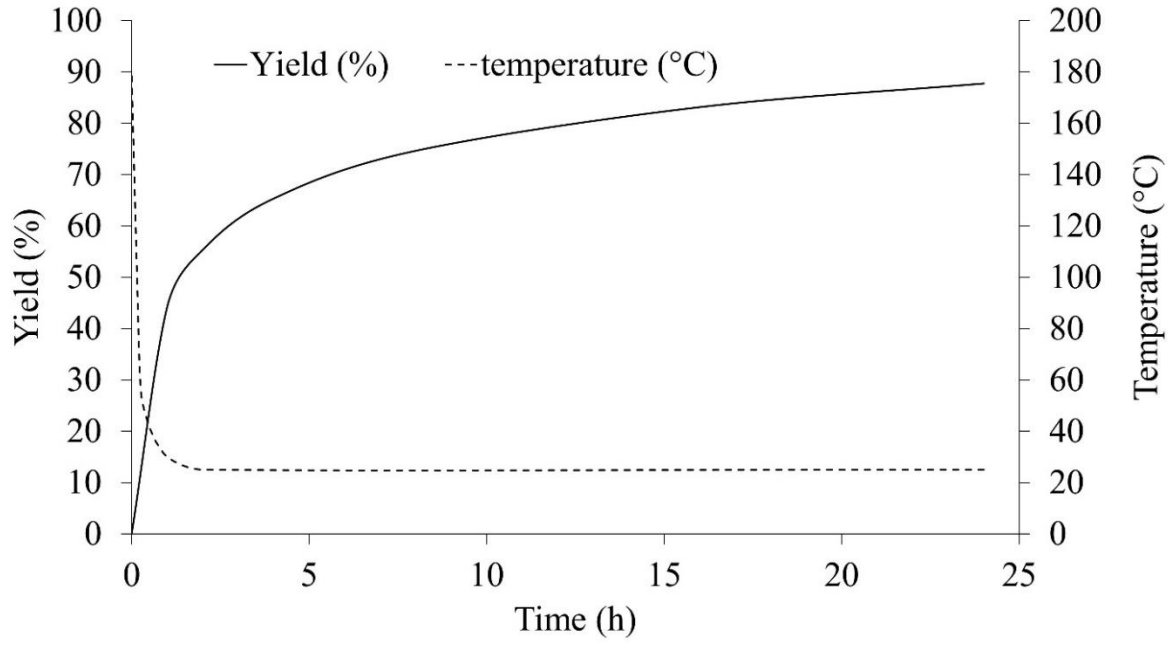

Figure 2.1 Yields of spherulites (25% solid) formed after cooling from 180°C to 25°C.

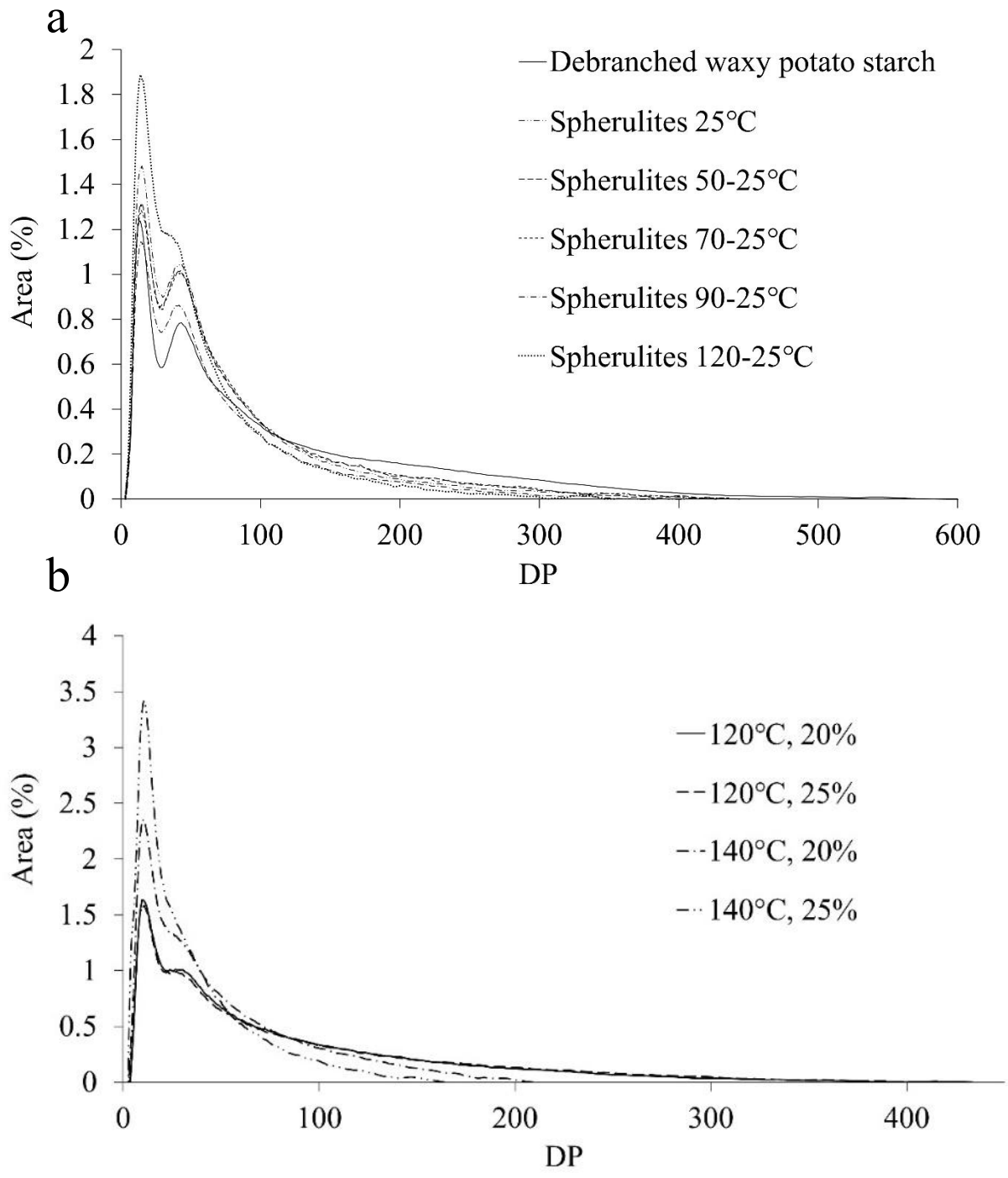

Figure 2.2 The molecular size distribution of (a) debranched waxy potato starch and spherulite formed at different temperatures, and (b) the spherulites modified by heat-moisture treatment (HMT).

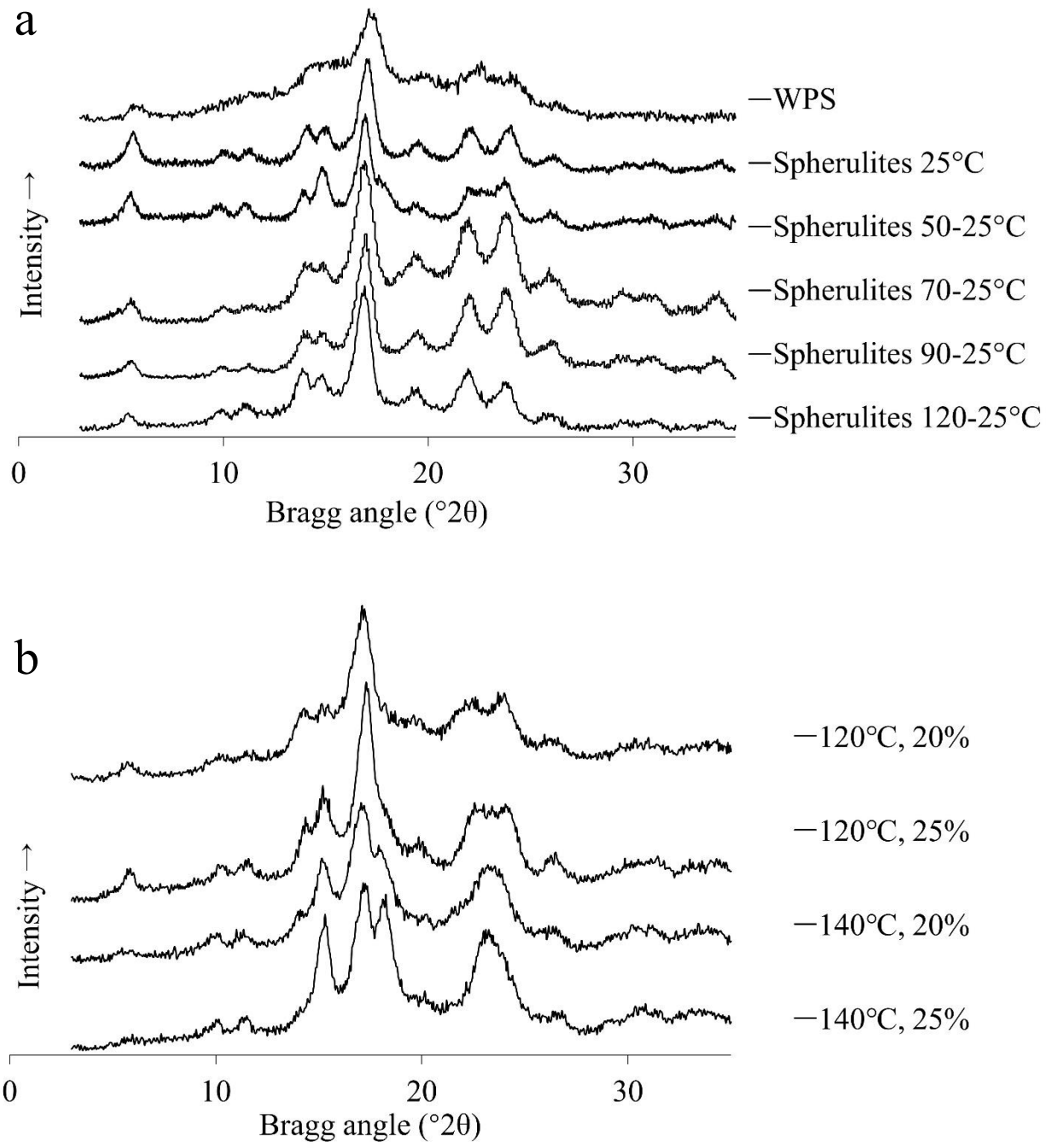

Figure 2.3 X-ray diffraction graphs of (a) waxy potato starch (WPS), spheurlites formed at different crystallization temperatures, and (b) the spherulites after the heat-moisture treatment (HMT).

Waxy potato starch

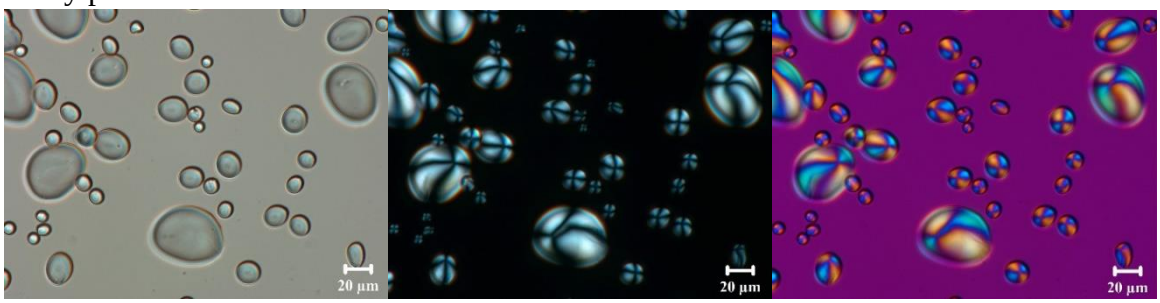

Spherulites at 25°C

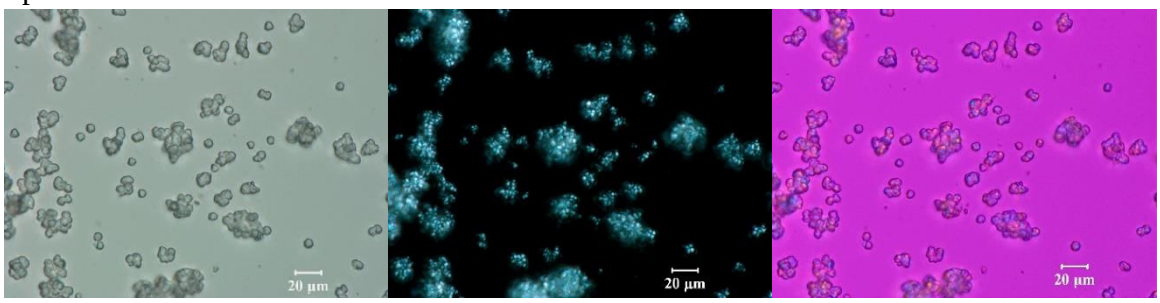

Spherulites at 50-25°C

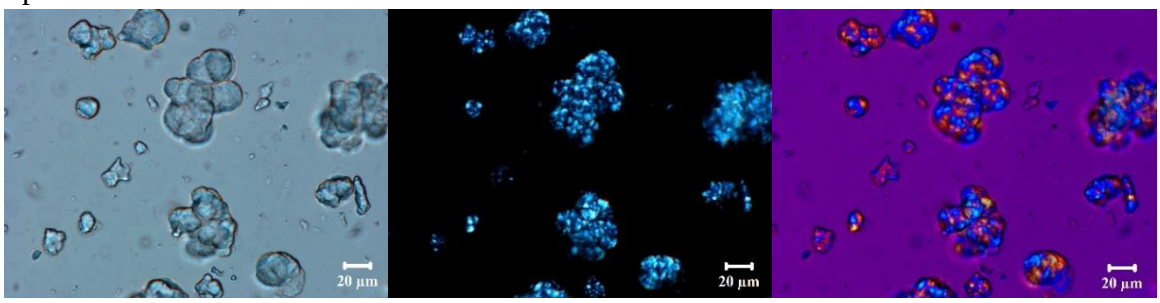

Spherulites at 70-25°C

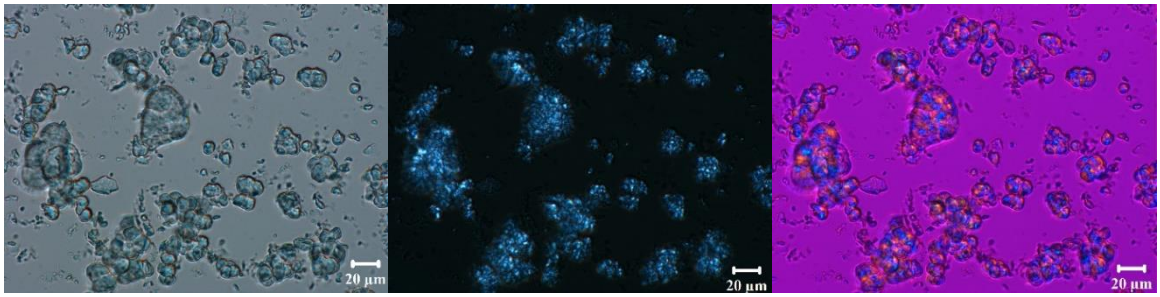

Spherulites at 90-25°C

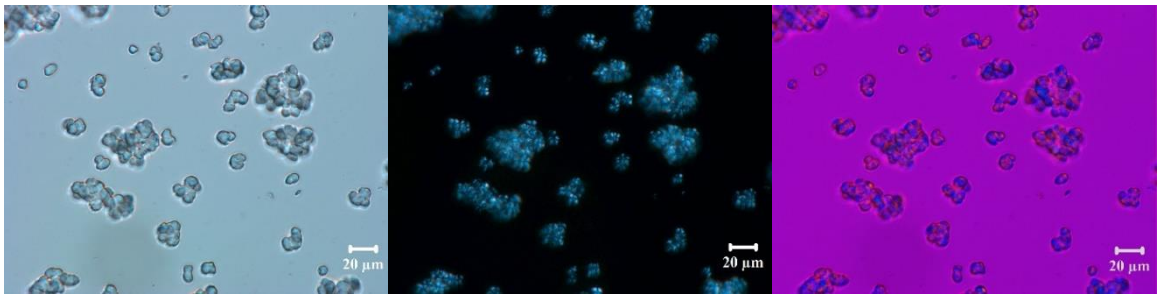

Spherulites at 120-25°C

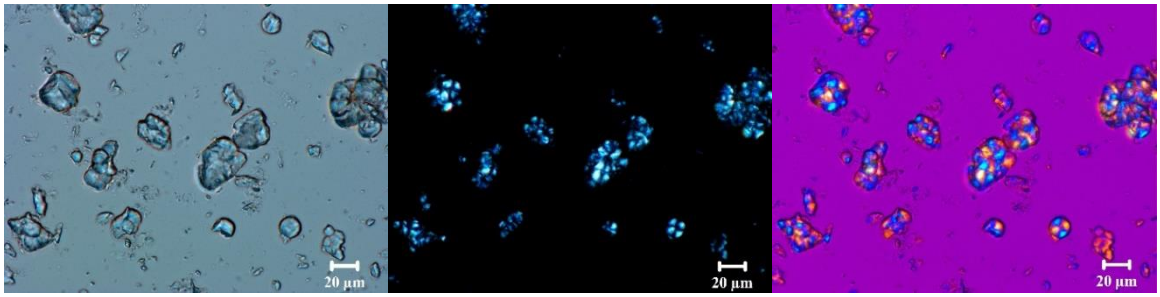

HMT 120°C, 20%

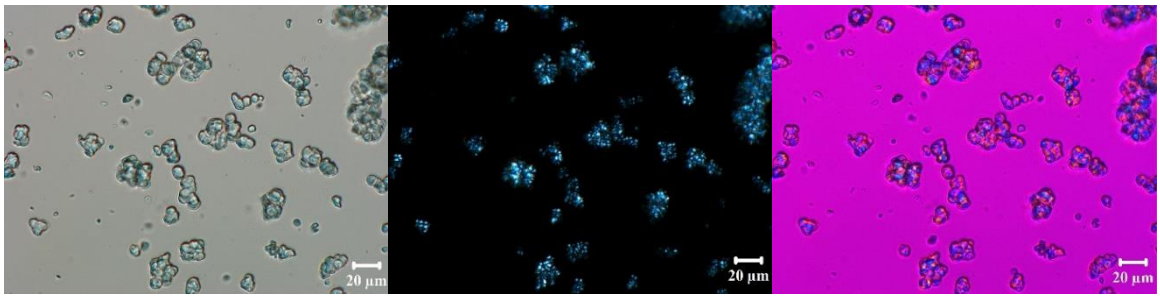

HMT 120°C, 25%

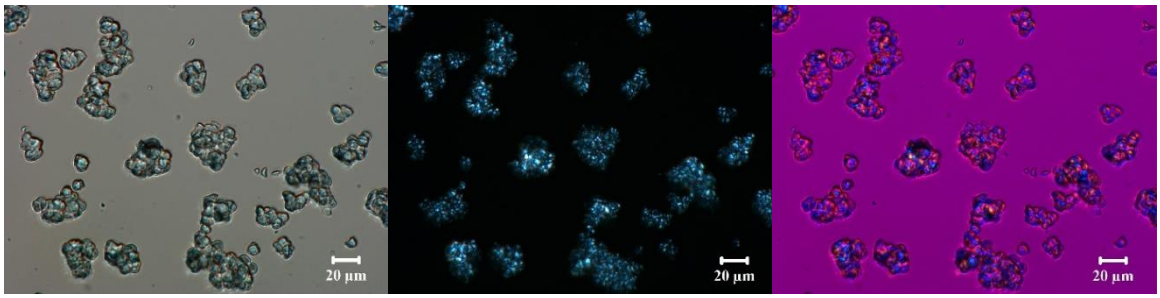

HMT 140°C, 20%

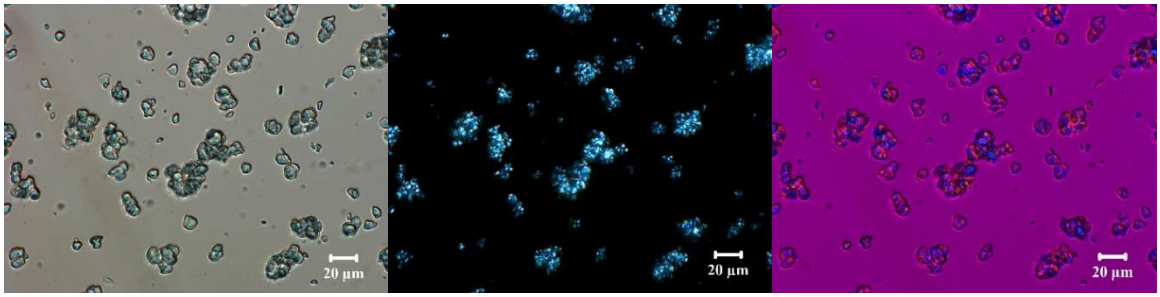

HMT 140°C, 25%

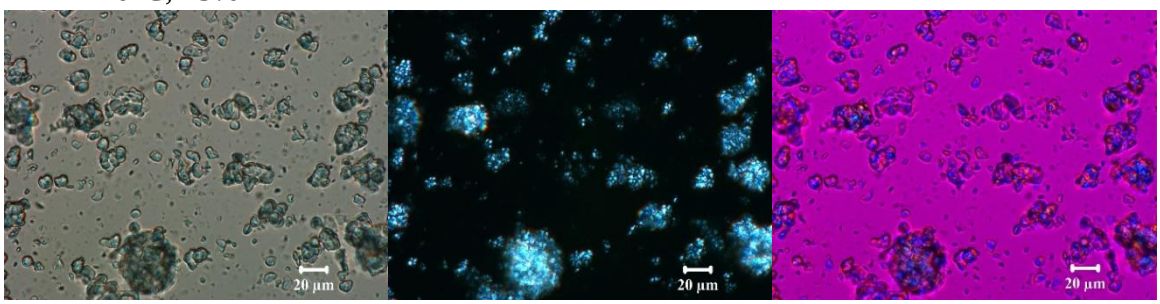

Figure 2.4 Morphology of waxy potato starch, spheurlites formed at different crystallization temperatures, and the spherulites after the heat-moisture treatment (HMT).

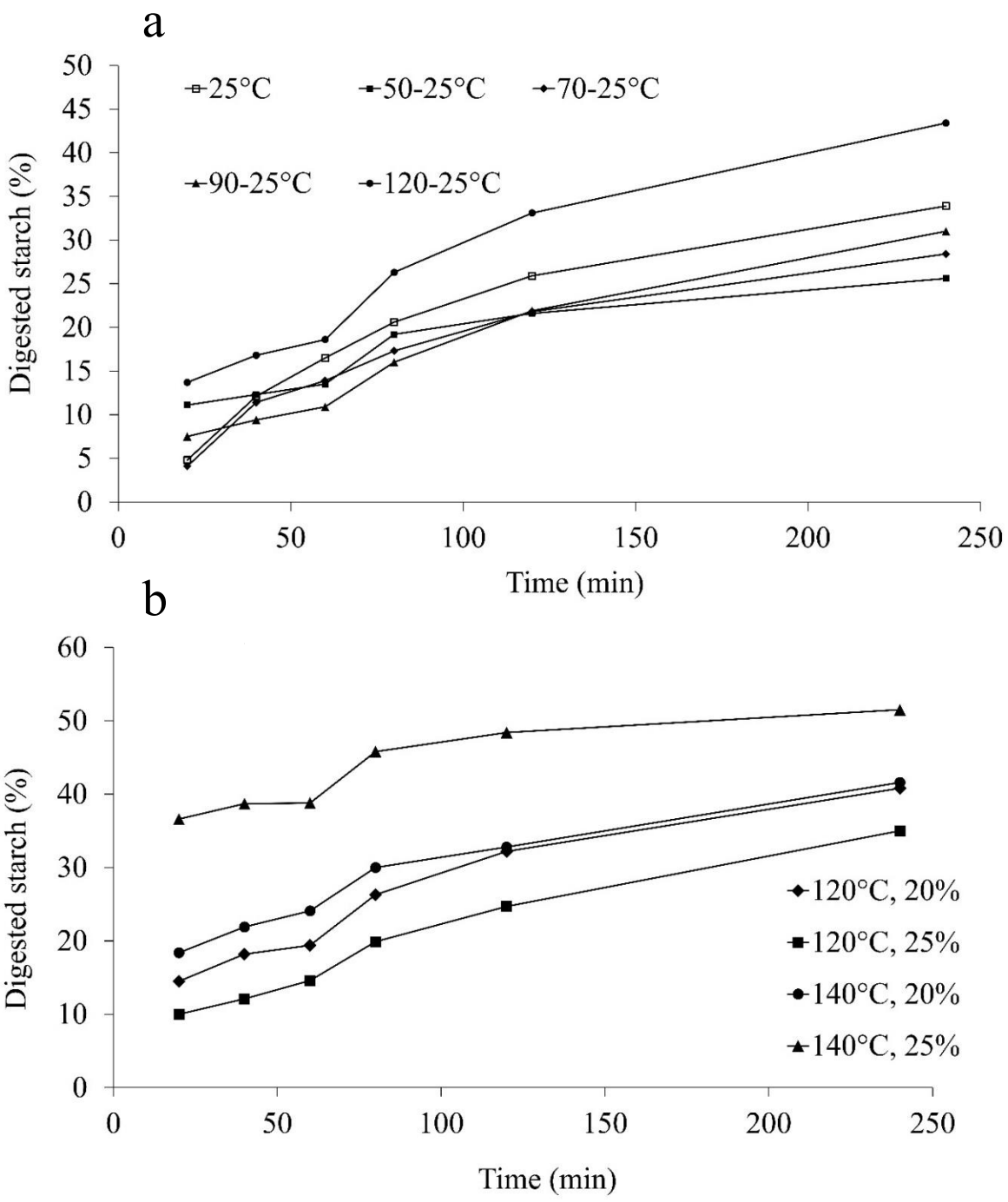

Figure 2.5 Digestion curve of (a) spherulites crystallized at different temperatures, and (b) the hydro-thermal treated spherulites.

Chapter 3 - Preparation, structure, and digestibility of spherulites with positive and negative birefringence from debranched high-amylose maize starch

Abstract

High-amylose maize starch was debranched to increase the level of linear molecules and enhance the formation of spherulites. Debranched high-amylose starch (25%, w/w) was heated to 180°C in a Parr reactor followed by crystallization at different temperatures between 50°C and 150°C. The yield, morphology, structure, digestibility, and crystallinity of the spherulites were investigated. When the crystallization temperature was 150°C, negative spherulites were observed. Meanwhile, the chain length, yields, degree of crystallinity and resistant starch content were smaller by comparing to spherulites crystallized at lower temperatures. When the formation temperature was lower than 150°C, all samples formed positive spherulites. The chain length of amylose, particle size, and degree of crystallinity were influenced by the formation temperature, but all spherulites were positive, highly crystallized, and highly resistant to enzyme digestion. Enzyme staining and confocal laser scanning microscopy showed that α-amylase hydrolyzed the surface of each first spherulite. This result was also reflected in the light microscopy images of digested spherulites. During digestion, spherulites were still observed, but the size was reduced after a longer digestion time.

Keywords

Birefringence sign, digestion, iodine staining, confocal microscopy

Introduction

Spherulites are crystalline materials showing a Maltese cross under a microscope with polarized light and having a rotational symmetry (Crist & Schultz, 2016; Haudin, 1986; Shtukenberg et al., 2012; Ziegler, 2020). The formation of starch spherulites is described as crystallization favored by linear molecules (Ziegler, 2020) or "high temperature retrogradation" (Fanta et al., 2002). In general, formation of spherulites is favored by a starch with a high level of amylose (Ma et al., 2011, Singh et al., 2010, Ziegler et al., 2003). To increase the level of linear chains, starches are debranched and the debranched starches are used to produce spherulites (Kiatponglarp et al., 2016; Cai and Shi 2013; Shi et al., 2021). Once a starch is dissolved (melted), a fast cooling rate enhances the formation of spherulites (Creek et al., 2006; Nordmark and Ziegler, 2002a). For pure amylose, spherulites are observed when a wide range of cooling rates (1–250°C) is used (Creek et al., 2006).

Many previous studies used a differential scanning calorimetry (DSC) to produce spherulites (Creek et al., 2006; Kiatponglarp et al., 2016; Ma et al., 2011; Singh et al., 2010; Ziegler, 2020; Ziegler et al., 2003). The amount of spherulites formed in a DSC pan is limited (about 10–20 mg), and is often not enough for digestibility, structure, and functional property studies. The yields of spherulites are often not quantified or reported (Helbert et al., 1993; Ma et al., 2011; Ziegler, 2020; Ziegler et al., 2005). Fanta et al. (2002) used a jet cooker to form spherulites with a large amount of starch (200 g), but the solid concentration was only

approximately 4%, and the yield was lower than 12%. Using pressure jars or pressure reactors, we are able to produce a larger amount of spherulites with a high yield (Cai & Shi, 2013; Shi et al., 2021).

As a crystallized material, the crystalline structure of spherulites is influenced by solid concentration, degree of polymerization (DP), crystallization temperature, and solvent used (Cai & Shi, 2013, 2014; Helbert et al., 1993; Kiatponglarp et al., 2016; Shi et al., 2021). High-solid concentration, high crystallization temperature, and low DP tend to form A-type crystalline spherulites (Cai & Shi, 2013; Helbert et al., 1993; Ring et al., 1987a, Shi et al., 2021). Debranched waxy maize starch has been used to form an A-type crystalline structure at 50°C (Cai & Shi, 2013, 2014, Shi et al., 2021). But few studies have applied the high crystallization temperature to produce spherulites with a high-amylose starch (Nordmark, 2002a; Singh et al., 2010a) and only B-type crystalline structure was observed when high-amylose maize starch was used (Fanta et al., 2002).

The Maltese cross of spherulites can be observed with an optical microscope using cross-polarization geometry (Crist & Schultz, 2016). By inserting a full-wave retardation plate with its principal axis being at 45° with respect to the polarizer (Kiatponglarp et al. 2016; Shi et al., 2021), an alternating pattern of blue and yellow hues appears in the four quadrants of a spherulite. This indicates the contrast in birefringence, positive and negative spherulites can be identified. The birefringence sign is given by $\Delta n = n_1 - n_2$, where n_1 is the refractive index along the radial direction of spherulites, and n_2 along the tangential direction. This method of classification is widely used in the characterization of spherulites (Crist & Schultz, 2016; Dingler et al., 2019; Haudin, 1986; Wang et al., 2002; Shi et al., 2021). In the

previous studies, positive spherulites were formed by long chain amylose (Kiatponglarp et al. 2016, Ziegler et al., 2003), but Shi et al. (2021) reported that spherulites with positive and negative signs could be produced from short-chain amylose (debranched waxy maize starch) by manipulating the crystallization conditions such as crystallization temperature and solvent used. Starch spherulites are a unique form of resistant starch (RS) (Cai & Shi, 2013). In our previous studies (Cai & Shi, 2010, 2014; Shi et al., 2021), debranched waxy maize starch crystallized and formed high quality RS. In this study, debranched high-amylose maize starch (DB-HAMS) was used to form spherulites. Our hypothesis is that debranching high-amylose maize starch produces essentially all linear chains with much longer chains than debranched waxy maize starch, and thus the DB-HAMS would form high quality spherulites with great RS content. The effects of crystallization temperature on spherulite formation were studied. High-amylose maize starch has a B-type crystalline structure (Brewer et al., 2012; Shi et al., 1997). We wondered if high crystallization temperatures would result in spherulites with an A-type crystalline structure from the DB-HAMS. Two steps of cooling were applied in this study (Shi et al., 2021). DB-HAMS was first crystallized at a high temperature, and then further crystallized at 25°C. The yield, crystalline structure (crystalline type and degree of crystallinity), birefringence sign, thermal properties and digestibility and digestion mechanism of the spherulites formed were studied. In addition, iodine staining was used to better understand the internal structure of the spherulites formed.

Materials and Methods

Materials

High-amylose maize starch (AmyloGel 03003) was obtained from Cargill (Wayzata, MN, US) and the amylose content was 69.3% as measured by the Con A method (Gibson et al., 1997) using an assay kit (K-AMYL) from Megazyem (Wicklow, Ireland); the ash content was 0.1% as measured by the AACC method 08-03.01; the protein content was 0.4% and measured by a Carbon/Nitrogen combustion analyzer (LECO Corporation, St. Joseph, MI). Isoamylase was obtained from Weissbiotech (Ascheberg, Germany); the enzyme activity was 77 IAU/mL, and one unit of isoamylase activity was defined as the amount of enzyme increasing 0.01 in absorbance at 600 nm per minute at 50°C and pH 6.0 (Ara et al., 1993; Li et al., 2016). Other chemicals were analytical grade.

Debranching starch

High-amylose maize starch (80 g, db) was mixed with sodium acetate buffer (240 mL, 0.01 M, pH 4) in a ball jar (32 oz, Ball Corporation, Westminster, CO), and heated in an oven at 140°C for 2 h. When the mixture was cooled to 50°C, another 80 mL of warm water (50°C) was added to dilute the mixture to ensure constant stirring. Isoamylase (1%, w/w) was added and the mixture was incubated in a water bath at 50°C and maintained at 50°C for 24 h with constant stirring (Cai et al., 2010; Cai & Shi, 2010). After incubation, the mixture was heated in a boiling water bath for 5 min to denature the enzyme and then dried by a spray dryer (180°C, Mini Spray Dryer B-290, BUCHI Corporation, DE, USA).

Formation of spherulites in a differential scanning calorimeter (DSC)

The DB-HAMS (20 mg, db) was loaded in a DSC pan, and 60 mg of water was added to the pan so that the starch concentration was 25% (w/w). Each sample was heated to 170, 180, or 190°C, maintained for 5 min followed by cooling to 25°C at a rate of 25, 50, or 100°C/min. After cooling to 25°C, each sample was maintained at this temperature for 5 min. Then the DSC pan was opened and placed in a centrifuge tube (Cat. 05-408-138, Fisherbrand™ Premium Microcentrifuge Tubes), all the solid (approximate 20 mg) was precipitated by ethanol (approximate 1~1.5 mL) and collected in the centrifuge tube. The DSC pan was washed by ethanol and removed from the centrifuge tube. After centrifuge processing (1000 g, 5 min), the supernatant was discarded, and the residue was dried in an oven (35°C) for 24 h and saved for further analysis.

Formation of spherulites in a pressure reactor

DB-HAMS (20 g) was dried and transferred to an aluminum can (PerkinElmer, Waltham, MA, USA) containing 60 mL of water with an aluminum foil cover, and heated in a parr reactor (4521M, PARR, Illinois, USA) to 180°C. When the temperature reached 180°C, the parr reactor was cooled by chilled water (2°C) to 100°C (the average cooling rate was 20°C/min) and then opened. The sample was cooled to 25, 50, 70, and 90°C in a water bath for 24 h, and other two samples were cooled to 120 and 150°C in the parr reactor for 4 h, respectively. The samples crystallized 25°C were filtered after 24 h. The samples formed at 50, 70, 90, 120 and 150°C were further crystallized at 25°C for 24 h. All samples were filtered and dried in an oven at 40°C for 24 h.

After the crystallization at 25°C, the spherulites were collected by filtration and the yield was calculated by measuring the soluble carbohydrate content with a portable refractometer (Fisher Scientific Inc., Pittsburgh, PA, USA). The yields of spherulites formed were calculated by the difference between the soluble carbohydrate content and solid concentration applied.

The time when the cooling started was considered as the crystallization time 0 h. The yields after 1, 2, 4, 8, and 24 h were recorded and used to plot the yield curve.

Gel permeation chromatography (GPC)

The molecular size of the high-amylose maize starch, DB-HAMS, and recovered crystalline debranched starch products was determined by GPC. A dried sample (4 mg) was dispersed in 4 mL of dimethyl sulfoxide (DMSO) (HPLC grade) containing lithium bromide (LiBr) (0.5% w/w) (Vilaplana & Gilbert, 2010). To fully dissolve the sample, the sample was sealed and heated in a boiling water bath for 24 h with stirring. After heating and cooling to 25°C, the dissolved sample was filtered through a 2 μm filter when cooled to 25°C. The filtrate was injected into a PL-GPC 220 (Polymer Laboratories, Inc., Amherst, MA, USA) using three Phenogel columns (Phenomenex, Inc., Torrance, CA, USA) and a guard column (Phenomenex, Inc., Torrance, CA, USA) as previously described (Cai et al., 2010). The mobile phase was DMSO containing 0.5% (w/w) LiBr, and the flow rate was 0.8 mL/min. The columns temperature was maintained at 80°C. Pullulan standards were used for universal calibration (Vilaplana & Gilbert, 2010). Molecular size obtained by GPC was further

calculated to the degree of polymerization (DP) and the method was described in a previous study (Li et al., 2020).

Light microscopy

Morphology and birefringent properties of the high-amylose maize starch and crystallized DB-HAMS products were examined by light microscopy. Each sample (1 mg) was mixed with 50% glycerol solution (100 µL), and a drop of the mixture (10 µL) was deposited on a microscope slide with a coverslip. The sample was examined by a microscope (Olympus BX51TF) attached with a retardation plate (Olympus Optical Co. Ltd., Shinjuku-ku, Tokyo, Japan). Normal light, cross-polarized light, and cross-polarized light with full-wave red retardation were applied to investigate the morphology and birefringence. The images were captured by an attached camera (SPOT 18.2 Color Mosaic, Diagnostic Instruments Inc., Sterling Heights, MI, USA).

X-ray diffraction (XRD)

The moisture content was adjusted to about 17% by placing samples in a humidity chamber containing a saturated sodium chloride solution. An XRD (PANalytical, Almelo, the Netherlands) was employed to identify the allomorph and determine the crystallinity of the partial-crystalline starches (Chakraborty et al., 2021; Komiya & Nara, 1986). The measurements were conducted at a voltage of 35 kV and a current of 20 mA, using a copper X-ray source. The Bragg angle was between 3 and 35° (2θ).

Small angle neutron scattering (SANS)

Small angle neutron scattering (SANS) was performed at the beamline NG-7 30 m SANS at the National Institute of Standards and Technology (NIST) center for Neutron Research (NCNR). The neutron wavelength was 6 Å and the wavelength spread was 14.8%. Data collection in a q-range (q was defined as $|\boldsymbol{q}| = 4\pi\sin\theta/\lambda$, where $\boldsymbol{q}$ was the scattering vector, θ and λ were half of the scattering angle and the neutron wavelength, respectively) between 0.003 and 0.5 $Å^{-1}$ was fulfilled by using three instrumental configurations, at a sample-to-detector distance (SDD) of 1, 4, and 13 m. An extended low-q data registration down to q = 0.001 $Å^{-1}$ was archived by using a focused beam configuration with SDD = 15 m and neutron wavelength was 8.09 Å.

Starch samples were D_2O-exchanged before the SANS experiments (Mao et al., 2023). Approximately 60 mg of the as-is (ca. 10% moisture) or hydrated (ca. 50% D_2O) sample was sealed in an aluminum pouch. The pouch was fixed by a rectangular aperture mounted on a cadmium mask. The size of beam was 19 mm, which covered the pouch. Data reduction including background subtraction and conversion of the 2D scattering image to the 1D profile was carried out using an Igor-based package developed by Steven Kline (2006).

Particle size analysis

The particle size (volume diameter) of recovered crystalline debranched starch products was measured by a laser scattering particle size analyzer (LA-910, Horiba Ltd., Kyoto, Japan) at room temperature (Qiu et al., 2015).

Differential scanning calorimetry (DSC)

Thermal properties of high-amylose maize starch and crystallized samples were investigated by using a DSC (DSC 25, TA Instruments, New Castle, DE, USA). Sample (about 10 mg) was loaded in a high-volume stainless DSC pan, and water (twice the weight of the solid) was added to the sample. The DSC pan was sealed and heated from 10°C to 180°C at a rate of 10°C/min. The results were analyzed by using the TRIOS software (TA Instruments, New Castle, DE, USA). The onset, peak, and conclusion temperatures (T_o, T_p, and T_c, respectively) and enthalpy (ΔH) were calculated from the DSC thermogram.

Iodine staining

Sample (10 mg) was loaded in a tube (2 mL) and stained by 1 mL of iodine solution (Cai et al., 2014). The stock iodine solution contained 0.5% sodium acetate buffer (pH 4.5), 25% glycerol, 0.04% I_2, and 0.06% KI (Evans et al., 2003). Each sample was stained for 30 min in darkness (Cai et al., 2014). Stained samples were viewed by an Olympus BX51 polarized light microscope equipped with a camera. Normal and polarized lights were used to observe stained samples.

Enzyme labeling

The enzyme labeling was performed based on a procedure reported in previous studies (Bhattarai et al., 2016; Dhital et al., 2014). Sodium carbonate buffer (0.1 M) was mixed with sodium bicarbonate buffer (0.1 M) as 20:80 (v: v). The pancreas α-amylase (70 µl, A6255, Sigma-Aldrich, Inc., St. Louis, MO) was mixed with the buffer mixture (330 µl), and then further mixed with 20 µl of fluorescein isothiocyanate isomer I (FITC, F7250,

Sigma-Aldrich, Inc., St. Louis, MO). This mixture was vortexed for 2 h, and then the labeled enzyme (yellow) was separated by a PF-10 desalting column (17-0851-01, GE Healthcare, Chicago, IL). The labeled enzyme (50 µl) was diluted by water (200 µl), then 50 µl of diluted enzyme was mixed with a sample suspension containing 20 mg starch and 200 µl of phosphate buffered saline buffer (pH 7.2, P4417, Sigma-Aldrich, Inc., St. Louis, MO). When the sample was incubated at 37°C for 0, 30, 60, and 120 min, the hydrolyzed sample was placed in an ice bath to stop an enzyme reaction. All samples were washed by distilled water (200 µl) and centrifuged (3000 rpm, 2 min) twice, and the residue was viewed by a confocal microscope (Carl Zeiss 700, One North Broadway, White Plains, NY) with an excitation wavelength of 488 nm.

Digestibility of spherulites

Digestibility of high-amylose maize starch and spherulites samples were measured by a modified Englyst method (Englyst et al., 1992; Sang & Seib, 2006) as described in our previous work (Shi et al., 2021).

Statistical analysis

Minitab 17 Statistical Software Program (Minitab Inc. State College PA, USA) was used for the statistical analysis. Mean value and standard deviation from the duplicated experiments were reported.

Results and Discussion

Formation of spherulites in DSC pans

When the DB-HAMS was heated to 160°C, small particles developed and formed aggregates, without showing birefringence (Figure 3.1). In contrast, when heating the debranched starch to 170°C and 180°C, spherulites were formed and showed positive birefringence (Figure 3.1). Cooling rate significantly affected the spherulite size. When the debranched starch was heated to 170°C, the cooling rate of 100℃/min resulted in spherulites with a larger size than those formed by the cooling rates of 25 and 50°C/min. After the debranched starch was heated to 180°C, the cooling rate showed less influences on the spherulites' morphology, as the spherulites were large, had similar size at different cooling rates, and the Maltese cross was clearly defined (**Error! Reference source not found.**).

In previous studies, starches were heated to 180°C to form spherulites (Cai & Shi, 2013; Creek et al., 2006; Kiatponglarp et al., 2015; Ma et al., 2011; Nordmark, 2002; Shi et al., 2021; Singh et al., 2010; Ziegler, 2020; Ziegler et al., 2003, 2005). Lower temperatures, such as 120°C or 170°C, were also used to produced spherulites, when acid-hydrolyzed starches were used (Ring et al., 1987; Ziegler et al., 2003). According to Nordmark and Ziegler (2002a), spherulites formed by high-amylose starches were supported when the cooling rate was faster than 10°C/min, and the particle size increased with an increase in the cooling rate to 100°C/min (Ziegler et al., 2005). When the sample was heated by using an autoclave parr reactor, the cooling rate was not constant. When the sample was cooled from 180°C to 100°C, the average cooling rate was about 20°C/min. However, it took

approximately 45 min to cool the sample from 100°C to 25°C. Three temperatures, 170°C, 180°C, and 190°C were used to investigate the effects of the heating temperature on the formation of spherulites in the parr reactor.

Effects of crystallization temperature on yield

When the DB-HAMS was heated to170°C, spherulites were not formed (Figure A.1). Although spherulites were formed when the starch was heated to 190°C, the crystallized material was brown. As a result, the debranched high-amylose starch was used to form spherulites in the pressure reactor by heating to 180°C. The yield of spherulites was dependent on the crystallization temperature (**Error! Reference source not found.**). When the formation temperature was lower than 150°C, the yields were higher than 90%. When the formation temperature was 150°C, the yield dramatically dropped to 33.5%. In our previous studies (Cai et al., 2010; Cai & Shi, 2013; Shi et al., 2021), the yields were low when short-chain amylose was crystallized at a high temperature (50°C or 60°C). When a further cooling to 25°C was applied, the yields of spherulites were increased (Cai & Shi, 2013, Shi et al., 2021), since cooling enhanced the crystallization. In this study, the yields of samples held at 25~120°C were higher than 90%. When the sample was held at 150°C, the starch was highly degraded, and the product was brown. As a result, the yields of spherulites decreased.

The spherulites crystallized at 25°C were selected to plot the curve of yields. After 1 h, the temperature was cooled to 25°C, and the yield was approximately 80%. After that, the yield increased slowly, and the yield curve was almost a straight line (Figure 3.2). The yield

increased to 92.5% after 24 h. The yield curve was fitted to the equation $y = 4.4041 \times \ln(x) + 78.677$, where the x was the crystallization time (h), and y was the yield.

A yield curve of debranched waxy maize starch was reported in our previous study (Shi et al., 2018). Compared to the DB-HAMS, the yield increased more slowly when debranched waxy maize starch crystallized. After 4 h, the yield of crystallized debranched waxy maize starch was approximately 78% and then the yield increased as a straight line. After 24 h, the yield of debranched waxy maize starch was approximately 87% (Shi et al., 2018). DB-HAMS contained longer linear molecules; therefore, the crystallization was faster and yield after 24 h was higher (92.5%).

Molecular size distribution

Molecular size distribution was measured by a gel permeation chromatograph (GPC). After debranching, three peaks were observed, and the largest molecules were approximately DP 1000 (Figure 3.3). When spherulites were formed by the DB-HAMS, the molecular size was reduced during the formation. The formed spherulites showed a smaller DP (DP <800), and the distribution was influenced by the crystallization temperature (Figure 3.3). The spherulites formed at 25, 50, 70, 90, and 120°C showed peaks around DP 60 and a shoulder around DP 30. Higher crystallization temperatures or a longer heating time could cause more heating damage. When the crystallization temperature was 150°C, the samples were more degraded. As a result, the spherulites formed at 150°C with shorter molecules (DP <150), and showed two peaks at DP 30 and 60, respectively.

High yields indicated that most materials were involved in the formation of spherulites. However, the molecules forming spherulites were smaller than the debranched high-amylose starch. High temperature degraded the starch molecules, but the molecular chain length was still long enough to form spherulites. When samples were held at 150°C, the degradation was severe, and the peak of DP distribution was reduced from DP 60 to DP 30. Consequently, the yield of spherulites was reduced.

According to Ziegler (2020), positive spherulites were formed by the molecule sizes of DP 120 and DP 642. In our previous study (Shi et al., 2021), the debranched waxy maize starch could form positive and negative spherulites, the molecule sizes were between DP 6 and DP 60, and they showed a peak around DP 15. In this study, when the formation temperature was lower than 150°C, the molecules involved in spherulites formation showed a wide DP range, and the peaks appeared around DP 60. By observing them under a light microscopy, these spherulites showed positive birefringence. When the formation temperature was 150°C, the highest peak appeared at DP 30, and negative spherulites were formed (Figure 3.3). This result agrees with the work of Ziegler (2020) and Shi et al. (2021). When chain length was long (DP >60), positive spherulites were more easily formed.

Morphology and birefringence

When a parr reactor was used, most samples clearly showed positive birefringence (Table 3.1 and Figure 3.4), except for the sample held at 150°C. When DB-HAMS was held at 150°C, although the morphology under the normal light was not dramatically changed, the

orientation of the Maltese cross was different and negative spherulites were formed (Figure 3.4).

Particle size was also influenced by the crystallization temperature. When the crystallization temperature was 25°C or 50°C, the average diameter of spherulites measured by a particle size analyzer was around 33~34 μm; when it was 70°C or 90°C, the diameter was increased to around 55 μm; and when the crystallization temperature was higher than 120°C, the diameter was between 40 and 50 μm (Table 3.1). This result was also reflected in Figure 3.4. When the crystallization temperatures were 25°C or 50°C, the spherical particles were uniform (around 20 μm under the microscope); when the crystallization temperature was 70°C or 90°C, the particle sizes of most spherulites were larger than 20 μm, but a few smaller particles were also observed; when the crystallization temperature was higher than 120°C, more small particles (<20 μm) were observed.

The average diameter of spherulites measured by a particle size analyzer was affected by two factors: the aggregation of particles and the diameter of a single spherulite. When viewed under the microscope, the aggregation of spherulites was also noted (Figure 3.4), which may increase the measured diameter by the particle size analyzer. When preparing the microscopy slides, shaking, or sonicating was conducted to disperse the spherulites better, but the aggregation persisted. It is possible that two different spherulites were formed during crystallization and then these two spherulites were aggregated. The solid concentration was 25% in this study. Some spherulites seemed to adhere to each other during formation. The average diameter of spherulites observed by the particle size analyzer was larger than the diameter that was observed by a light microscopy.

The influence of amylose content on the formation of spherulites has been reported (Ma et al., 2011; Nordmark and Ziegler, 2002b; Ziegler et al., 2003). Compared to the spherulites formed in previous studies (Nordmark and Ziegler, 2002a; Ziegler, 2020; Ziegler et al., 2003), the Maltese cross of spherulites in this study was as obvious and uniform as the one formed by isolated amylose, and better than those formed by native high-amylose maize starch. Our results suggested that DB-HAMS was a suitable material for the formation of spherulites. After debranching, more linear chains were produced. When spherulites were formed at a higher temperature, some molecules were degraded by heat. Crystallization temperature and chain length can influence morphology. When the formation temperature was 150°C, the chain length was reduced as described above (Figure 3.2), and negative spherulites were formed.

Crystalline structure

All spherulites had a B-type crystalline pattern (Figure 3.5). The degree of crystallinity decreased with an increase in crystallization temperature. When the crystallization temperature was increased from 25°C to 120°C, the degree of crystallinity decreased from 83.5% to 74.6%. When the crystallization temperature was 150°C, the degree of crystallinity dropped to 58.8% (Table 3.1). The crystalline structure of starch crystallites depended on the degree of polymerization, the crystallization temperature, and the solid concentration (Buléon et al., 2007; Jane, 2004; Gidley & Bulpin, 1987). In our previous studies on debranched waxy maize starch (Cai & Shi, 2013, 2014; Shi et al., 2021), when the solid concentration was 25%, and the crystallization temperature was 25°C, B-type

spherulites were formed. After increasing the formation temperature to 50°C, A-type crystallites were formed. Meanwhile, two steps of cooling were also used to form the A-type crystalline structure, since A-type crystallites were formed at a high temperature, and the further crystallization resulted in the A-type crystalline structure. However, when the spherulites were formed by 25% solid concentration of DB-HAMS in this study, a higher crystallization temperature did not change the type of crystallites, since the molecular chain length was longer than that of debranched waxy maize starch, which always resulted in a B-type crystalline structure. Cai and Shi (2014) compared the crystals formed by debranched waxy maize and debranched waxy potato starches. When the formation temperature was 50℃, debranched waxy potato starch formed B-type crystalline structures, since the average DP was 32, which was longer than that of debranched waxy maize starch (average DP = 24). Compared to Cai and Shi's work (2014), debranched high-amylose starch contained more long molecules (DP > 60), and A-type crystallites were not formed even when DHAMS was crystallized at 150°C. In our previous study (Shi et al., 2021), a high crystallization temperature (50°C) produced A-type spherulites with short-chain amylose. Shamai et al. (2003) used high-amylose maize starch (about 70% amylose) to produce resistant starch by re-crystallization. A mixture of B- and A- type crystalline structures was observed when the high-amylose maize starch was crystallized at 95°C, although the product was not a spherulite. However, no spherulites with an A-type crystalline structure were formed in this study even though crystallization was performed at high temperatures. It seems that it is difficult to form spherulites with an A-type crystalline structure from the debranched high-

amylose maize starch (mostly long chains). In general, the B-type crystalline structure is favored by long chains (Cai et al., 2012; Gidley & Bulpin, 1987).

Small angle neutron scattering (SANS)

When the intensity and q were used to plot the curve, a peak was detected between 0.023 and 0.14 $Å^{-1}$. By plotting the curve using $I \times q^{22}$ vs. q, where I was the intensity, the peak was enhanced and detected at 0.06 $Å^{-1}$ (Figure 3.6). Using equation $L = 2\pi/q$ to estimate the long period L, the peak appeared between 4.6 and 27.1 nm with a peak at 10.47 nm. Compared with the native high-amylose maize starch (Mao et al., 2023), this peak from the spherulites was much broader and weaker, suggesting that at the nanoscale, the repeating ordered structure (long periods) had a great variation in size, but the debranched chains are oriented well toward the surface of the spherulites, giving strong birefringence with a Maltese cross.

Thermal properties

The native high-amylose maize starch started to gelatinize at 68.9°C and the conclusion temperature (T_c) was 113.4°C (Table 3.2). After debranching and formation of spherulites, the melting peak of most samples shifted to higher temperatures, except for the sample formed at 150°C. When sample was formed between 25°C and 120°C, the onset temperatures (T_o) increased to 70~85°C, and the peak temperatures (T_p) were 106~116°C. The enthalpy was also increased from 24 J/g to 32~41 J/g. When the crystallization temperature was increased to 150°C, the melting peak shifted to a lower temperature (T_o: 51.5°C; T_p: 86.1°C; T_c: 102.8°C), but the enthalpy was high (38.3 J/g).

Gelatinization was the process of starch granules swelling and the crystallites melting. Unlike starch granules, spherulites in this study were crystallized by DB-HAMS and showed a high degree of crystallinity, which increased the enthalpy (ΔH) (Lopez-Rubio et al., 2008). At 150°C the degree of polymerization was dramatically reduced (Figure 3.3), causing the development of smaller crystals with a broad size distribution and poor perfection, which was attributed to the observed lower melting temperature and broader melting of crystallites.

Structure of spherulites revealed by iodine staining

Based on the type of birefringence sign, the spherulite formed at 25°C was selected as a model positive spherulite sample; and the spherulite with 25% solid content and formed at 150°C followed by cooling to 25°C was selected as a model negative spherulite sample. Both spherulites and native high-amylose maize starch were stained by an iodine solution, and the results were shown in **Error! Reference source not found.**. Native high-amylose maize s tarch contained spherical, elongated, and aggregated granules. After iodine staining, those granules were dark under normal light, and Maltese crosses were observed by applying polarized light. When a full wavelength waveplate was attached, the Maltese crosses were less obvious since the granules were dark. Compared to the native high-amylose maize starch, both spherulites were larger. After staining, positive spherulites showed purple color under a normal light. The stained level was heterogeneous, some granules were darker than others. Under a polarized light, two types of Maltese cross were observed. The darker particles under normal light also showed a purple Maltese cross. The lighter particles under normal light showed a Maltese cross with bright parts and purple parts. For negative

spherulites, which had a short chain length (Figure 2), the Maltese crosses were brighter under polarized light, and more pink parts appeared at the edge of the Maltese cross.

It is known that the iodine staining of starch is influenced by (1) iodine solution concentration, (2) amylose content, (3) the chain length, and (4) the crystalline structure (Bailey & Whelan, 1961; Bates et al., 1943; Bradbury & Bello, 1993). Evans et al. (2003) stained high-amylose starch with iodine solutions of different I_2 concentrations (0.02% – 0.075%). When I_2 concentration was lower than 0.04%, high-amylose starch granules were less stained; when I_2 concentration was higher than 0.04%, high-amylose starch granules were stained to be dark blue, but the birefringence was less bright due to the dark stain. As a result, Cai et al. (2014) also used an iodine solution of 0.04% I_2 to stain high-amylose starch, and spherical, elongated, and aggregated granules were observed. Based on Figure 4.1, native high-amylose starch had the largest molecular size. When spherulites were formed at 25°C with 25% concentration of debranched high-amylose starch, the peak was at DP 60, which was smaller than that of the amylose peak of native high-amylose starch. When spherulites were formed at 150°C, the molecular size was further reduced. Based on Figure 5, both spherulites showed the same type of crystalline structure. Therefore, the iodine staining should be mainly influenced by the chain length. Bailey and Whelan (1961) used iodine solution to stain amylose of different degrees of polymerization (DP). When the DP was smaller than 30, the stained amylose was red. When the DP of amylose was larger than 45, the staining color was blue. When the DP was between 30 and 45, the color was purple. Degrees of polymerization explained the stained color in this study. Under the polarized light, the center of a positive spherulite could be bright, and the edge could be purple. The negative

spherulites showed a bright center under the polarized light, and some spherulites also showed purple on the edge. This phenomenon revealed that shorter chains were crystallized at the initial stage and located in the center parts of the spherulites. Longer chains were located on the edge of the spherulites, and the long-chain amylose content was higher in positive spherulites.

Digestion

The resistant starch (RS) contents of the spherulites were all higher than 89%, except the samples formed at 150°C, which contained 47.9% RS content (Table 3.3). When samples were formed at 25°C and 50°C, the RS contents were 91.9% and 89.3%, respectively. And their rapidly digested starch (RDS) contents were less than 7%. When the formation temperature was 70°C ~ 120°C, the RS contents were higher than 94%, and the RDS contents were lower than 4%. When the formation temperature was 150°C, the RS content was reduced to 47.9% and the RDS content was 22.5% (Table 3.3).

In addition to the digestion time of 20 min and 120 min, the digested starch was also measured after digestion times of 40, 60, 80, and 240 min. The digested starch contents at different time points were used to plot the digestion curve (Figure 3.8). When samples were formed at 70°C, 90°C, and 120°C, the digestion curves were overlapped and almost linear. When the formation temperature was 25°C and 50°C, the digestion curves were separated, and the digestion rate was increased to between 80 min and 120 min of digestion time. When the formation temperature was 150°C, the digested starch content after 20 min was higher

than other spherulites digested for 240 min, and the digestion rate was increased more between 60 min and 80 min of digestion.

Positive spherulites showed similar digestion pattern, and the sample formed at 25°C was used to investigate the spherulites' digestion by observing the digested sample under a microscope (Figure 3.9). Before the digestion, the spherulites were spherical and showed the positive Maltese cross. After 20 min of digestion, although some particles were still around 20 μm and the positive birefringence was clear, smaller particles and fragments were observed too. With the longer digestion time, more fragments may be observed after 60 min of digestion, and these fragments barely showed birefringence. It may be due to the digestion of fragments, so that the digestion rate was increased. After 240 min of digestion, the fragments were small particles showing no birefringence. Meanwhile, most residues were not as spherical as they were before digestion, and the size was reduced to a smaller diameter (approximately 10 μm). Positive birefringence was clearly observed after 240 min of digestion.

Based on the morphology of the digested samples, it seems that the surfaces of the spherulites were digested first, then the enzymes could move into the particles. Consequently, those particles were digested into fragments. If the enzyme was not able to move into the particles, the enzyme only digested the outer layer, so that the birefringence sign was still observed. Ziegler (2020) used amylose with molecule sizes of DP 120 and DP 642 to produce spherulites in a pressure vessel. The solid concentration was 11% and spherulites were formed by cooling the pressure vessel from 180°C to 10°C in an ice-water slush. The spherulites formed by amylose molecule sizes of DP 120 and DP 642 were digested by

AOAC method 2002.02, and the RS content was 61.7 and 36.6%, respectively. In contrast to Englyst's method, the enzyme hydrolysis duration was 16 h in AOAC method 2002.02. As a result, more spherulites were digested.

In this study, α-amylase was stained, and digested samples were observed under a scanning laser confocal microscope. The spherulites were formed by cooling the sample to 25°C directly, and were digested by α-amylase for 0, 30, 60, and 120 min. At 0 min, the α-amylase was added to samples placed in an ice bath. Spherical particles were observed during the digestion, and the green parts indicated the α-amylase location. The α-amylase was not able to penetrate the inside of spherulites (Figure 3.10), indicating that the spherulites were compact. Little enzyme was detected on the spherulites at 0 min, and then the enzyme was always located on the outer surface of the particles with a longer digestion time. However, the morphology of the spherulites was not changed. In the 3D images, it was clear that there was no enzyme inside the spherulites. As a result, the spherulites were highly resistant to α-amylase hydrolysis, and the particle size was not clearly reduced (Figure 3.10).

Conclusions

Both positive and negative spherulites were produced from DB-HAMS. When the solid concentration was 25%, the high quality positive spherulites and medium quality negative spherulites were formed, and they showed B-type allomorphs. During the formation of spherulites, the molecules were degraded due to the heating, and the degradation increased with increasing temperatures. Since the chain length of amylose was long, the spherulites mostly had positive birefringence. However, when the formation temperature was 150°C, the

chain length became short (DP < 150) and negative spherulites could be formed. Since the chain length was shorter in spherulites, the color of iodine staining was lighter than that of native high-amylose starch. The negative spherulites showed a lower degree of crystallinity and resistance to enzyme digestion. But all the positive spherulites had a high level of resistant starch (89% ~ 94%). The confocal laser scanning microscopy images and the light microscopy images revealed that the enzyme hydrolyzed the surface of each spherulite particle first, and then the spherulites were gradually digested from the outside to inside.

Acknowledgements

The project is supported by the U.S. Department of Agriculture National Institute of Food and Agriculture (Award No. 2018-67017-27562). This is contribution no. 23-255-J from the Kansas Agricultural Experiment Station. The authors also thank the College of Veterinary Medicine Core Facilities from Kansas State University for their help on confocal microscopy.

Reference

Bailey, J. M., & Whelan, W. J. (1961). Physical properties of starch. *Journal of Biological Chemistry*, *236*(4), 969–973.

Bates, F. L., French, D., & Rundle, R. E. (1943). Amylose and amylopectin content of starches determined by their iodine complex formation. *Journal of the American Chemical Society*, *65*(2), 142–148.

Bhattarai, R. R., Dhital, S., & Gidley, M. J. (2016). Interactions among macronutrients in wheat flour determine their enzymic susceptibility. *Food Hydrocolloids*, 61, 415–425.

Bradbury, A. G. W., & Bello, A. B. (1993). Determination of molecular size distribution of starch and debranched starch by a single procedure using high-performance size-exclusion chromatography. *Cereal Chemistry*, *70*, 543–547.

Brewer, L. R., Cai, L., & Shi, Y.-C. (2012). Mechanism and Enzymatic Contribution to In Vitro Test Method of Digestion for Maize Starches Differing in Amylose Content. *Journal of Agricultural and Food Chemistry*, *60*(17), 4379–4387.

Buléon, A., Véronèse, G., & Putaux, J.-L. (2007). Self-association and crystallization of amylose. *Australian Journal of Chemistry*, *60*(10), 706–718.

Cai, L., Bai, Y., & Shi, Y.-C. (2012). Study on melting and crystallization of short-linear chains from debranched waxy starches by in situ synchrotron wide-angle X-ray diffraction. *Journal of Cereal Science*, *55*(3), 373–379.

Cai, C., Zhao, L., Huang, J., Chen, Y., & Wei, C. (2014). Morphology, structure and gelatinization properties of heterogeneous starch granules from high-amylose maize. *Carbohydrate Polymers*, *102*, 606–614.

Cai, L., & Shi, Y. C. (2013). Self-assembly of short linear chains to A- and B-type starch spherulites and their enzymatic digestibility. *Journal of Agricultural and Food Chemistry*, *61*, 10787–10797.

Cai, L., & Shi, Y.-C. (2010). Structure and digestibility of crystalline short-chain amylose from debranched waxy wheat, waxy maize, and waxy potato starches. *Carbohydrate Polymers*, *79*(4), 1117–1123.

Cai, L., & Shi, Y.-C. (2014). Preparation, structure, and digestibility of crystalline A- and B-type aggregates from debranched waxy starches. *Carbohydrate Polymers*, *105*, 341–350.

Cai, L., Shi, Y.-C., Rong, L., & Hsiao, B. S. (2010). Debranching and crystallization of waxy maize starch in relation to enzyme digestibility. *Carbohydrate Polymers*, *81*(2), 385–393.

Chakraborty, I., Govindaraju, I., Rongpipi, S., Mahato, K. K., & Mazumder, N. (2021). Effects of hydrothermal treatments on physicochemical properties and in vitro digestion of starch. Food Biophysics, 16(4), 544–554.

Creek, J. A., Ziegler, G. R., & Runt, J. (2006). Amylose Crystallization from Concentrated Aqueous Solution. *Biomacromolecules*, *7*(3), 761–770.

Crist, B., & Schultz, J. M. (2016). Polymer spherulites: A critical review. *Progress in Polymer Science*, *56*, 1–63.

Dhital, S., Warren, F. J., Zhang, B., & Gidley, M. J. (2014). Amylase binding to starch granules under hydrolysing and non-hydrolysing conditions. *Carbohydrate Polymers*, 113(0), 97-107.

Dingler, C., Dirnberger, K., & Ludwigs, S. (2019). Semiconducting polymer spherulites-from fundamentals to polymer electronics. *Macromolecular Rapid Communications*, *40*(1), 1800601.

Evans, A., McNish, N., & Thompson, D. B. (2003). Polarization colors of lightly iodine-stained maize starches for amylose-extender and related genotypes in the W64A inbred line. *Starch – Stärke*, *55*(6), 250–257.

Fanta, G. F., Felker, F. C., & Shogren, R. L. (2002). Formation of crystalline aggregates in slowly-cooled starch solutions prepared by steam jet cooking. *Carbohydrate Polymers*, *48*(2), 161–170.

Fanta, G. F., Felker, F. C., Shogren, R. L., & Salch, J. H. (2008). Preparation of spherulites from jet cooked mixtures of high amylose starch and fatty acids. Effect of preparative conditions on spherulite morphology and yield. *Carbohydrate Polymers*, *71*(2), 253–262.

Fanta, G. F., Kenar, J. A., Byars, J. A., Felker, F. C., & Shogren, R. L. (2010). Properties of aqueous dispersions of amylose–sodium palmitate complexes prepared by steam jet cooking. *Carbohydrate Polymers*, *81*(3), 645–651.

Fanta, G. F., Kenar, J. A., & Felker, F. C. (2013). Preparation and properties of amylose complexes prepared from hexadecylamine and its hydrochloride salt. *Carbohydrate Polymers*, *98*(1), 555–561.

Fanta, G., Felker, F., Shogren, R., & Salch, J. (2006). Effect of fatty acid structure on the morphology of spherulites formed from jet cooked mixtures of fatty acids and defatted cornstarch. *Carbohydrate Polymers*, *66*(1), 60–70.

Felker, F. C., Kenar, J. A., Fanta, G. F., & Biswas, A. (2013). Comparison of microwave processing and excess steam jet cooking for spherulite production from amylose-fatty acid inclusion complexes. *Starch – Stärke*, *65*(9–10), 864–874.

Gibson, T. S., Solah, V. A., & McCleary, B. V. (1997). A Procedure to Measure Amylose in Cereal Starches and Flours with Concanavalin A. *Journal of Cereal Science*, *25*(2), 111–119. https://doi.org/10.1006/jcrs.1996.0086

Gidley, M. J., & Bulpin, P. V. (1987). Crystallization of malto-oligosaccharides as models of the crystalline forms of starch: minimum chain-length requirement for the formation of double helices. *Carbohydrate Research*, *161*, 291–300

Gránásy, L., Pusztai, T., Tegze, G., Warren, J. A., & Douglas, J. F. (2005). The growth and form of spherulites. *Phys Rev E Stat Nonlin Soft Matter Phys.* 72 (1 Pt 1) 011605. https://doi.org/10.1103/PhysRevE.72.011605.

Helbert, W., Chanzy, H., Planchot, V., Buléon, A., & Colonna, P. (1993). Morphological and structural features of amylose spherocrystals of A-type. *International Journal of Biological Macromolecules*, *15*(3), 183–187.

Htoon, A., Shrestha, A. K., Flanagan, B. M., Lopez-Rubio, A., Bird, A. R., Gilbert, E. P., & Gidley, M. J. (2009). Effects of processing high amylose maize starches under controlled conditions on structural organization and amylase digestibility. *Carbohydrate Polymers*, *75*(2), 236–245.

Kiatponglarp, W., Rugmai, S., Rolland-Sabaté, A., Buléon, A., & Tongta, S. (2016). Spherulitic self-assembly of debranched starch from aqueous solution and its effect on enzyme digestibility. *Food Hydrocolloids*, *55*, 235–243.

Kline, S. R. (2006). Reduction and Analysis of SANS and USANS Data Using IGOR Pro. *J. Appl. Crystallogr.*, *39* (6), 895–900.

Kobayashi, S., Hobson, L. J., Sakamoto, J., Kimura, S., Sugiyama, J., Imai, T., & Itoh, T. (2000). Formation and structure of artificial cellulose spherulites via enzymatic polymerization. *Biomacromolecules*, *1*(2), 168–173.

Komiya, T., & Nara, S. (1986). Changes in crystallinity and gelatinization phenomena of potato starch by acid treatment. *Starch - Stärke*, *38*, 9–13.

Lin, J.-H., Wang, S.-W., & Chang, Y.-H. (2008). Effect of molecular size on gelatinization thermal properties before and after annealing of rice starch with different amylose contents. *Food Hydrocolloids, 22,* 156-163.

Lopez-Rubio, A., Flanagan, B. M., Gilbert, E. P., & Gidley, M. J. (2008). A novel approach for calculating starch crystallinity and its correlation with double helix content: A combined XRD and NMR study. *Biopolymers*, *89*(9), 761–768.

Ma, U. V. L., Floros, J. D., & Ziegler, G. R. (2011). Effect of starch fractions on spherulite formation and microstructure. *Carbohydrate Polymers*, *83*(4), 1757–1765.

Mao, Y., Shi, J., Cai, L., Hwang, W., and Shi, Y.-C. (2023). Microstructures of starch granules with different amylose contents and allomorphs as revealed by scattering techniques. *Biomacromolecules*. 10.1021/acs.biomac.2c01240.

Nordmark, T. S., & Ziegler, G. R. (2002a). Spherulitic crystallization of gelatinized maize starch and its fractions. *Carbohydrate Polymers*, *49*(4), 439–448.

Nordmark, T. S., & Ziegler, G. R. (2002b). Structural features of non-granular spherulitic maize starch. *Carbohydrate Research*, *337*(16), 1467–1475.

Ring, S. G., Miles, M. J., Morris, V. J., Turner, R., & Colonna, P. (1987). Spherulitic crystallization of short chain amylose. *International Journal of Biological Macromolecules*, *9*(3), 158–160.

Shamai, K., Bianco-Peled, H., & Shimoni, E. (2003). Polymorphism of resistant starch type III. *Carbohydrate Polymers*, 54(3), 363–369.

Shang, Y., Chao, C., Yu, J., Copeland, L., Wang, S., & Wang, S. (2018). Starch spherulites prepared by a combination of enzymatic and acid hydrolysis of normal corn starch. *Journal of Agricultural and Food Chemistry*, *66*(25), 6357–6363.

Shi, J., Sweedman, M. C., & Shi, Y.-C. (2018). Structural changes and digestibility of waxy maize starch debranched by different levels of pullulanase. *Carbohydrate Polymers*, *194*, 350–356.

Shi, J., Sweedman, M. C., & Shi, Y.-C. (2021). Structure, birefringence and digestibility of spherulites produced from debranched waxy maize starch. *International Journal of Biological Macromolecules*, *183*, 1486–1494.

Shi, Y.-C., Capitani, T., Trzasko, P., & Jeffcoat, R. 1998. Molecular structure of a low-amylopectin starch and other high-amylose maize starches. *J. Cereal Sci.* 27:289-299.

Shtukenberg, A. G., Punin, Y. O., Gunn, E., & Kahr, B. (2012). Spherulites. *Chemical Reviews*, *112*(3), 1805–1838.

Singh, J., Kaur, L., & McCarthy, O. J. (2007). Factors influencing the physico-chemical, morphological, thermal and rheological properties of some chemically modified starches for food applications—A review. *Food Hydrocolloids, 21*, 1–22.

Singh, J., Lelane, C., Stewart, R. B., & Singh, H. (2010). Formation of starch spherulites: Role of amylose content and thermal events. *Food Chemistry*, *121*(4), 980–989.

Vilaplana, F., & Gilbert, R. G. (2010). Characterization of branched polysaccharides using multiple-detection size separation techniques: Liquid Chromatography. *Journal of Separation Science*, *33*(22), 3537–3554.

Wang, C., Chen, C.-C., Cheng, Y.-W., Liao, W.-P., & Wang, M.-L. (2002). Simultaneous presence of positive and negative spherulites in syndiotactic polystyrene and its blends with atactic polystyrene. *Polymer*, *43*(19), 5271–5279.

Whittam, M. A., Noel, T. R., & Ring, S. G. (1990). Melting behaviour of A- and B-type crystalline starch. *International Journal of Biological Macromolecules*, *12*(6), 359–362.

Ziegler, G. R. (2020). Enzyme-resistant starch spherulites. *Starch/Staerke*, 72, [1900217].

Ziegler, G. R., Creek, J. A., & Runt, J. (2005). Spherulitic crystallization in starch as a model for starch granule initiation. *Biomacromolecules*, *6*(3), 1547–1554.

Ziegler, G. R., Nordmark, T. S., & Woodling, S. E. (2003). Spherulitic crystallization of starch: Influence of botanical origin and extent of thermal treatment. *Food Hydrocolloids*, *17*(4), 487–494.

Table 3.1 Yield, crystalline type, degree of crystallinity, birefringence sign and size of the spherulites formed at different temperatures.

Crystallization temperature (°C)	Yields (%)	Crystalline type	Degree of crystallinity (%)	Birefringence sign (quality)*	Average diameter (μm)
25	92.5±0.2[a]	B	83.5±0.8[a]	Positive (good)	34.7±1.4[c]
50–25	91.8±0.4[a]	B	81.4±0.2[a]	Positive (good)	33.3±2.0[c]
70–25	92.8±0.3[a]	B	80.5±0.9[a]	Positive (good)	54.3±2.2[a]
90–25	92.8±0.2[a]	B	76.7±1.2[b]	Positive (good)	55.6±2.2[a]
120–25	90.1±0.4[b]	B	74.6±0.9[b]	Positive (good)	43.2±0.9[b]
150–25	33.5±0.5[c]	B	58.8±1.8[c]	Negative (medium)	47.6±0.2[b]

Values within columns bearing the same small letter superscript(s) do not significantly differ at $p < 0.05$.

*The quality was rated by the observed Maltese cross. “Good” quality indicated well developed Maltese cross. “Medium” quality indicated Maltese cross was observed, but some particles did not show Maltese cross.

Table 3.2 Thermal properties of high-amylose maize starch and spherulites formed at different temperatures

Sample	T_o (°C)	T_p (°C)	T_c (°C)	ΔH (J/g)
High-amylose starch	68.9±1.0^{f}	88.6±0.7^{d}	113.4±0.4^{d}	24.4±0.2^{e}
Crystallization Temperature (°C)				
25	71.1±1.0^{e}	107.4±0.0^{c}	127.8±0.5^{c}	31.9±0.6^{d}
50–25	84.5±0.5^{a}	115.2±0.4^{a}	134.4±1.1^{b}	39.2±0.5^{b}
70–25	79.7±0.4^{c}	110.7±0.1^{b}	127.3±0.7^{c}	35.6±0.4^{c}
90–25	77.2±1.0^{d}	106.5±1.0^{c}	128.1±0.8^{c}	32.0±0.5^{d}
120–25	82.4±0.6^{b}	116.5±0.1^{a}	137.0±1.1^{a}	41.4±1.0^{a}
150–25	51.5±0.5^{g}	86.1±0.5^{e}	102.8±0.5^{e}	38.3±1.2^{bc}

Values within columns bearing the same small letter superscript(s) do not significantly differ at $p < 0.05$.

Table 3.3 Degree of crystallinity (%) of samples formed in ethanol at 4°C (ES4), in water at 4°C (WS4), in water at 50°C (WS50) and in water from 50°C to 4°C (WS50-4), respectively. Rapidly digestible starch (RDS), slowly digestible starch (SDS) and resistant starch (RS) content of high-amylose maize starch (HAMS) and spherulites formed at 25% solid concentration, and different crystallization temperatures.

Samples	RDS (%)	SDS (%)	RS (%)
HAMS	19.0±0.1^{b}	18.7±1.1^{b}	62.3±1.0^{d}
Spherulites			
Crystallization temperature (°C)			
25	4.5±0.4^{d}	3.6±0.1^{d}	91.9±0.3^{b}
50–25	6.1±0.3^{c}	4.6±0.1^{c}	89.3±0.4^{c}
70–25	3.7±0.0^{e}	2.1±0.4^{e}	94.2±0.4^{a}
90–25	3.8±0.0^{e}	1.4±0.3^{f}	94.8±0.3^{a}
120–25	3.7±0.0^{e}	1.5±0.3^{f}	94.8±0.3^{a}
150–25	22.5±0.2^{a}	29.6±0.2^{a}	47.9±0.0^{e}

Values within columns bearing the same small letter superscript(s) do not significantly differ at $p < 0.05$.

Normal light Polarized light Polarized light with a waveplate

High-amylose maize starch

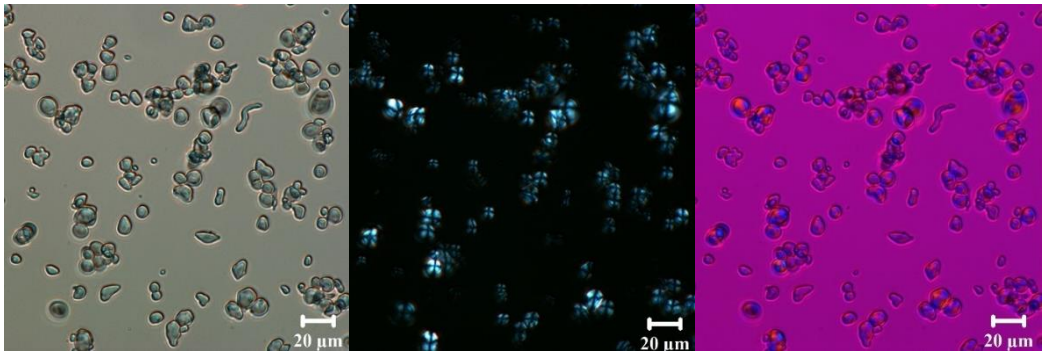

Heat to 160°C, Cooling rate: 25°C/min

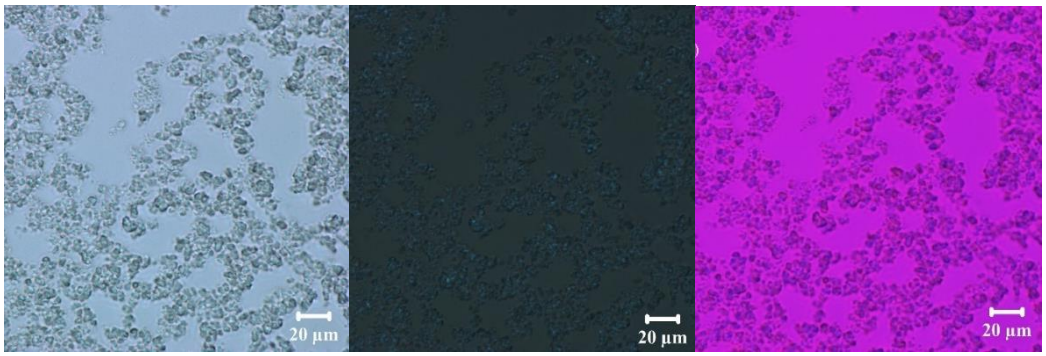

Heat to 160°C, Cooling rate: 50°C/min

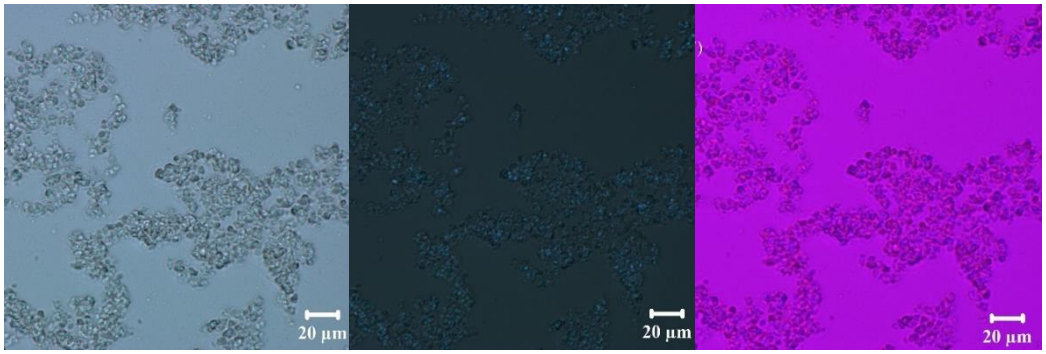

Heat to 160°C, Cooling rate: 100°C/min

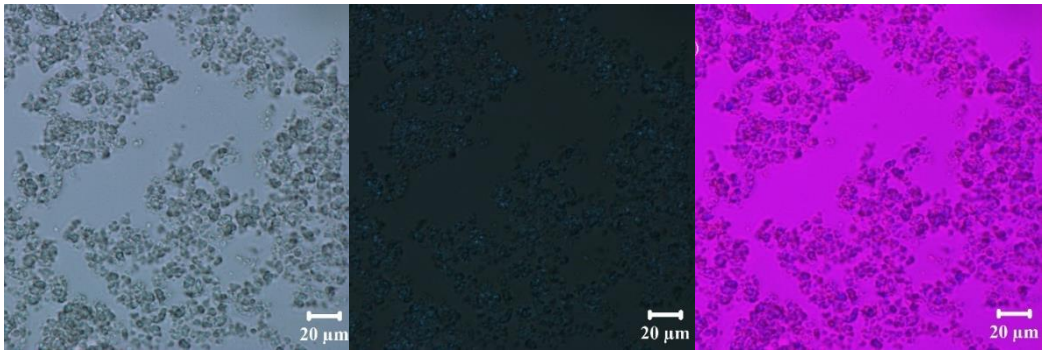

Heat to 170°C, Cooling rate: 25°C/min

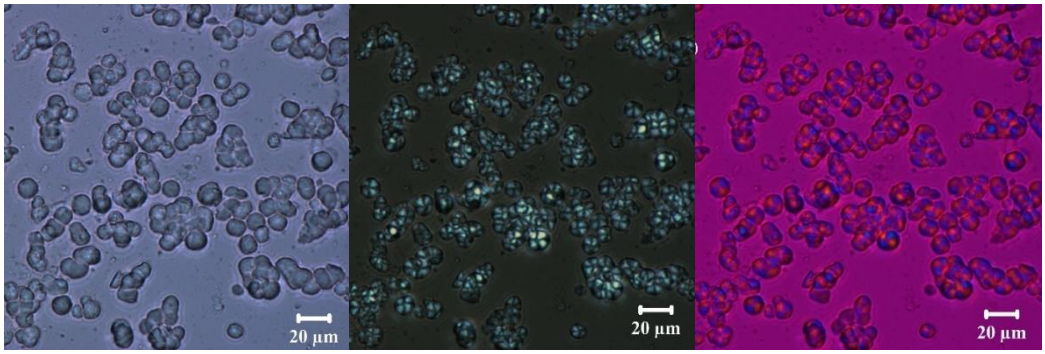

Heat to 170°C, Cooling rate: 50°C/min

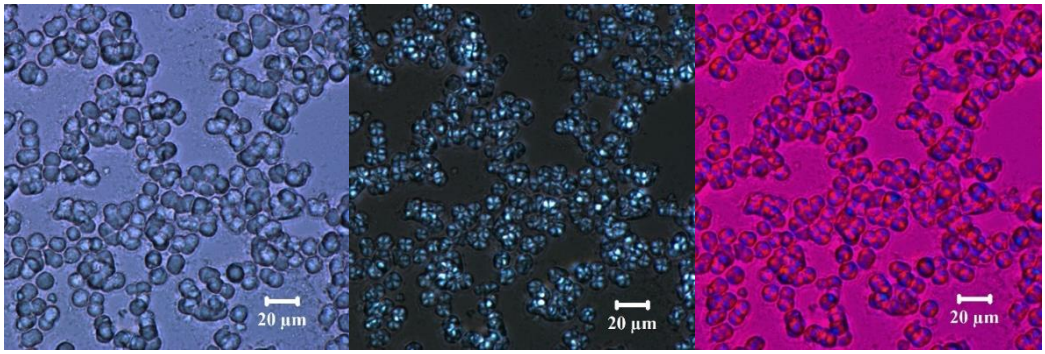

Heat to 170°C, Cooling rate: 100°C/min

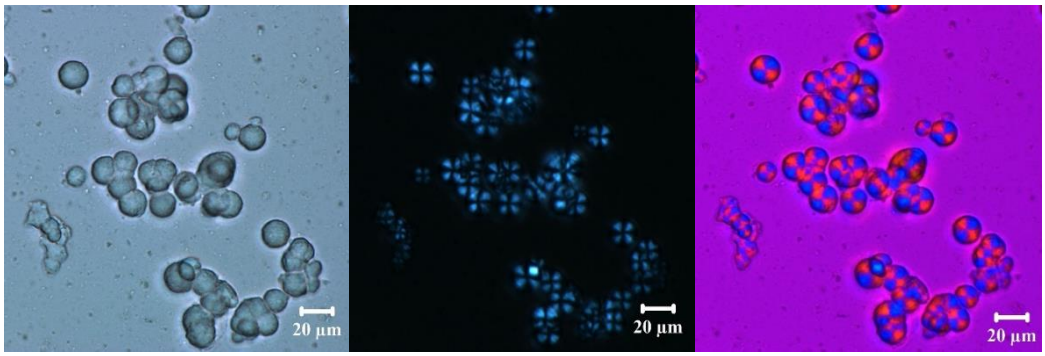

Heat to 180°C, Cooling rate: 25°C/min

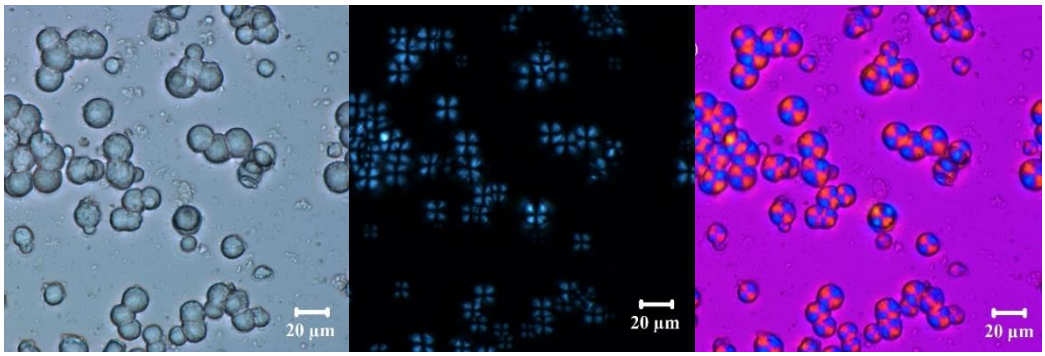

Heat to 180°C, Cooling rate: 50°C/min

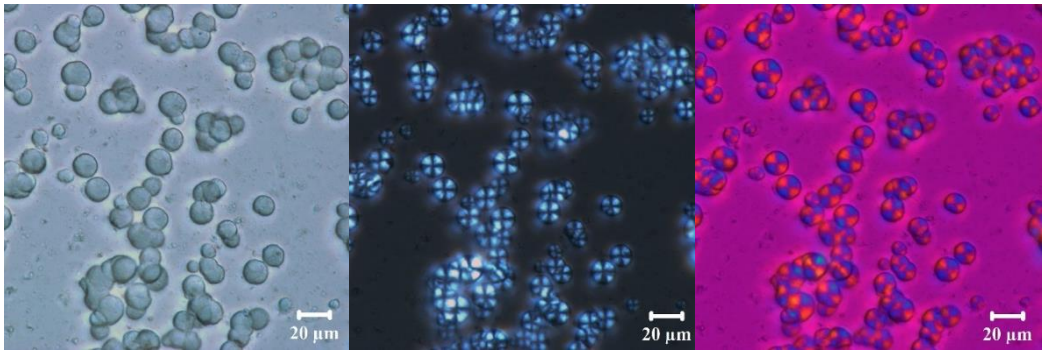

Heat to 180°C, Cooling rate: 100°C/min

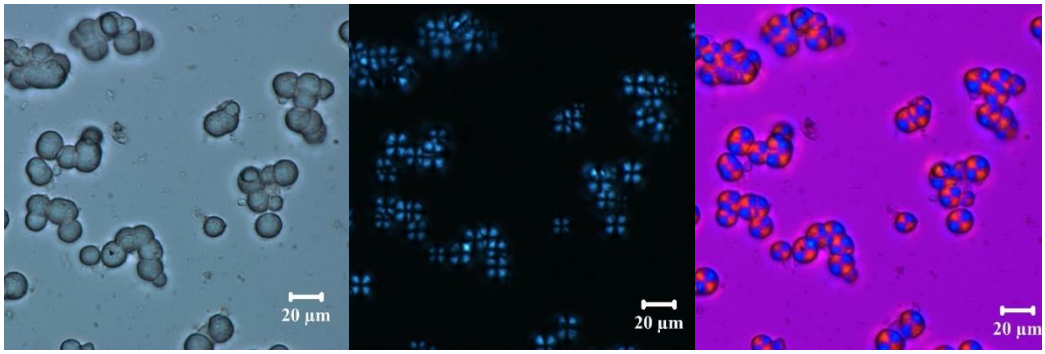

Figure 3.1 Morphology of high-amylose starch and spherulites formed by debranched high-amylose starch in a differential scanning calorimetry (DSC) pan. The solid concentration was 25%, and three cooling rates: 25°C/min, 50°C/min, and 100°C/min were applied. The debranched material was heated to 160°C, 170°C, and 180°C. Bright field images under normal light, images under polarized light, and the images under polarized light with a waveplate were recorded.

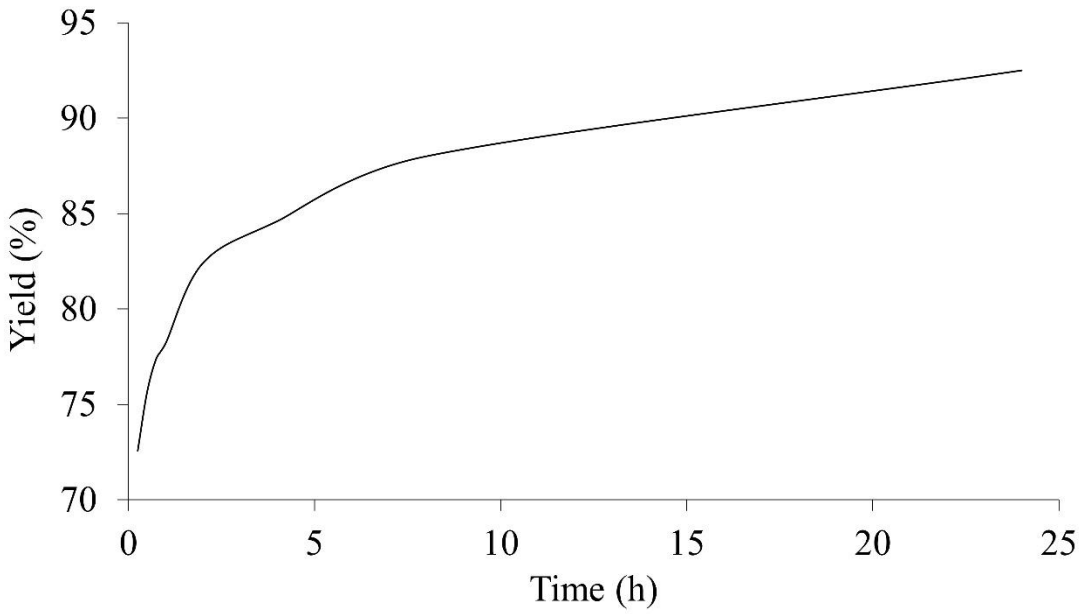

Figure 3.2 The yields of spherulites during the crystallization. The crystallization temperature was 25°C, and the solid concentration was 25%. The 0 h of crystallization was the time when sample started cooling at 180°C. After 1, 2, 4, 8, and 24 h, the yields were recorded and used to plot the yields curve.

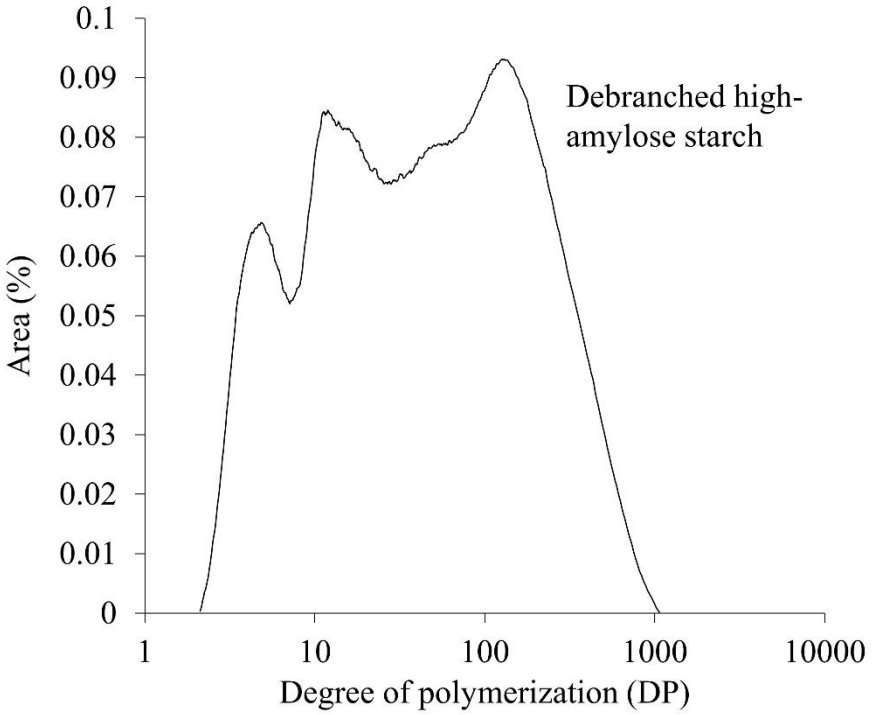

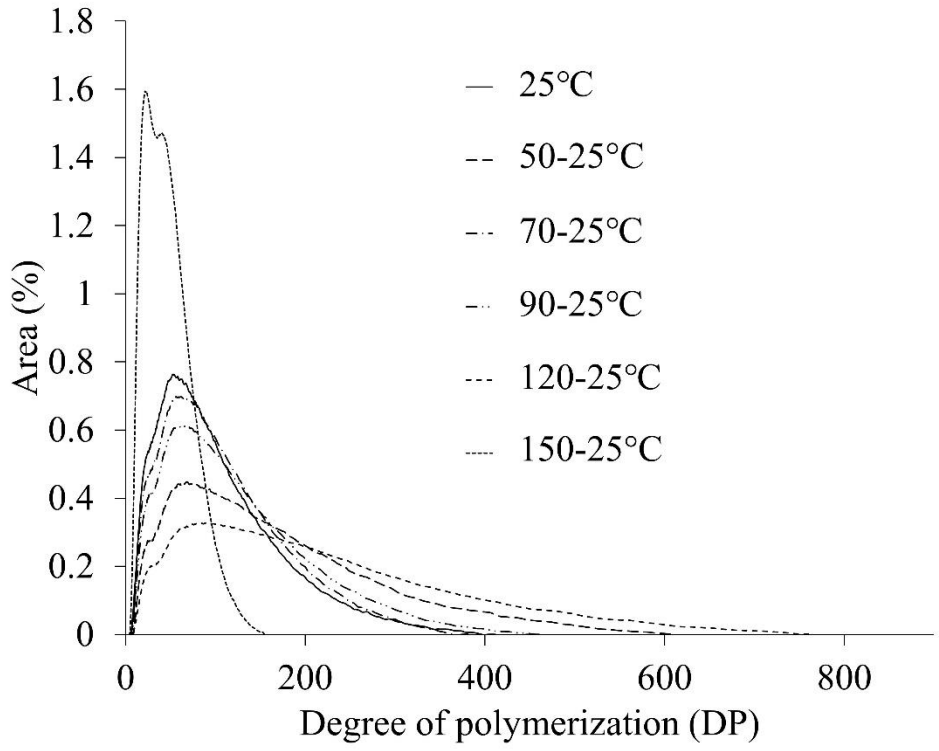

Figure 3.3 Molecular size distribution of high-amylose starch, debranched high-amylose starch, and spherulites formed by debranched high-amylose starch. The crystallization temperatures were indicated.

Bright light Polarized light Polarized light with a waveplate

Crystallization temperature 25°C

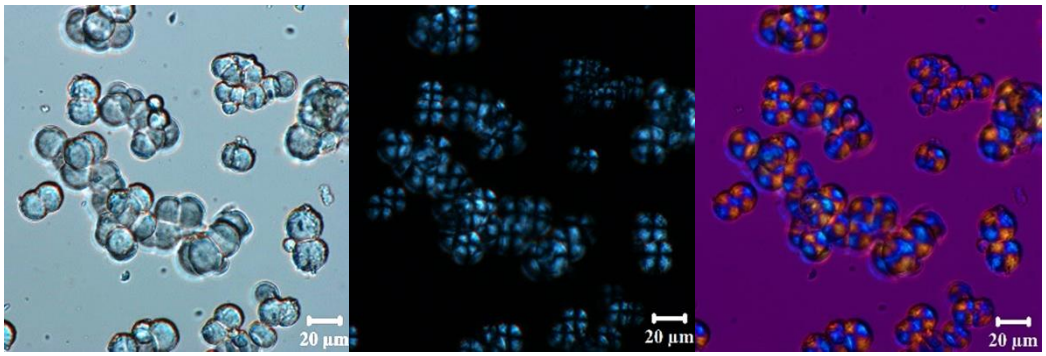

Crystallization temperature 50–25°C

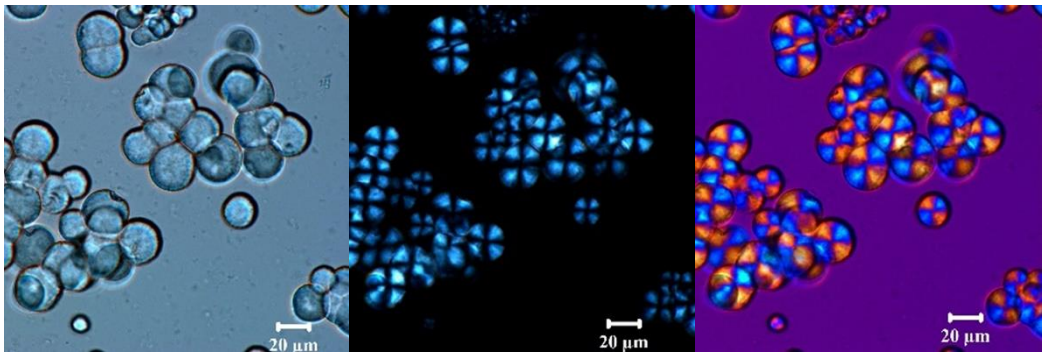

Crystallization temperature 70–25°C

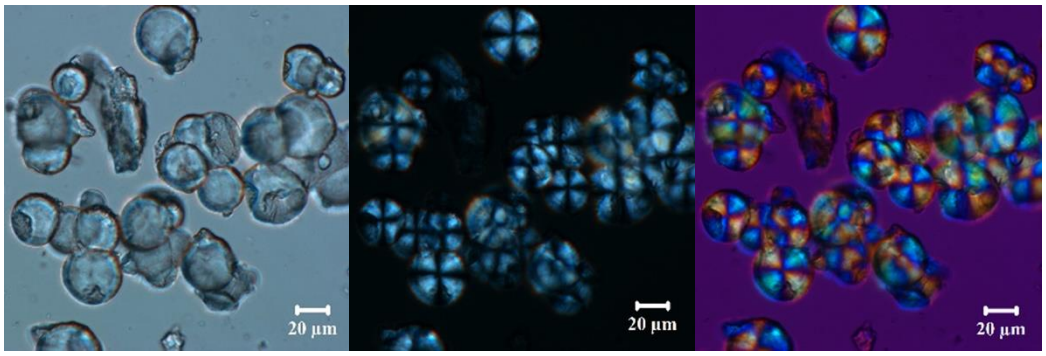

Crystallization temperature 90–25°C

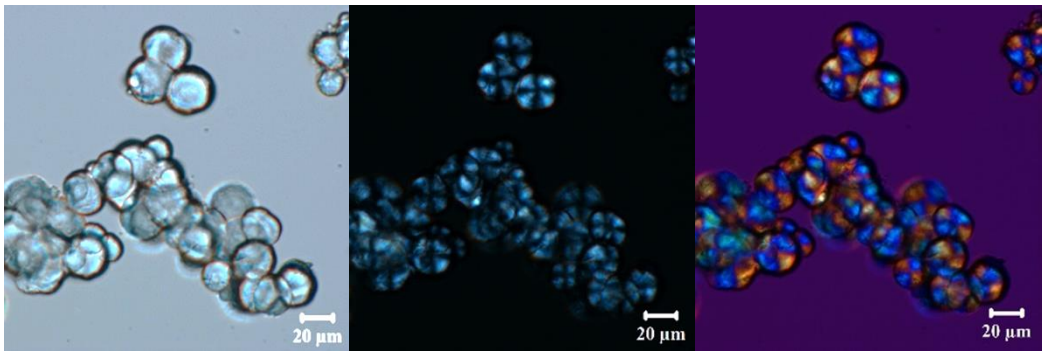

Crystallization temperature 120–25°C

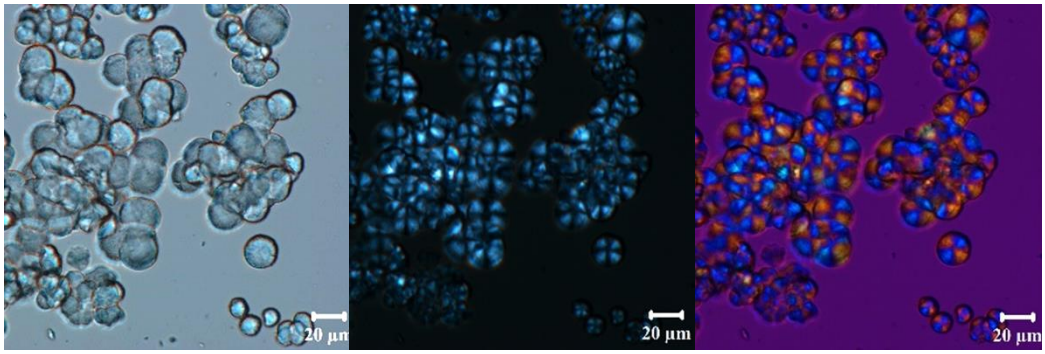

Crystallization temperature 150-25°C

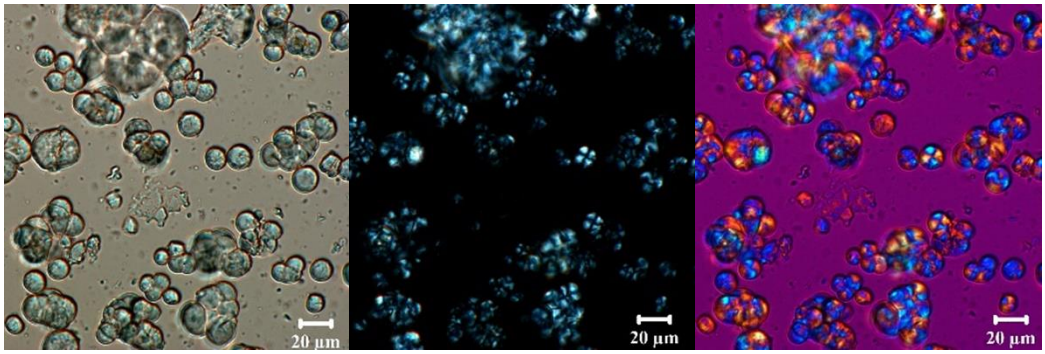

Figure 3.4 Spherulites formed at different temperatures (25°C~150°C). Bright field images under normal light, images under polarized light, and the images under polarized light with a waveplate were recorded.

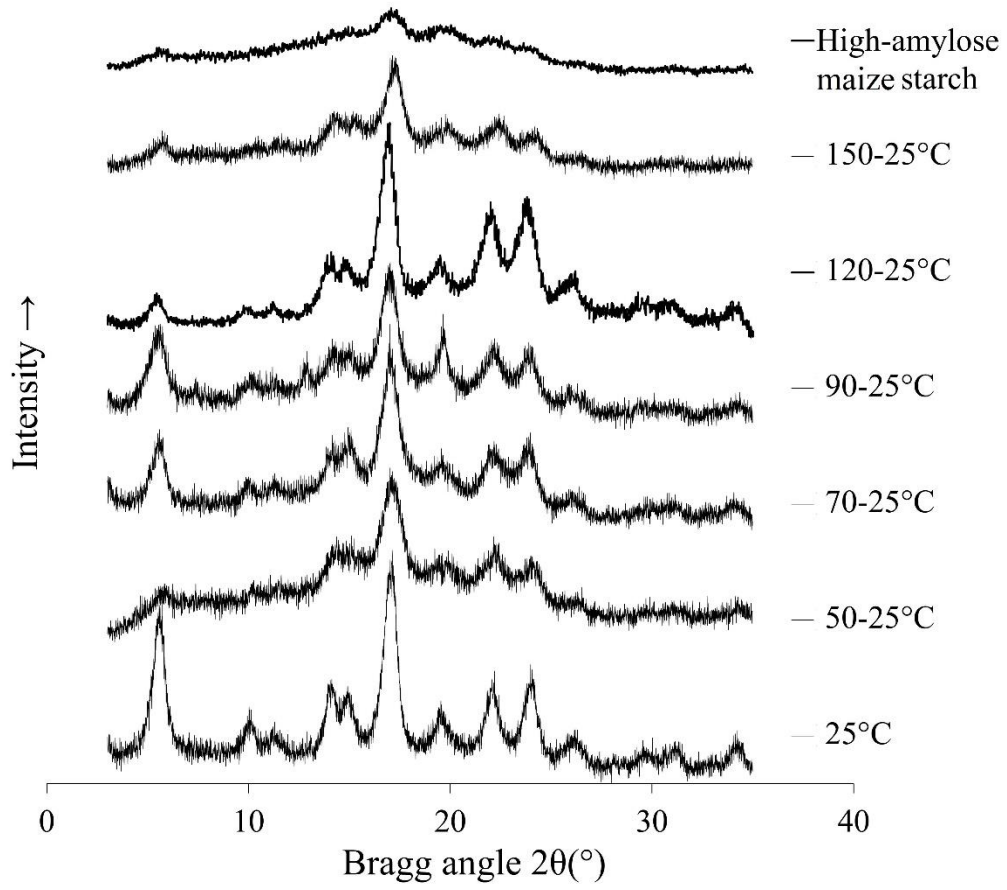

Figure 3.5 X-ray diffraction patterns of high-amylose maize starch and spherulites formed at different temperatures.

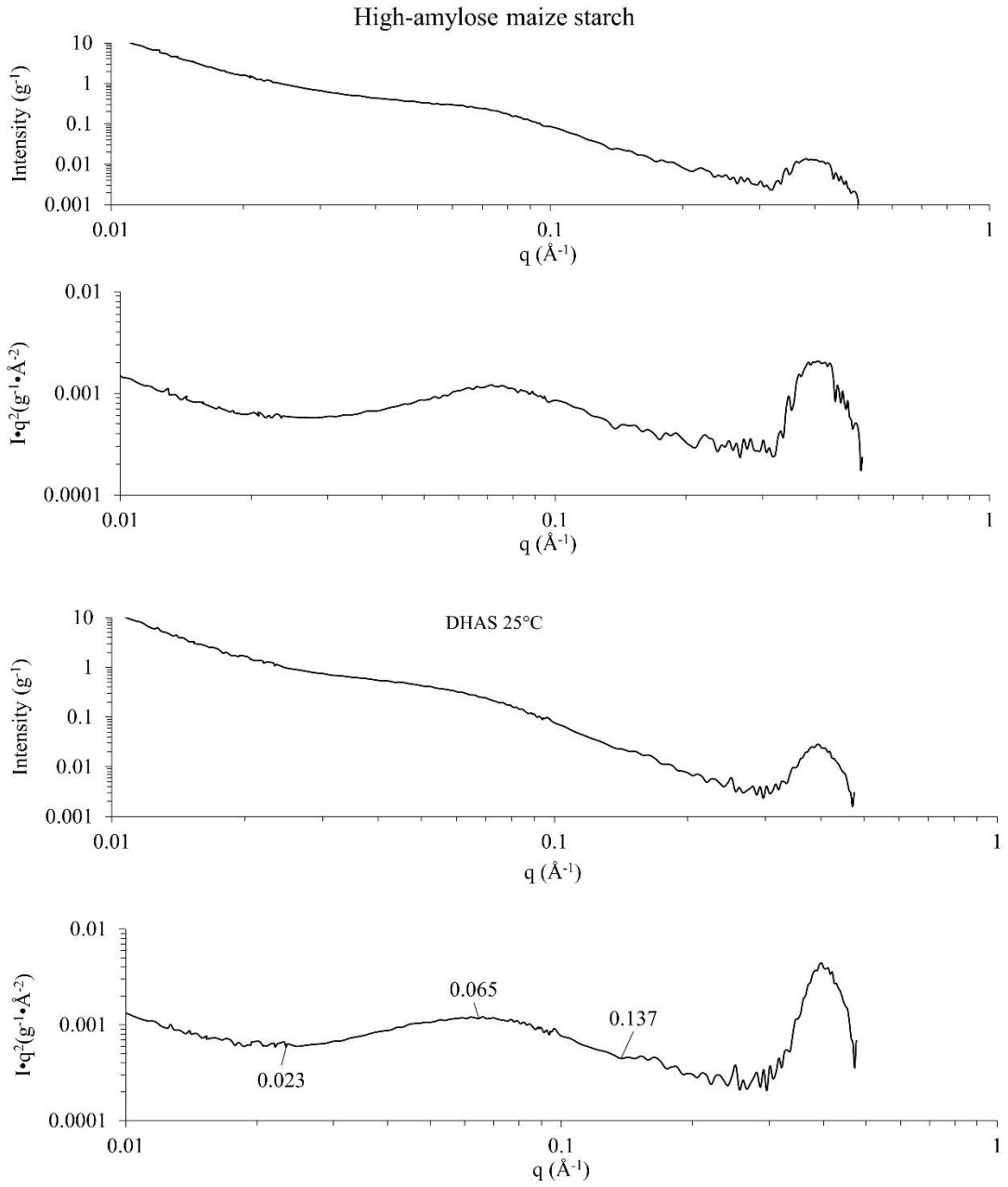

Figure 3.6 Small angle neutron scattering (SANS) of native high-amylose maize starch and spherulites crystallized at 25°C (DHAS 25°C). The curve was plotted as Intensity (I) vs. q, and $I \cdot q^2$ vs. q.

Bright light Polarized light Polarized light with a waveplate

High-amylose starch

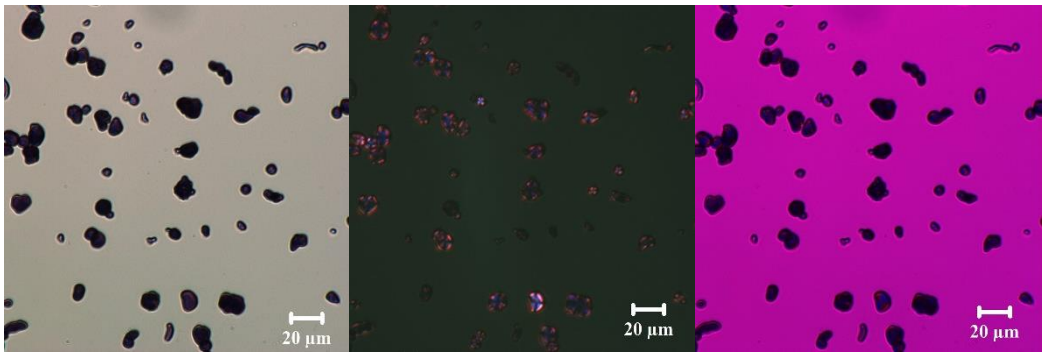

Positive spherulites

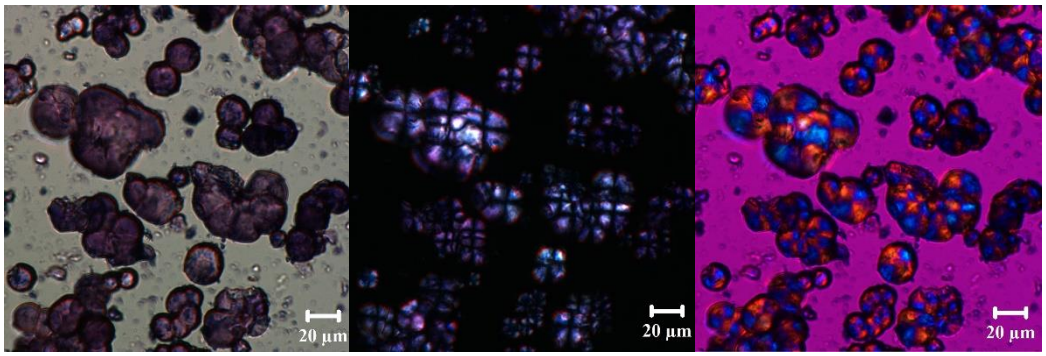

Negative spherulites

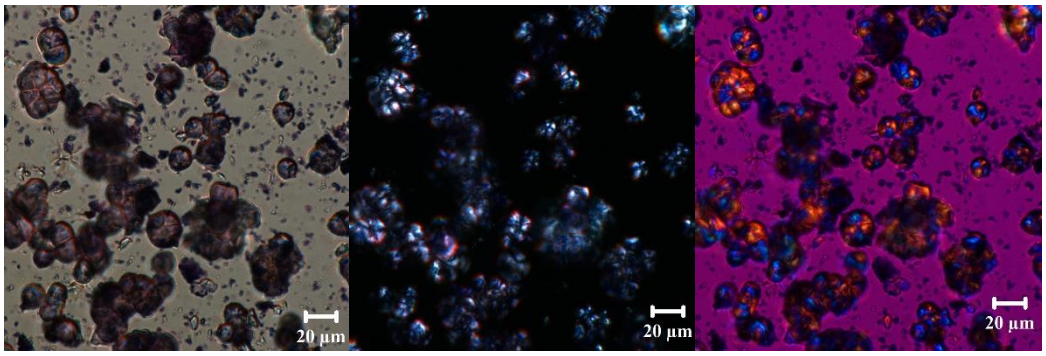

Figure 3.7 Iodine staining of native high-amylose starch, positive spherulites (25°C) and negative spherulites (150–25°C). The solid concentration was 25%, and the formation temperature was 25°C for positive spherulites, and 150–25°C for negative spherulites. The images of bright field, polarized light, and polarized light with a waveplate were recorded.

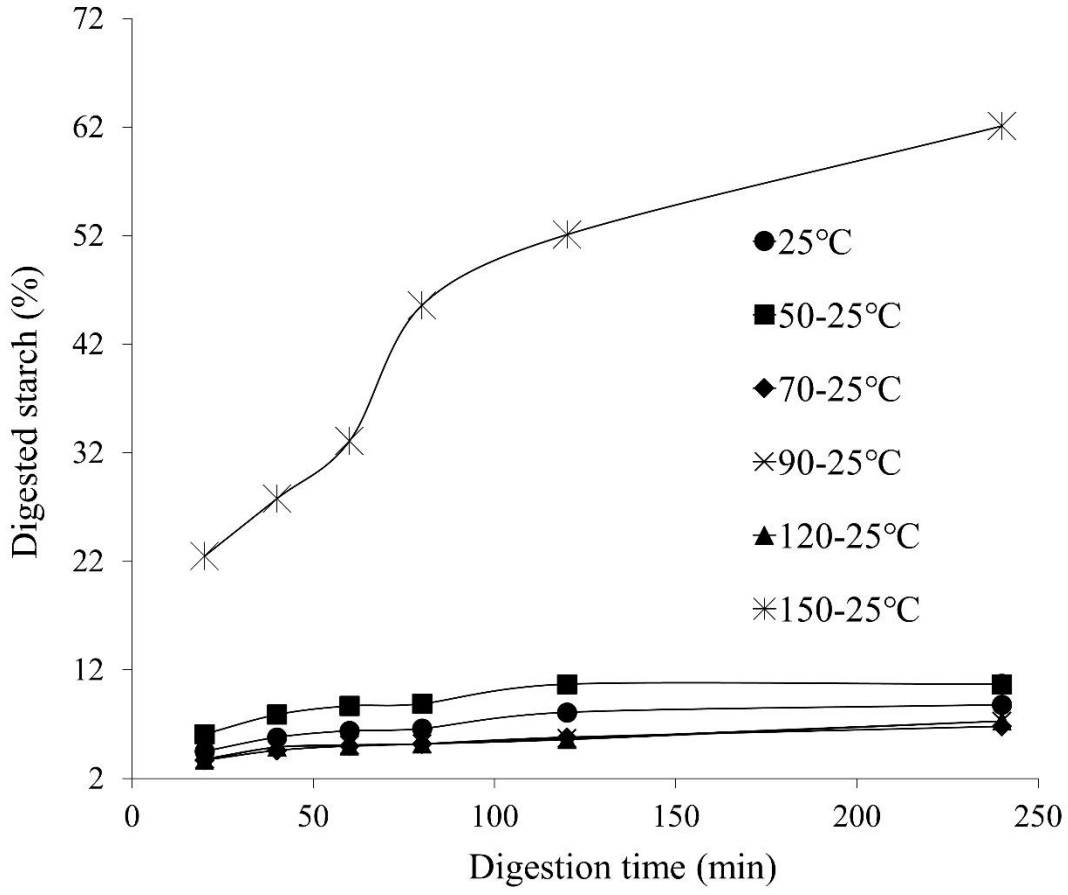

Figure 3.8 Digestion curve of the spherulites formed by 25% solid concentration of debranched high-amylose starch. The crystallization temperatures are indicated in the figure.

Bright light Polarized light Polarized light with a waveplate

Digestion time: 20 min

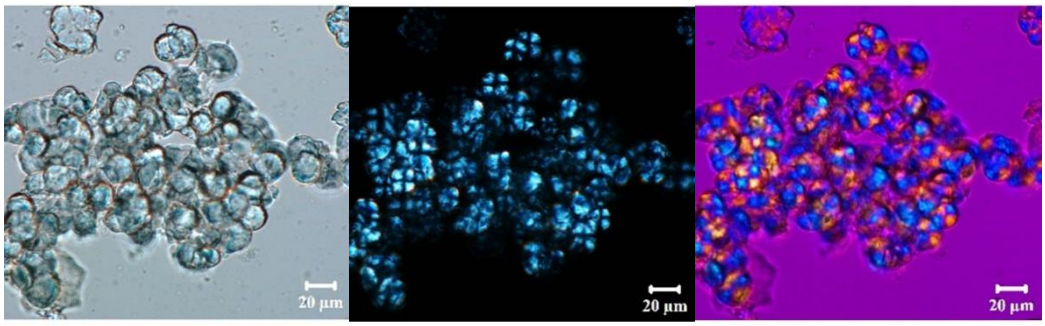

Digestion time: 60 min

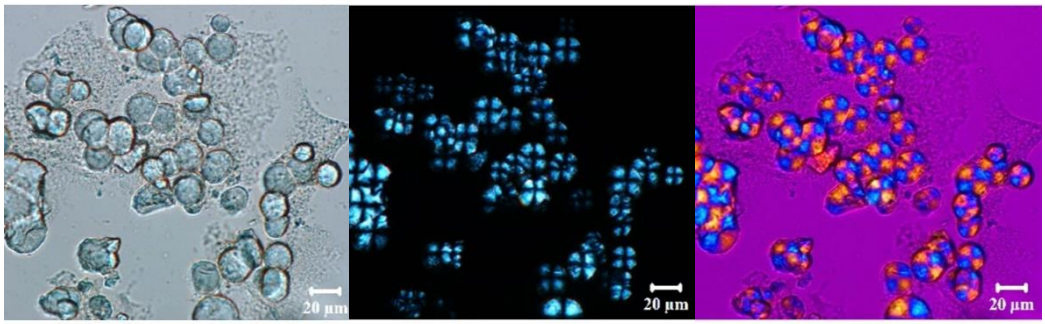

Digestion time: 120 min

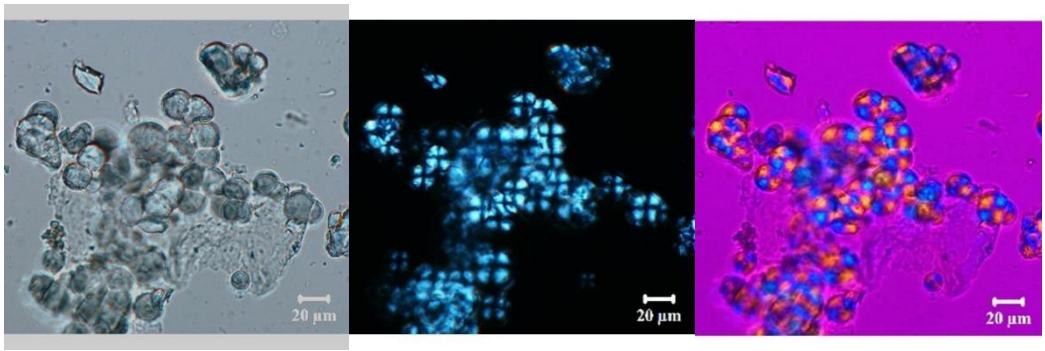

Digestion time: 240 min

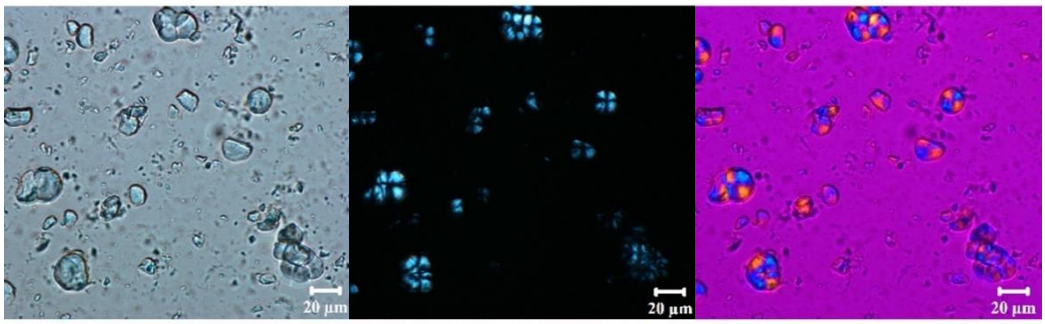

Figure 3.9 Morphology of spherulites during digestion. The spherulites were formed at 25°C and the solid concentration was 25%.

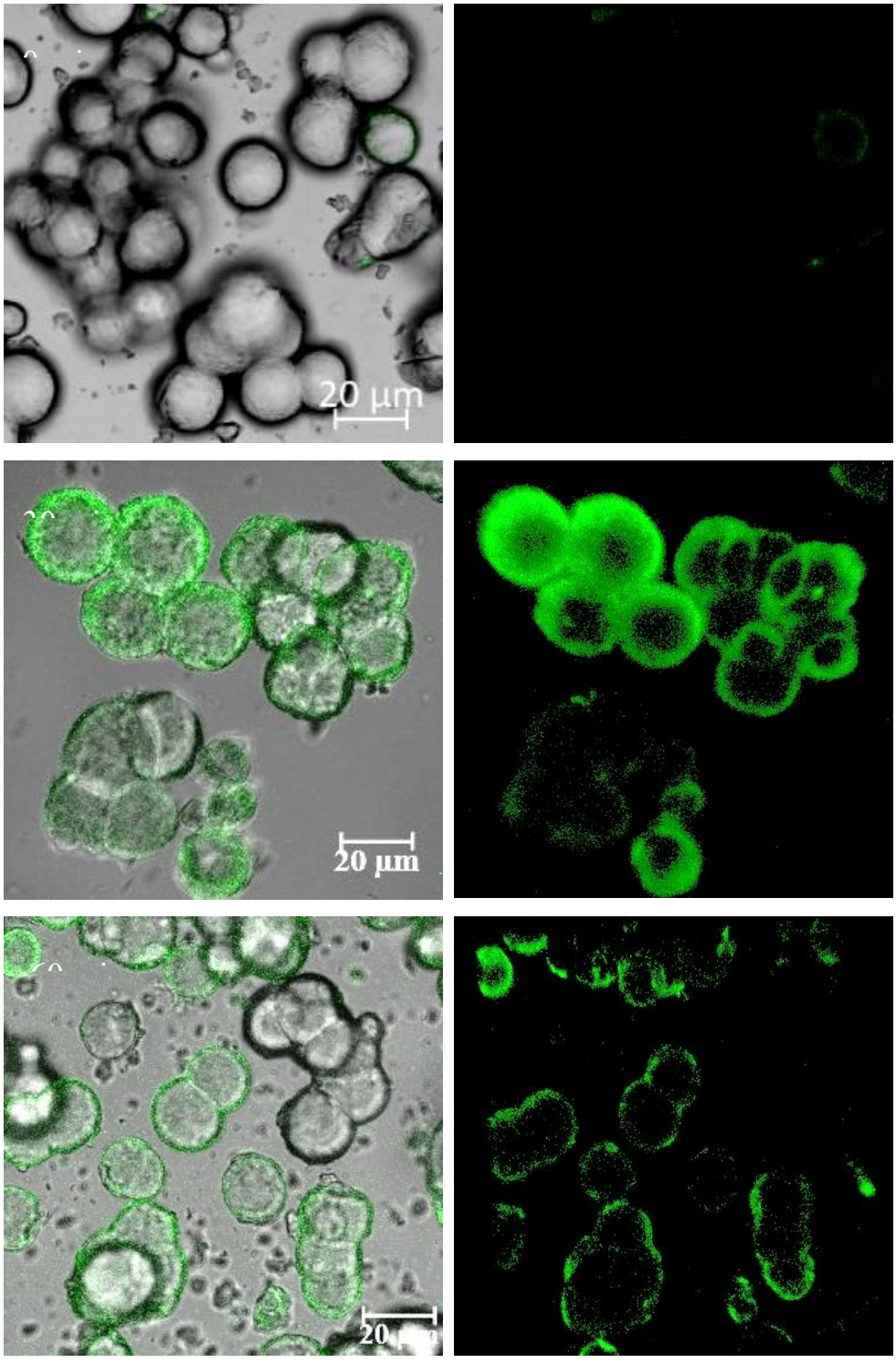
20 µm
20 µm

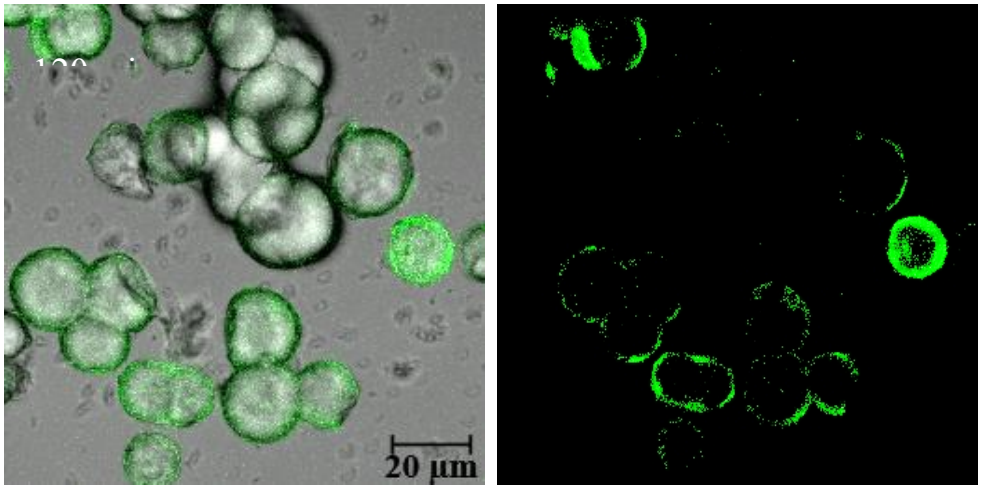

Figure 3.10 Confocal laser scanning microscope of spherulites formed by cooling debranched high-amylose starch from 180℃ to 25°C directly. Stained α-amylase was added to these spherulites and samples were incubated for 0, 30, 60, and 120 min. The green area indicated the location of α-amylase.

Chapter 4 - Developing products with A-type crystalline structure from debranched high-amylose maize starch

Abstract

The objective of this study was to develop products with A-type crystalline structure from debranched high-amylose starch. The debranched high-amylose maize starch was heated to 190°C, and then crystallized at high temperatures, 90°C, 120°C, and 150°C. The relatively high solid concentrations 30%, 40% and 50% were used. By increasing the crystallization temperature and the solid concentration, products with A-type and C-type crystalline structure were developed. But the crystallinities of A-type products were 35.1% and 46.2%, when the solid concentrations were 40% and 50%, respectively. The crystallinity of C-type crystallites was the highest (80.3%). Meanwhile, the resistant starch (RS) contents of A-type products formed at 40% and 50% solid concentrations were 75.9% and 69.8%, respectively. The RS content of C-type products was 55.6%. In addition to adjusting the crystallization conditions, heat-moisture treatment (HMT) was used to alter the B-type crystalline structure to A-type. The A-type crystalline structure was observed when the temperature of HMT was 150°C, and the morphology was maintained. Although the crystallinity was reduced to 43 - 47%, the RS content was high (90%), and the melting peak appeared between 133°C and 140°C.

Keywords

Crystalline structure, solid content, heat-moisture treatment, digestion

Introduction

Native starches normally contain two types of crystallites: A-type crystalline structure exists in waxy and normal cereal starches; B-type crystalline structure exists in high amylose content starches, such as high-amylose maize starches (Pérez, et al., 2009). During gelatinization, the crystallites are lost changing to a dis-ordered structure. After cooling, the starch molecules re-crystallized, which is called retrogradation. This procedure could be influenced by the crystallization temperature, solid concentrations, molecular chain length, and other additives such as ethanol (Buleon et al., 2007; Cai & Shi, 2013, 2014; Helbert et al., 1993; Jane, 2004). Previous studies have used shorter chains, higher crystallization temperatures, and higher solid concentrations to produce A-type crystalline structure (Buléon et al., 2007; Cai & Shi, 2010, 2014; Cai et al., 2010; Gidley & Bulpin, 1987; Shi et al., 2021). High-amylose maize starch was less used to produce A-type crystalline structure since the chain length was longer than that of debranched waxy maize starch. But heat-moisture treatment (HMT) was applied to high-amylose spherocrystals and transited B-type allomorphic to A-type (Nishiyama et al., 2010).

Crystalline structure is determined by the crystallization temperature, solid concentration, and chain length (Cai & Shi, 2013, 2014; Helbert et al., 1993; Jane, 2004). Debranched waxy maize and waxy potato starches were debranched to produce short chain amylose. When the solid concentration was 25%, debranched waxy maize starch formed B-type crystallites at 25°C, and A-type crystallites at 50°C. But only B-type crystallites were formed by debranched waxy potato starch due to a longer chain length. When the solid concentration was 15%, only B-type crystalline structure was formed by debranched waxy

maize starch since the solid concentration was reduced (Cai & Shi, 2013, 2014; Shi et al. 2021).

In previous studies, re-crystallized starch showed resistance to α-amylase digestion, which was called resistant starch (RS) (Cai & Shi, 2010, 2014; Cai et al., 2010; Shi et al., 2018, 2021; Eerlingen et al., 1993). Resistant starch was classified as five types. RS 1 was physically inaccessible to the enzyme, RS 2 was the raw starches from plant species, RS 3 was formed by retrogradation, RS 4 was formed by chemical modification, and RS 5 was formed by amylose-lipid complex (Topping et al., 2003; Hasjim et al., 2013). During the retrogradation, a higher DP (up to 100) and a higher content of amylose increased RS3 content (Eerlingen et al., 1993). In previous studies, enzyme debranching was applied to increase the amylose and RS content (Cai & Shi, 2010, 2013, 2014; Cai et al., 2010; Shi et al., 2018, 2021). Some studies compared the digestibility of A- and B- type crystalline. Cai et al. (2010) found the A-type crystals were more resistant to enzyme digestion. So, the relationship between types of crystalline and digestibility are not fully understood.

The objective of this study was to produce A-type spherulites. Spherulites was a crystallized material showing Maltese crosses. When the solid concentration was 25°C, spherulites with B-type crystalline structure were produced by debranched high-amylose maize starch. Spherulites of A-type crystalline structure were expected by increasing the solid concentration and crystallization temperature. HMT was another approach applied to produce spherulites of A-type crystalline structure. Then the digestibility and structure of crystallized material were investigated. This information will offer more insights on the crystalline formation, and further investigate the digestibility of two different types of crystallinities.

Materials and Methods

Materials

High-amylose maize starch was provided by Cargill (Wayzata, MN, US). The amylose content, ash content, protein content and the degree of crystallinity were 69.3%, 0.1%, 0.4%, and 25.0%, respectively. The isoamylase was from Weissbiotech (Ascheberg, Germany), and the activity was 77 IAU/ml. One unit of isoamylase activity was defined as the amount of enzyme increasing 0.01 in absorbance at 600 nm per minute (Ara et al., 1993; Li et al., 2016). Other chemicals were analytical grade.

Debranching

High-amylose maize starch (80 g, db) was loaded in a ball jar (32 oz, Ball Corporation, Westminster, Co.) and suspended in sodium acetate buffer (240 ml, pH 4). The suspension was heated at 140°C in an oven for 2 h. Then the sample was placed in a water bath of 50°C. When the sample was cooled to 50°C, isoamylase (1%, w/w, starch base) was added and the debranching was carried out at 50°C with a constant overhead stirring for 24 h (Cai et al., 2010; Cai & Shi, 2010; Shi et al., 2021). Distilled water (80 g) of 50°C was added to thin the mixture for constant stirring, and the mixture was heated in a boiling water bath for 5 minutes to denature the enzyme. The debranched product was collected by a spray dryer (Mini Spray Dryer B-290, BUCHI Corporation, DE. USA). The inlet temperature of spray drying was 180°C.

Crystallinity formation at different crystallization temperatures

The spray dried debranched material (20g) was weighed to an aluminum can and suspended in water of 46, 30, or 20 ml, so that the solid concentration was 30%, 40%, or 50%, respectively. After a well mixing, samples were heated to 190°C in a Parr reactor (4521M, PARR, Illinois, USA), and then cooled to 25, 90, 120, and 150°C, respectively. The sample crystallized at 25°C were held for 24h, the samples crystallized at 90°C were held for 24 h, and then cooled to 25 °C for another 24 h. The samples crystallized at 120 and 150°C were held for 4 h, and then cooled to 25 °C for another 24 h. All crystallized debranched starch was filtered and dried in an oven at 40°C.

Heat-moisture treatment (HMT) of B-type spherulites

The spray dried debranched material (20g) was weighed to an aluminum can and mixed well with water (60 ml) to form a 25% solid concentration. The mixture was heated to 180℃ in the Parr reactor, and then cooled to the room temperature (25°C) immediately. After crystallization at ambient for 24 h, B-type spherulites were collected by a filtration and drying at 40℃ in an oven.

To conduct further heat-moisture treatment, the moisture contents of the dried sample was adjusted to 20% and 25% by adding water. The samples were held at ambient for 24 h to equilibrate the moisture contents. Then samples were heated to 140°C or 150°C for 4 h in an oven. The heated samples were cooled to 25°C and dried in an oven for 24 h.

Gel permeation chromatography (GPC)

The native starch and crystallized debranched starch were mixed with dimethyl sulfoxide (DMSO) containing lithium bromide (0.5% w/w) as 1 mg/ml and dissolved at 80°C for 24 h with occasionally stirring to prevent from aggregates formation. The dissolved sample was filtered by a 2 μm filter when cooled to 25°C, and then injected into a PL-GPC 220 (Polymer Laboratories, Inc., Amherst, MA, USA). The separation was archived by three Phenogel columns and a guard column (Cai et al., 2010) (Phenomenex, Inc., Torrance, CA, USA). The flow rate was 0.8 ml/min, and the solvent was same to what was used to dissolve the samples. Pullulan standards were used for universal calibration (Vilaplana & Gilbert, 2010).

X-ray diffraction (XRD)

Starch samples were placed in a humidity chamber containing saturated sodium chloride solution for 24 h, and the moisture content was reached to about 17%. Then samples were analyzed by a wide-angle X-ray diffraction (PANalytical, Almelo, The Netherlands). This analysis was conducted using 35 kV and 20 mA, theta-compensating slit, and a diffracted beam monochromator. The Bragg angle was between 3 and 35° (2θ). The degree of crystallinity was calculated as the ratio of the peaks representing crystals to the total area (Chakraborty et al., 2021; Komiya & Nara, 1986).

Light Microscopy

The dried samples produced with different solid content, B-type spherulites formed by 25% debranched high-amylose maize starch and HMT spherulites were suspended in 50%

glycerol solution as 1% of solid concentration. An aliquot of suspension was dropped on a glass microscope slide and covered by a coverslip. The sample was viewed under a light microscope (Olympus BX51TF, Olympus Optical Co. Ltd., Shinjuku-ku, Tokyo, Japan) attached with a retardation plate (Olympus Optical Co. Ltd., Shinjuku-ku, Tokyo, Japan). Normal light, cross-polarized light, and a retardation plate were used to investigate morphology. The images were recorded by a camera (SPOT 18.2 Color Mosaic, Diagnostic Instruments Inc., Sterling Heights, MI, USA).

Differential scanning calorimetry (DSC)

Thermal properties including the onset, peak, conclusion, and enthalpy (T_o, T_p, T_c, and ΔH) were measured by a DSC (DSC 25, TA Instruments, New Castle, DE, USA). A sample (approximate 10 mg, db) was loaded in a stainless DSC pan, then water (two times of solid weight) was added to the sample. The DSC pan was sealed and heated from 10°C to 180°C at a rate of 10°C/min in a DSC (high-amylose starch and crystallized samples were measured by a DSC (DSC 25, TA Instruments, New Castle, DE, USA). The DSC thermogram was analyzed by TRIOS (TA Instruments, New Castle, DE, USA).

Digestibility

Modified Englyst's method (Englyst et al., 1992; Sang & Seib, 2006) was used to determine the digestibility of produced samples. The digestion times were 20, 40, 60, 80, 120, and 240 min. The digested starch contents at 20 min and 120 min were used to calculate the rapidly digested starch (RDS), slowly digested starch (SDS) and resistant starch (RS)

contents. The digestion curve was plotted based on the digested starch content at each time point (Shi et al., 2018, 2021).

Total dietary fiber (TDF)

The TDF contents were measured by the AOAC method 991.43. The B-type spherulites and HMT samples were selected for the TDF measurement.

Statistical analysis

Minitab 17 Statistical Software Program (Minitab Inc. State College PA, USA) was used for the statistical analysis. Mean value and standard deviation from the duplicated experiments were reported.

Results and Discussion

Yields of crystallinities formed by debranched high-amylose starch

When the crystallization temperature was lower than 150°C, the yield was higher than 95% and a higher solid concentration led to a slightly higher yield. When the solid concentration was 30%, 40%, and 50%, the yields were about 95.4 - 99.5% (Table 4.1). But when the crystallization temperature was 150°C, the yield was dramatically decreased. When the solid concentration was 30%, 40%, and 50%, the yield decreased to 36.6%, 54.6% and 57.0%, respectively (Table 4.1).

In our previous study, when debranched waxy maize starch (25% solid) was used to crystallize at 25°C, the yield was higher than 82% (Shi et al. 2018, 2021). In this study, although the crystallization temperature was high, chain length of the debranched high-

amylose maize starch was longer and a higher solid concentration was used. These two factors resulted in a yield greater than 90%, when the crystallization temperature was lower than 120°C. But when the crystallization temperature was 150°C, the debranched high-amylose maize starch was significantly degraded (as discussed in Section of molecular size distribution), so that the yield was low.

Molecular size distribution

The molecular size distribution of the crystallized products was shown in Figure 4.1. when the solid concentrations were 30%, 40%, and 50%, higher formation temperature resulted in a smaller molecular size. When the samples were crystallized at 25°C directly, the molecular size was not influenced by the solid concentration. The degree of polymerization (DP) was in a wide range (DP 6 ~ DP 860), and a sholder appeared at DP 30. The DP of the products crystallized at 90°C and 30% solid concentration was in the range from DP 6 to DP 760. Compared to the samples of lower crystallization temperatures, more molecules between DP 6 and DP 300 were crystallized. When the crystallization temperature was 120°C, the chain length (DP) was shorter (DP 6 ~ 300), and the peak appeared at DP 60. When the crystallization temperature was 150°C, the molecular size was further reduced to lower than DP 120. When the solid concentrations were 40%, the DP distribution was between DP 6 and DP 860 if the crystallization temperature was lower than 90°C. At the crystallization temeperature of 120°C, the DP distribution range was also between DP 6 and DP 300, and the peak was DP 60. When the crystallization temperature was 150°C, the molecular size was also reduced to lower than DP 120. When the solid concentration was 50%, the DP

distribution was similar when the crystallization temperature was lower than 90°C. The carystallization temperature of 120°C also resulted the reduced DP, but the distribution was similar to that of sample formed at 90°C with a solid concentration of 30%, which had a range from DP 6 to DP 760 and more crystallized molecules between DP 6 and DP 300. At 150°C, the DP distribution was similar to the samples of 30% and 40% solid, the molecular size was also reduced to lower than DP 120.

When the solid concentration was 25%, all molecules were shorter than DP 800, and a peak appeared at approximately DP 60. After heat-moisture treatment, the molecules were samller than DP 500, and a peak appeared at DP 60 too (Figure 4.1).

In chanpter 3, the native high-amylose maize starch had a molecular size range from DP 6 to DP 7000. After debranching, the largest molecules was reduced to about DP 1000, and a peak appeared at DP 140. After the crystallization, all molecular size was reduced lower than DP 900 (Figure 4.1). Instead of showing a peak at DP 140, crystallized samples showed a smooth curve and a shoulder at DP 30 when the crystallization temperature was 25°C (Figure 4.1). This could be explained by the heating degradation and the peak was appeared at DP 60 or DP 30. As mentioned in the yield results, the debranched high-amylose starch was degraded when the formation temperature was higher, and lower solid concentration may be more easily degraded by heating. The molecular size distribution matched to the yields results.

When the solid concentration was 25%, the molecules were lower than DP 800, which also agreed to the phenonmenon above. After the heat-moisture treatment (HMT), the

molecules were further reduced, but due to the moisture content was low (20% or 25%), the molecular size range was not affected by the HMT conditions.

Crystalline structure

Two approaches were used to produce A-type crystalline products from debranched high-amylose maize: (1) crystallization at high temperatures and high solid content, and (2) heat-moisture treatment of B-type spherulites. When the solid concentration was 30%, 40%, and 50%, the degree of crystallinity was mostly lower than 50%. When the crystallization temperature was 150°C, the samples of 40% and 50% solid concentrations showed 74.0% and 80.3% degrees of crystallinity, respectively. When the crystallization temperature was 120°C, the sample of 50% solid concentration showed 50.3%. Except for these three samples above, the crystallinity degrees of other samples were lower than 50%. When the solid concentration was 30%, all the degrees of crystallinity were less than 40% (Table 4.1).

When the solid concentration was reduced to 25%, the degree of crystallinity dramatically increased to 81.2%. However, the HMT reduced the degree of crystallinity. When the moisture content was 20%, the degree of crystallinity was about 42%~43%, and the temperature of HMT showed few influences. However, when the moisture content was 25%, the degree of crystallinity increased from 44.4% to 46.8%, when the temperature increased from 140°C to 150°C.

According to the XRD graph, all samples showed B-type of crystalline, when the solid concentration was 30%. But when the solid concentrations were 40 and 50%, the crystalline turned to A-type at 90°C. At 150°C, the sample of 40% solid showed B-type

crystalline, but the sample of 50% solid showed dominantly A-type crystalline with a small peak at 5° indicating B-type crystalline (Figure 4.2).

Before the HMT, the crystallites were B-type. When the temperature of HMT was 140°C, all samples were still B-type. But when the temperature of HMT was 150°C, the B-type crystallites changed to A-type. However, the degree of crystallinity was also reduced after HMT. The B-type crystallites showed a crystallinity of 81.2%. When the temperature of HMT was 140°C, the moisture contents were 20% and 25%, the degrees of crystallinity were 42.6% and 44.4%, respectively. When the temperature of HMT was 150°C, the moisture contents were 20% and 25%, the degrees of crystallinity were 42.9% and 46.8%, respectively (Table 4.2).

Generally, high solid concentration, shorter chains, and high crystallization temperature can enhance the formation of A-type of crystalline. In this study, A-type crystalline structure was formed when the products were crystallized at 90°C, 40% or 50% solid content. And according to the molecular size distribution (Figure 4.1), when the formation temperatures were lower than 90°C, the molecular chains were similar, so the main factors affecting the crystalline types were temperature and solid concentration. But when the crystallization temperatures were higher, only samples formed at 150°C with 50% solid concentration showed C-type crystalline structure, due to a shorter chain length and a higher solid concentration.

In chapter 3, solid concentration of 25% was used and B-type crystallites were formed at 25°C. The degree of crystallinity was 81.2% in this study, which also matched the previous study. But after HMT, the reduced chain length indicated heating degradation

occurred, so that the crystalline structure was influenced. Different native starches, such as potato and maize starches, have been applied to HMT. The crystalline structure changed from B-type to A-type, and the reduced crystallinity were also observed (Chakraborty et al., 2021; Nishiyama et al., 2010; Yang et al., 2016). However, native starch contained amylopectin which could be degraded during HMT, so that the crystallinity was reduced (Yang et al., 2016; Chakraborty et al., 2021). Compared to low-amylose potato starch, high-amylose potato starch showed crystalline structure changes at a higher temperature, but less clearly identified. Meanwhile, the B to A type transition was not observed for high-amylose maize starch (Nishiyama et al., 2010). The crystalline structure transition from B to A type was described as a compaction of double helices. During the HMT, the crystal lattice of B-type crystallites expanded, the water molecules in the center of B-type double helices could be released and denser helices could be packed, which was the A-type crystalline structure formed. This re-packing required enough mobility of the helices (Perez et al. 1990). According to Jenkins et al. (1995), long chains amylose lacks the mobility to re-organize the helices during the structure transition. After debranching, the amylose content was further increased, but linear short chains were produced and included. As a result, when the temperature of HMT was 140°C, the samples still showed B-type crystalline structure. But when the temperature was 150°C, the samples turned to A-type crystallites. The B-type crystallites by debranched high-amylose starch showed a high degree of crystallinity (81.2%), although the degradation caused by HMT reduced the crystallinity, the samples were still more crystallized than native starches.

Morphology

The morphology of the crystallized products with A-type and C-type crystalline structure, spherulites before and after HMT is shown in Figure 4.3. The A-type products did not show Maltese crosses and the particles were not spherical. The C-type products showed spherical particles, but the Maltese crosses were observed. As the results, no spherulites were formed by using 40% and 50% solid. When the solid concentration was 25%, spherical particles were formed, and Maltese crosses were observed under polarized light and indicated they were positive spherulites (Shi et al., 2021). After the HMT, some fragments were observed, but most particles were still spherical, and the Maltese crosses were not altered (Figure 4.3). The positive birefrigence indicated the radial orentation of crystals (Cai & Shi, 2013; Crist & Schultz, 2016; Shi et al., 2021). The microscope images indicated the orentation of crystals was not changed by the HMT, and the conditions of HMT showed few influences on the morphology of the spherulites.

Thermal properties

Thermal properties of crystallized products formed at different solid contents and temperatures are shown in Table 4.3. When a higher solid concentration was applied, two thermal peaks were observed in most samples. But when products were crystallized at 120°C and 150°C followed by 25°C, only one thermal peak was observed with 30 and 40% solid concentration. When the solid content was 50%, a single thermal peak was observed when the crystallization temperature was 150°C followed by 25°C. And compared to other samples, those samples with one thermal peak showed a lower thermal stability.

A previous study (Ziegler et al., 2003) also reported two thermal peaks of crystallized products. Higher solid concentration could enhance the crystallization at high temperatures, so some crystals may be formed at a high temperature, and then some were formed at 25°C. As a result, two thermal peaks were observed. When the formation temperature was 120°C, the molecular size distribution of samples formed by 30 and 40% solid concentration was similar. And when the formation temperature was 150°C, all the samples of three solid concentration (30%, 40%, and 50%) were similar. These five samples only showed one peak, and it may be due to two factors. First, the temperature was too high to form crystals; second, the molecules were degraded, and the molecular size distribution was narrow so that the crystallization was more uniform.

Our previous study used the debranched high-amylose starch at 25% solid to form B-type crystallites. The crystallites showed a melting peak between 71.1°C and 127.9°C, the enthalpy was 32 J/g. After the HMT, the melting peaks appeared at higher temperatures. Lower heating temperature and lower moisture content resulted in a higher onset temperature. When the temperature was 140°C, the onset temperature was 114.1°C at the moisture content of 20%. The onset temperature decreased slightly to 111.4°C when the moisture content increased to 25%. When the crystallized debranched starch was treated at 150°C, 20% moisture content, the highest onset temperature was 110.9°C, and the moisture content was 20%. When the moisture content increased to 25%, the onset temperature reduced to 92.9°C. Compared to onset temperature, peak temperature and conclusion temperature were less influenced by HMT. When the sample was treated at 25% moisture content and 150°C, the peak temperature was the highest (140.3°C). Except for this HMT condition, all the others

resulted in a peak temperature approximate 133~134°C. The conclusion temperatures were 164~165°C at all the four HMT conditions. HMT also influenced the enthalpy. After HMT, the lowest enthalpy was 39.6 J/g and observed at 150°C and 20% moisture content. When the temperature reduced to 140°C, the enthalpy was increased to 46.3 J/g. When the moisture content increased to 25%, the enthalpy was increased to 47.3 J/g. When the temperature was reduced to 140°C, and the moisture content was 25%, the enthalpy was the highest as 52.6 J/g.

HMT did not cause melting of crystallites and crystallization but influenced the crystalline structure. After the HMT, the degree of crystallinity decreased, so the crystals having a lower melting temperature may disappear after HMT. Although the crystalline type was not changed when the heating temperature was 140°C, the arrangement of double helices could be affected. Meanwhile, the temperature and moisture content of HMT also influenced the degradation. As a result, when the temperature was higher, the onset temperature and enthalpy could be lower. But when the temperature was the same, a higher moisture may reduce the onset temperature, but increased the enthalpy.

Digestibility

Rapidly digested starch (RDS), slowly digested starch (SDS) and resistant starch (RS) contents of the crystallized products from the debranched high-amylose maize starch are shown in Table 4.5. When the products were crystallized at temperature lower than 150°C, the RS contents were between 70% and 77%, except the sample crystallized at 120°C and 30% solid, which the RS content was 84.2%. When the crystallization temperature was

150°C, the RS content was reduced to lower than 55.6%, and a higher solid concentration resulted in a higher RS content (Table 4.5).

However, the products of 25% solid showed the RS content increased to 92%. After HMT, the RS contents were approximately 89% ~ 90%. The HMT conditions showed little influence on the RS content (Table 4.6).

By measuring the digested starch after different hydrolysis time, digestion curve could be plotted (Figure 4.4). The RS contents were also reflected by the digestion curve. When the crystallization temperature was 150°C, the digestion curves were higher than those crystallized at other temperatures, which indicated more starch were digested after the same hydrolysis time. Based on Figure 4.4, when the solid concentration was 30% and the crystallization temperature was 150°C, the digestion rate dramatically increased between 60 min and 80 min. This phenomenon was also observed in other samples, but less obvious. Especially when the crystallization temperature was 150°C, and the solid concentrations were 40% and 50%. The digestion curve of these two samples were straight lines. HMT samples also showed this digestion rate change, and the digestion rate increased most when least digestible when samples were heated at 150°C and moisture content was 25%.

In our previous study, crystallites were formed by debranched high-amylose maize starch, and the solid concentration was 25%. When the samples were crystallized at different temperatures (<150°C), the RS content was always higher than 90%. But when the solid concentration was higher, the crystallinity was reduced, which decreased the RS content. In chapter 3, when the crystallization occurred at 150°C and the solid concentration was 25%, the RS content was 47.9%. Meanwile, the crystallinity was also reduced when samples

crystallized at 150°C. However, crystallization at 150°C increased the crystallinity, and the RS content was still reduced. At 150°C, degradation also occurred (Figure 4.1), which could be the cause of a lower RS content. When the solid concentration was 30%, this degradation also resulted in a lower crystallinity. With a higher solid concentration, the crystallization was enhanced, so the crystallinity was increased. Based the Figure 4.1 and Figure 4.4, the RS content was mainly influenced by degradation. When the crystallization was 150°C, the molecules were degraded into a same range, the higher solid concentration showed obvious influences on the RS, since the crystallinity was affected. The increased digestion rate between 60 min and 80 min was also observed in our previous study, and it could be caused by the digested starch fragments. When the crystallized starch was digested, the enzyme hydrolyzed the surface of a particle first, and produced fragments. These fragments were more digestible and hydrolyzed between 60 min and 80 min. So, the digestion rate increased. When the fragments were hydrolyzed, the digestion rate was also decreased. It also explained the straight curve of samples crystallized at 150°C, when the solid concentration was 40% and 50%.

The B-type spherulites were formed as described in chapter 3; the digestibility of the spherulites was repeated in this chapter. After HMT, the degree of crystallinity decreased to lower than 50%. However, the RS content was still approximately 90%. HMT was used to alter the crystalline structure but did not change the morphology. In our previous study, the enzyme hardly penetrated the particles, and only the most outer layer was hydrolyzed. It explained the high RS content of the HMT samples.

Total dietary fiber (TDF)

The TDF contents were measured by AOAC method 991.43. TDF content of the B-type spherulites before HMT was the lowest (48.3%). After HMT, the TDF content increased to 72.1% when the temperature was 140°C, and the moisture content was 20%. When the moisture was 25%, the TDF content was 70.4%. After increasing the temperature of HMT to 150°C, the TDF contents were further reduced. When the moisture content was 20%, the TDF content was 60.0%. When the moisture content was 25%, the TDF content was 66.8% (Table 4.7).

The AOAC method 991.43 used thermal stable α-amylase, and samples were heated in a boiling water bath for the enzyme hydrolysis. As a result, the TDF contents were influenced by their thermal stability. Based on Table 4.6, the RS content of spherulites before HMT was the highest. However, the melting temperature was the lowest (Table 4.4). As a result, the crystalline structure was mostly affected during heating and the resistance to enzyme digestion was reduced, which resulted the lowest TDF content. When the temperature of HMT was 150°C, the onset temperature was lower, which resulted a lower TDF content. But when the temperature was 140°C, the onset temperature was higher than 111.4°C, so the sample was less affected by heating, and the TDF content was higher.

Conclusions

In this study, the crystallization conditions and the HMT were applied to produce the A-type spherulites. Debranched high-amylose maize starch was suspended in water and crystallized at 25°C, 90°C, 120°C, and 150°C. A higher crystallization temperature caused a

higher level of degradation, which affected the crystallinity, thermal properties, and the digestibility. When the solid concentration was 30%, no A-type crystallites were formed, and the crystallinity was lower than 40%. When the solid concentrations were 40% and 50%, the A-type products were crystallized at 90°C. But when the crystallization temperature increased, A-type crystalline structure was not observed. And the product crystallized at 150°C and 50% solid concentration showed C-type crystalline structure, meanwhile the crystallinity increased to 80.3%. When the crystallization temperature was 150°C, although the crystallinity was higher when the solid contents were 40% and 50%, the melting temperature and RS contents were reduced.

Heat-moisture treatment (HMT) successfully changed the crystalline structure of spherulites from B-type to A-type, when the HMT temperature was 150°C. Heating at a high temperature (140°C and 150°C) in a slightly hydrated condition (moisture contents were 20% and 25%) caused degradation, too. And the degrees of crystallinity were lower than 47%. But these samples maintained the morphology and crystals orientations. The thermal stability also obviously increased, and the RS content was approximately 90%. As a result, the TDF content of spherulites was increased from 48.3% to 72.1%.

Reference

Bailey, J. M., & Whelan, W. J. (1961). Physical Properties of Starch. *Journal of Biological Chemistry*, *236*(4), 969–973.

Bates, F. L., French, D., & Rundle, R. E. (1943). Amylose and Amylopectin Content of Starches Determined by their Iodine Complex Formation [1]. *Journal of the American Chemical Society*, *65*(2), 142–148.

Bradbury, A. G. W., & Bello, A. B. (1993). Determination of Molecular Size Distribution of Starch and Debranched Starch by a Single Procedure Using High-Performance Size-Exclusion Chromatography. *Cereal Chemistry*, *70*, 543–547.

Buléon, A., Véronèse, G., & Putaux, J.-L. (2007). Self-Association and Crystallization of Amylose. *Australian Journal of Chemistry*, *60*(10), 706–718.

Cai, C., Zhao, L., Huang, J., Chen, Y., & Wei, C. (2014). Morphology, structure and gelatinization properties of heterogeneous starch granules from high-amylose maize. *Carbohydrate Polymers*, *102*, 606–614.

Cai, L., & Shi, Y. C. (2013). Self-Assembly of Short Linear Chains to A- and B-Type Starch spherulites and Their Enzymatic Digestibility. *Journal of Agricultural and Food Chemistry*, *61*, 10787–10797.

Cai, L., & Shi, Y.-C. (2010). Structure and digestibility of crystalline short-chain amylose from debranched waxy wheat, waxy maize, and waxy potato starches. *Carbohydrate Polymers*, *79*(4), 1117–1123.

Cai, L., & Shi, Y.-C. (2014). Preparation, structure, and digestibility of crystalline A- and B-type aggregates from debranched waxy starches. *Carbohydrate Polymers*, *105*, 341–350.

Cai, L., Shi, Y.-C., Rong, L., & Hsiao, B. S. (2010). Debranching and crystallization of waxy maize starch in relation to enzyme digestibility. *Carbohydrate Polymers*, *81*(2), 385–393.

Chakraborty, I., Govindaraju, I., Rongpipi, S., Mahato, K. K., & Mazumder, N. (2021). Effects of Hydrothermal Treatments on Physicochemical Properties and In Vitro Digestion of Starch. Food Biophysics, 16(4), 544–554.

Creek, J. A., Ziegler, G. R., & Runt, J. (2006). Amylose Crystallization from Concentrated Aqueous Solution. *Biomacromolecules*, *7*(3), 761–770.

Crist, B., & Schultz, J. M. (2016). Polymer spherulites: A critical review. *Progress in Polymer Science*, *56*, 1–63.

Dingler, C., Dirnberger, K., & Ludwigs, S. (2019). Semiconducting Polymer Spherulites-From Fundamentals to Polymer Electronics. *Macromolecular Rapid Communications*, *40*(1), 1800601.

Evans, A., McNish, N., & Thompson, D. B. (2003). Polarization Colors of Lightly Iodine-stained Maize Starches for Amylose-Extender and Related Genotypes in the W64A Inbred Line. *Starch - Stärke*, *55*(6), 250–257.

Fanta, G. F., Felker, F. C., & Shogren, R. L. (2002). Formation of crystalline aggregates in slowly-cooled starch solutions prepared by steam jet cooking. *Carbohydrate Polymers*, *48*(2), 161–170.

Fanta, G. F., Felker, F. C., Shogren, R. L., & Salch, J. H. (2008). Preparation of spherulites from jet cooked mixtures of high amylose starch and fatty acids. Effect of preparative

conditions on spherulite morphology and yield. *Carbohydrate Polymers*, *71*(2), 253–262.

Fanta, G. F., Kenar, J. A., Byars, J. A., Felker, F. C., & Shogren, R. L. (2010). Properties of aqueous dispersions of amylose–sodium palmitate complexes prepared by steam jet cooking. *Carbohydrate Polymers*, *81*(3), 645–651.

Fanta, G. F., Kenar, J. A., & Felker, F. C. (2013). Preparation and properties of amylose complexes prepared from hexadecylamine and its hydrochloride salt. *Carbohydrate Polymers*, *98*(1), 555–561.

Fanta, G., Felker, F., Shogren, R., & Salch, J. (2006). Effect of fatty acid structure on the morphology of spherulites formed from jet cooked mixtures of fatty acids and defatted cornstarch☆. *Carbohydrate Polymers*, *66*(1), 60–70.

Felker, F. C., Kenar, J. A., Fanta, G. F., & Biswas, A. (2013). Comparison of microwave processing and excess steam jet cooking for spherulite production from amylose-fatty acid inclusion complexes. *Starch - Stärke*, *65*(9–10), 864–874.

Gránásy, L., Pusztai, T., Tegze, G., Warren, J. A., & Douglas, J. F. (n.d.). *On the growth and form of spherulites*. 14.

Helbert, W., Chanzy, H., Planchot, V., Buléon, A., & Colonna, P. (1993). Morphological and structural features of amylose spherocrystals of A-type. *International Journal of Biological Macromolecules*, *15*(3), 183–187.

Htoon, A., Shrestha, A. K., Flanagan, B. M., Lopez-Rubio, A., Bird, A. R., Gilbert, E. P., & Gidley, M. J. (2009). Effects of processing high amylose maize starches under controlled

conditions on structural organisation and amylase digestibility. *Carbohydrate Polymers*, *75*(2), 236–245.

Jenkins, P. J., & Donald, A. M. (1995). The influence of amylose on starch granule structure. *International Journal of Biological Macromolecules, 17(6)*, 315–321.

Kiatponglarp, W., Rugmai, S., Rolland-Sabaté, A., Buléon, A., & Tongta, S. (2016). Spherulitic self-assembly of debranched starch from aqueous solution and its effect on enzyme digestibility. *Food Hydrocolloids*, *55*, 235–243.

Kobayashi, S., Hobson, L. J., Sakamoto, J., Kimura, S., Sugiyama, J., Imai, T., & Itoh, T. (2000). Formation and Structure of Artificial Cellulose Spherulites via Enzymatic Polymerization. *Biomacromolecules*, *1*(2), 168–173.

Lopez-Rubio, A., Flanagan, B. M., Gilbert, E. P., & Gidley, M. J. (2008). A novel approach for calculating starch crystallinity and its correlation with double helix content: A combined XRD and NMR study. *Biopolymers*, *89*(9), 761–768.

Ma, U. V. L., Floros, J. D., & Ziegler, G. R. (2011). Effect of starch fractions on spherulite formation and microstructure. *Carbohydrate Polymers*, *83*(4), 1757–1765.

Nishiyama, Y., Putaux, J., Montesanti, N., Hazemann, J.-L., & Rochas, C. (2010). B→A Allomorphic Transition in Native Starch and Amylose Spherocrystals Monitored by In Situ Synchrotron X-ray Diffraction. Biomacromolecules, 11(1), 76–87.

Nordmark, T. S., & Ziegler, G. R. (2002a). Spherulitic crystallization of gelatinized maize starch and its fractions. *Carbohydrate Polymers*, *49*(4), 439–448.

Nordmark, T. S., & Ziegler, G. R. (2002b). Structural features of non-granular spherulitic maize starch. *Carbohydrate Research*, *337*(16), 1467–1475.

Perez, S.; Imberty, A.; Scaringe, R. P. (1990). In Computer modeling of carbohydrate molecules; French, A. D., Brady, J. W., Eds.; ACS Symposium Series 430; American Chemical Society, Washington, DC, pp 281-299.

Ring, S. G., Miles, M. J., Morris, V. J., Turner, R., & Colonna, P. (1987). Spherulitic crystallization of short chain amylose. *International Journal of Biological Macromolecules*, *9*(3), 158–160.

Shang, Y., Chao, C., Yu, J., Copeland, L., Wang, S., & Wang, S. (2018). Starch Spherulites Prepared by a Combination of Enzymatic and Acid Hydrolysis of Normal Corn Starch. *Journal of Agricultural and Food Chemistry*, *66*(25), 6357–6363.

Shi, J., Sweedman, M. C., & Shi, Y.-C. (2018). Structural changes and digestibility of waxy maize starch debranched by different levels of pullulanase. *Carbohydrate Polymers*, *194*, 350–356.

Shtukenberg, A. G., Punin, Y. O., Gunn, E., & Kahr, B. (2012). Spherulites. *Chemical Reviews*, *112*(3), 1805–1838.

Singh, J., Lelane, C., Stewart, R. B., & Singh, H. (2010). Formation of starch spherulites: Role of amylose content and thermal events. *Food Chemistry*, *121*(4), 980–989.

Vilaplana, F., & Gilbert, R. G. (2010). Characterization of branched polysaccharides using multiple-detection size separation techniques: Liquid Chromatography. *Journal of Separation Science*, *33*(22), 3537–3554.

Wang, C., Chen, C.-C., Cheng, Y.-W., Liao, W.-P., & Wang, M.-L. (2002). Simultaneous presence of positive and negative spherulites in syndiotactic polystyrene and its blends with atactic polystyrene. *Polymer*, *43*(19), 5271–5279.

Whittam, M. A., Noel, T. R., & Ring, S. G. (1990). Melting behaviour of A- and B-type crystalline starch. *International Journal of Biological Macromolecules*, *12*(6), 359–362.

Yang, J., Xie, F., Wen, W., Chen, L., Shang, X., & Liu, P. (2016). Understanding the structural features of high-amylose maize starch through hydrothermal treatment. International Journal of Biological Macromolecules, 84, 268–274.

Ziegler, G. R. (2020). *Enzyme-Resistant Starch Spherulites*. 10.

Ziegler, G. R., Creek, J. A., & Runt, J. (2005). Spherulitic Crystallization in Starch as a Model for Starch Granule Initiation. *Biomacromolecules*, *6*(3), 1547–1554.

Ziegler, G. R., Nordmark, T. S., & Woodling, S. E. (2003). Spherulitic crystallization of starch: Influence of botanical origin and extent of thermal treatment. *Food Hydrocolloids*, *17*(4), 487–494.

Table 4.1 Yields, crystalline structure and the degree of crystallinity of the samples crystallized by the debranched high-amylose starch. The crystallization temperatures were from 25℃ to 150℃. The solid concentrations were 30%, 40%, and 50%.

Solid concentration	Crystallization temperature (°C)	Yields (%)	Crystalline type	Degree of crystallinity (%)
30%	25	95.4±0.3^{h}	B	31.0±1.1^{h}
	90-25	97.2±0.4^{efg}	B	29.8±0.1^{h}
	120-25	96.0±0.0^{gh}	B	39.5±1.5^{e}
	150-25	36.6±0.2^{k}	B	36.3±1.0^{ef}
40%	25	98.4±0.4^{abc}	B	24.0±1.4^{i}
	90-25	98.1±0.1^{bcd}	A	35.1±0.2^{fg}
	120-25	97.2±0.1^{def}	B	39.0±0.6^{e}
	150-25	54.6±0.6^{j}	B	74.0±1.5^{b}
50%	25	99.5±0.5^{a}	B	23.6±1.1^{i}
	90-25	99.0±0.2^{ab}	A	46.2±1.0^{d}
	120-25	98.2±0.2^{bcd}	B	50.3±0.1^{c}
	150-25	57.0±1.0^{i}	C	80.3±1.3^{a}

Values within the same column bearing the same small letter superscript(s) do not significantly differ at $p < 0.05$.

Table 4.2 The degree of crystallinity of the B-type spherulites product formed by debranhced high-amylose starch, and its heat-moisture treated products.

Sample		Degree of crystallinity (%)	Crystalline type
Spherulites		81.2±0.5[a]	B
Temperatures (℃)	Moisture content (%)		
140	20	42.6±0.9[c]	B
	25	44.4±0.2[bc]	B
150	20	42.9±0.1[c]	A
	25	46.8±0.4[b]	A

Values within the same column bearing the same small letter superscript(s) do not significantly differ at $p < 0.05$.

Table 4.3 Thermal properties of crystallized products formed at different solid contents and different temperatures.

Solid concentration	Temperature (°C)	T_o (°C)	T_p1 (°C)	T_p2 (°C)	T_c (°C)	ΔH (J/g)
30%	25	82.4±0.9^{d}	121.4±0.6^{b}	134.0±1.2^{f}	143.0±1.3^{e}	39.0±1.4^{efg}
	90-25	97.4±1.3^{a}	117.0±0.8^{d}	147.5±1.3^{a}	160.2±1.0^{a}	38.8±0.8^{efg}
	120-25	77.2±1.2^{e}	107.7±0.3^{f}		126.2±0.5^{f}	40.7±1.4^{def}
	150-25	43.6±1.0^{i}	80.9±0.4^{hi}		95.2±0.4^{i}	40.2±1.1^{def}
40%	25	76.8±0.4^{e}	124.0±1.0^{a}	141.8±1.3^{cd}	151.4±0.7^{c}	41.5±1.0^{de}
	90-25	94.4±1.2^{b}	117.7±0.7^{d}	147.4±1.3^{a}	152.4±1.0^{bc}	38.7±0.9^{efg}
	120-25	64.8±0.3^{b}	99.9±0.1^{g}		115.3±1.5^{g}	38.4±0.9^{fg}
	150-25	51.4±0.2^{h}	79.5±0.9^{i}		108.9±0.5^{h}	49.0±1.3^{a}
50%	25	76.4±1.0^{e}	119.9±0.8^{bc}	143.2±0.8^{bc}	154.8±0.1^{bc}	37.8±1.1^{fg}
	90-25	93.2±1.3^{b}	112.7±0.0^{e}	144.9±1.1^{ab}	155.7±0.4^{b}	42.9±0.8^{cd}
	120-25	81.0±0.6^{d}	108.1±0.0^{f}	140.4±0.7^{de}	152.7±1.5^{bc}	40.1±1.3^{defg}
	150-25	58.1±0.4^{g}	82.7±0.1^{h}		144.6±1.0^{de}	45.2±1.4^{bc}

If two peaks were detected, the peak temperatures (T_p1 and T_p2) were recorded separately. Values within the same column bearing the same small letter superscript(s) do not significantly differ at $p < 0.05$.

Table 4.4 Thermal properties of the spherulites formed by debranhced high-amylose starch, and its heat-moisture treated products.

Sample		T_o (°C)	T_p (°C)	T_c (°C)	ΔH (J/g)
Spherulites		71.1±0.7^{d}	107.3±0.5^{c}	127.9±0.2^{b}	32.0±0.6^{d}
Temperature (°C)	Moisture content (%)				
140	20	114.1±0.7^{a}	134.4±0.3^{b}	165.2±0.7^{a}	46.3±1.3^{b}
	25	111.4±1.4^{a}	134.8±0.2^{b}	164.7±0.0^{a}	52.6±0.4^{a}
150	20	100.9±1.1^{b}	133.0±1.6^{b}	164.1±1.1^{a}	39.6±0.3^{c}
	25	92.9±0.8^{c}	140.3±0.5^{a}	164.2±0.3^{a}	47.3±0.2^{ab}

Values within the same column bearing the same small letter superscript(s) do not significantly differ at $p < 0.05$.

Table 4.5 Rapidly digested starch (RDS), slowly digested starch (SDS) and resistant starch (RS) content of crystallized products formed from debranched high-amylose maize starch.

Solid concentration (%)	Crystallization temperature (°C)	RDS (%)	SDS (%)	RS (%)
30	25	11.0±0.4^{g}	12.0±0.4^{d}	77.0±0.4^{b}
	90-25	19.3±0.7^{cde}	8.1±0.5^{efg}	72.6±0.9^{cd}
	120-25	9.5±0.0^{g}	6.3±0.2^{g}	84.2±0.2^{a}
	150-25	36.9±0.3^{a}	19.2±0.5^{c}	43.9±0.3^{g}
40	25	20.4±1.1^{c}	9.6±0.6^{def}	71.7±0.5^{d}
	90-25	16.1±0.3^{f}	8.0±0.5^{efg}	75.9±0.8^{bc}
	120-25	20.1±0.1^{cd}	6.9±0.2^{fg}	73.0±0.1^{cd}
	150-25	28.0±0.8^{b}	22.6±0.8^{b}	49.4±0.1^{f}
50	25	20.2±0.7^{cd}	6.6±0.8^{g}	73.1±1.2^{cd}
	90-25	12.0±0.0^{g}	18.2±0.2^{c}	69.8±0.2^{d}
	120-25	16.9±0.1^{ef}	10.8±0.3^{de}	72.4±0.5^{cd}
	150-25	17.5±0.0^{def}	26.9±0.7^{a}	55.6±0.7^{e}

Values within the same column bearing the same small letter superscript(s) do not significantly differ at $p < 0.05$.

Table 4.6 Rapidly digested starch (RDS), slowly digested starch (SDS) and resistant starch (RS) contents of the spherulites formed by debranched high-amylose starch, and the HMT samples.

Temperature (°C)	Moisture content (%)	RDS (%)	SDS (%)	RS (%)
140	20	7.6 ± 0.4^{ab}	3.2 ± 0.1^{a}	89.2 ± 0.1^{b}
	25	7.7 ± 0.2^{ab}	3.2 ± 0.1^{a}	89.1 ± 0.1^{b}
150	20	8.0 ± 0.2^{a}	2.0 ± 0.1^{a}	90.0 ± 0.1^{b}
	25	6.2 ± 0.1^{bc}	3.5 ± 0.0^{a}	90.3 ± 0.1^{b}
Spherulites		4.6 ± 0.5^{c}	3.4 ± 0.6^{a}	92.0 ± 0.6^{a}

Values within the same column bearing the same small letter superscript(s) do not significantly differ at $p < 0.05$.

Table 4.7 Total dietary fiber (TDF) contents of the spherulites formed by debranched high-amylose starch, and the HMT samples.

Temperature (°C)	Moisture content (%)	TDF (%)
140	20	72.1±0.9[a]
	25	70.4±0.2[a]
150	20	60.0±0.5[c]
	25	66.8±0.9[b]
Spherulites		48.3±0.5[d]

Values within the same column bearing the same small letter superscript(s) do not significantly differ at $p < 0.05$.

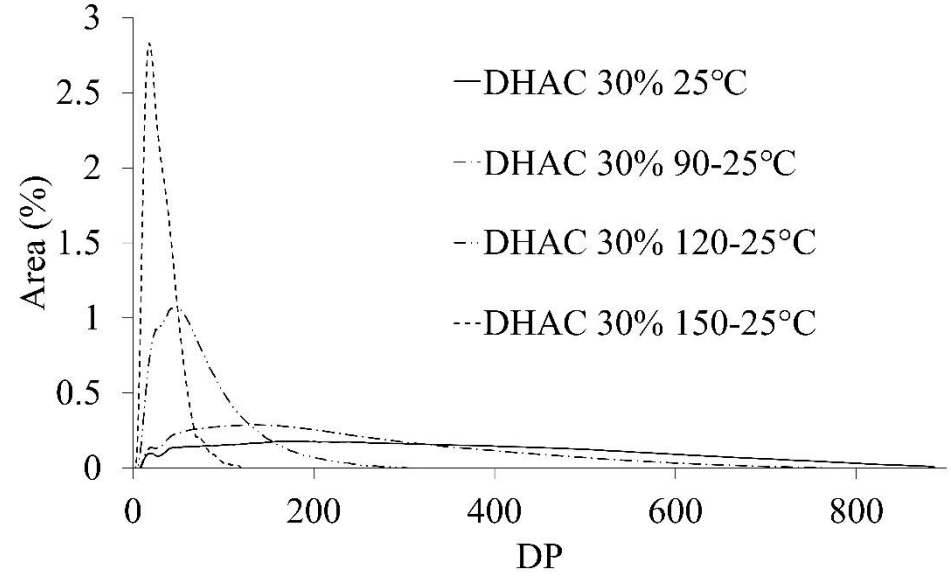
3
2.5
2
1.5
1
0.5
0
Area (%)
0
200
400
600
800
DP
DHAC 30% 25°C
DHAC 30% 90-25°C
DHAC 30% 120-25°C
DHAC 30% 150-25°C

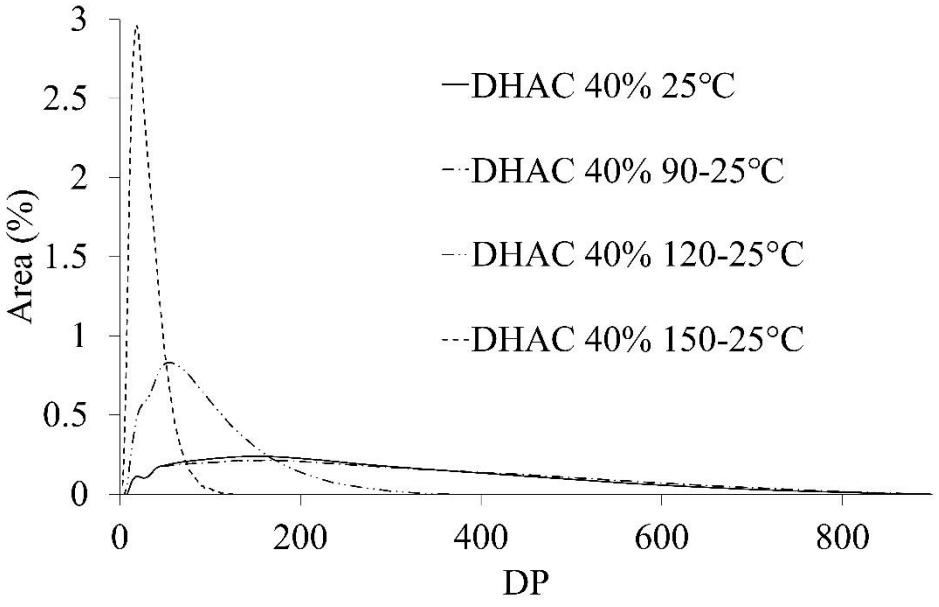
3
2.5
2
1.5
1
0.5
0
Area (%)
0
200
400
600
800
DP
DHAC 40% 25°C
DHAC 40% 90-25°C
DHAC 40% 120-25°C
DHAC 40% 150-25°C

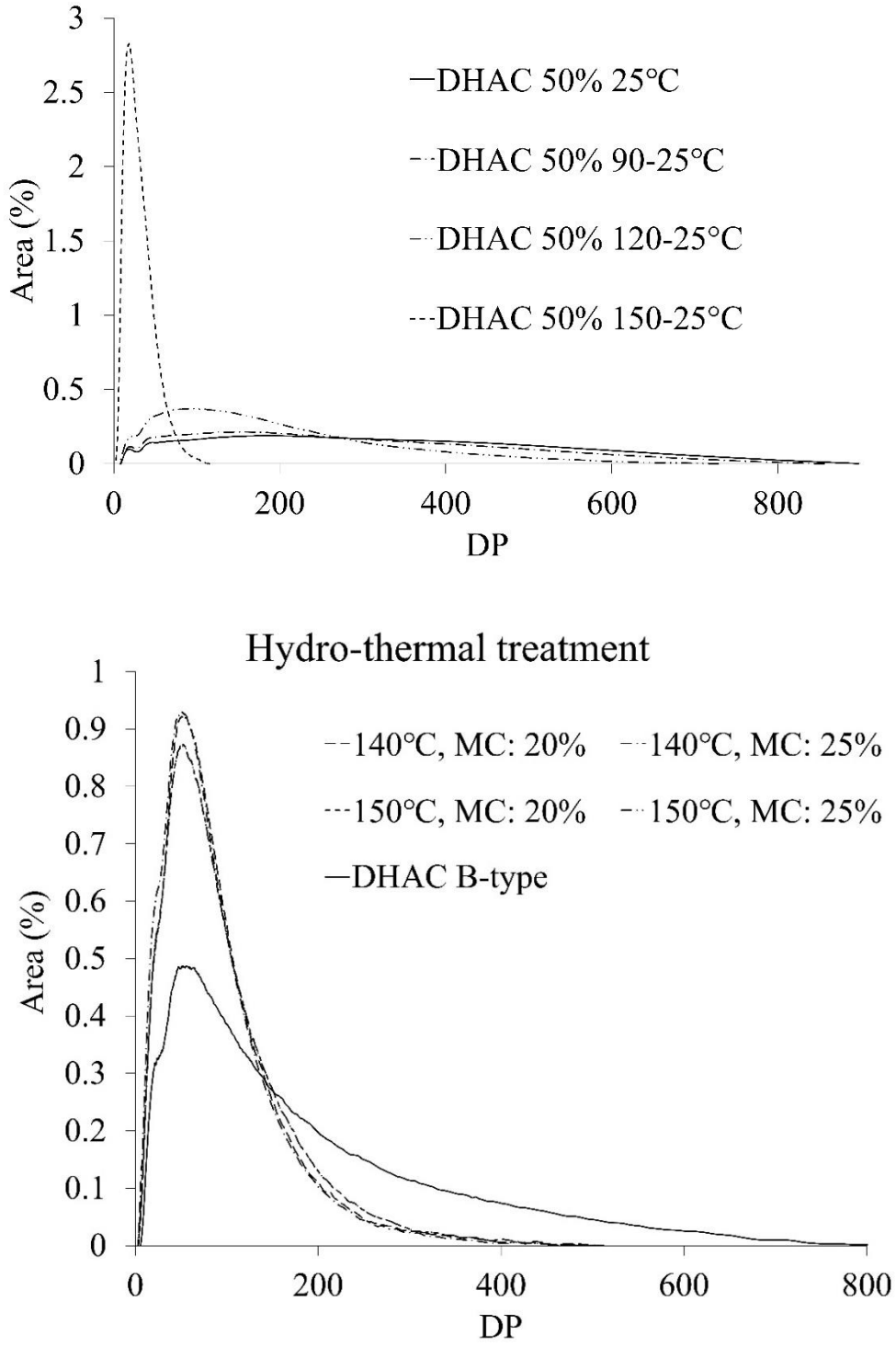

Figure 4.1 Degree of polymerization (DP) distribution of crystallites formed by debranched high-amylose starch. The solid concentrations were 30%, 40%, and 50%. The debranched high-amylose crystallites were formed at 25°C, 90°C, 120°C, and 150°C. All samples crystallized at temperatures higher than 25°C were further cooled to 25°C. The heat-moisture treatment used temperatures of 140°C and 150°C, moisture contents (MC) of 20% and 25%.

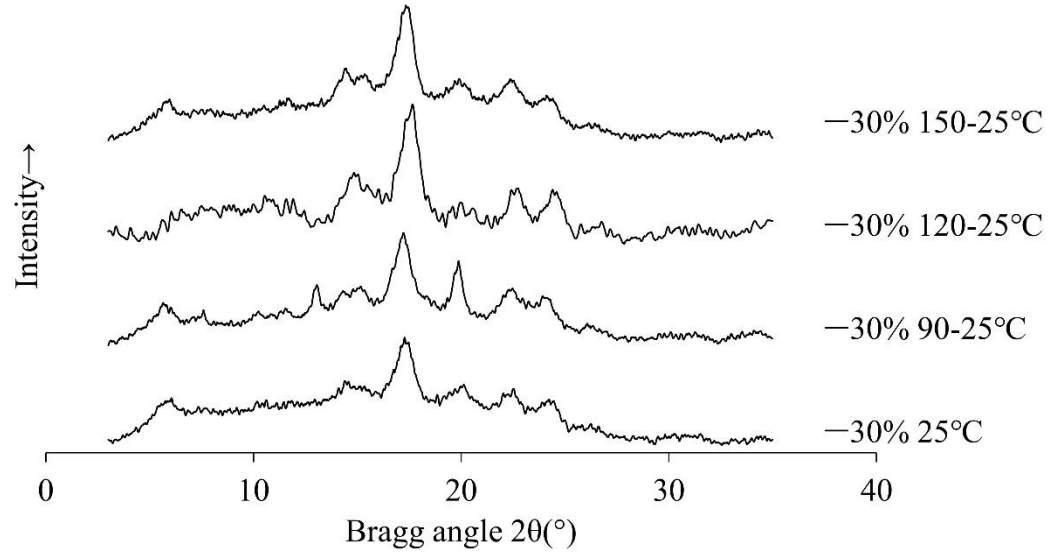
Intensity→
—30% 150-25°C
—30% 120-25°C
—30% 90-25°C
—30% 25°C
0
10
20
30
40
Bragg angle 2θ(°)

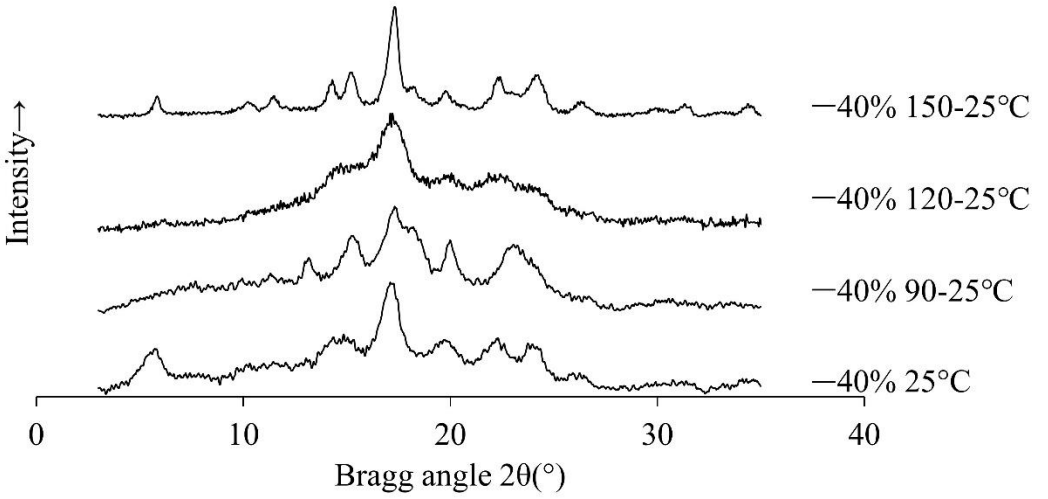
Intensity→
—40% 150-25°C
—40% 120-25°C
—40% 90-25°C
—40% 25°C
0
10
20
30
40
Bragg angle 2θ(°)

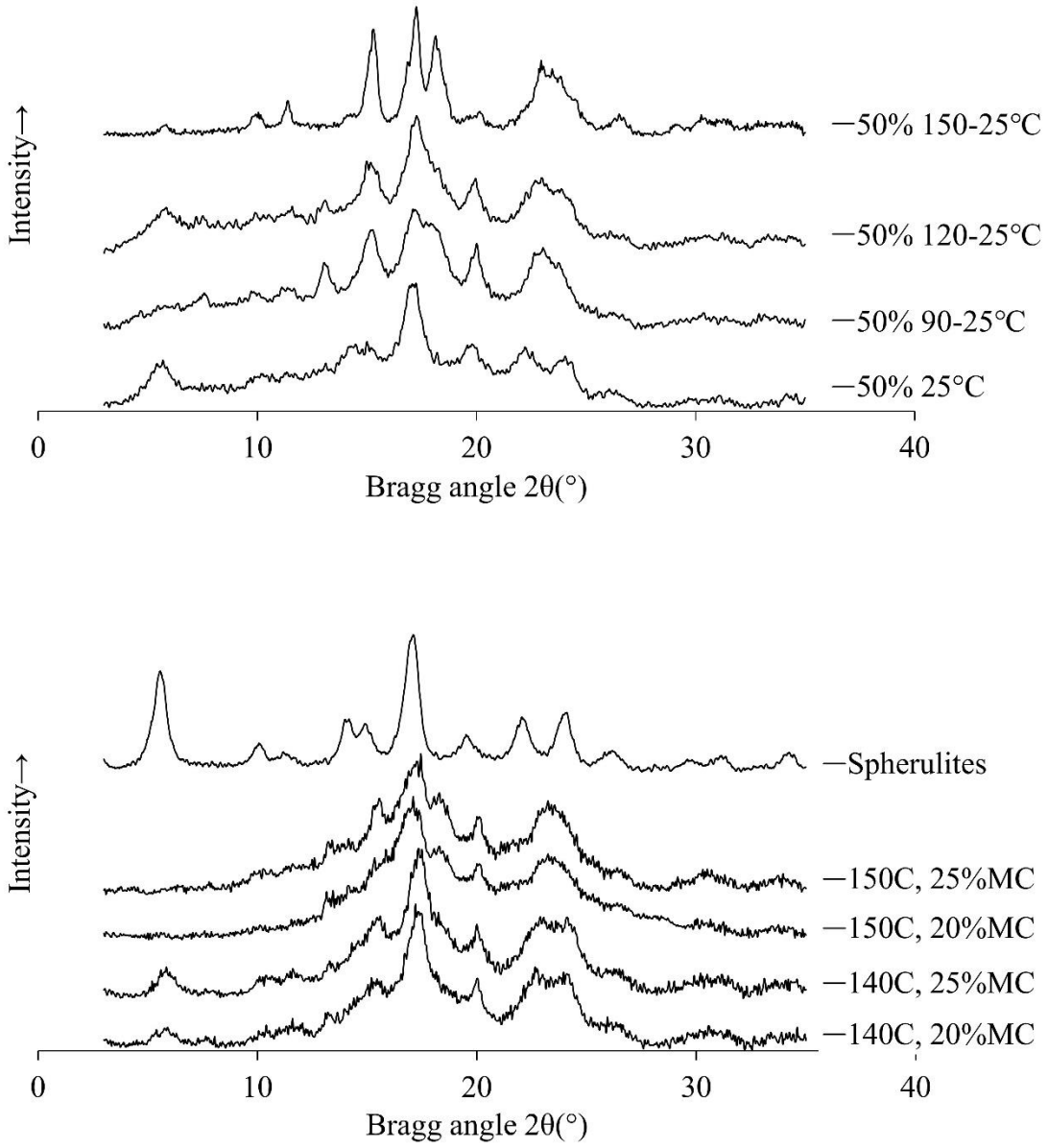

Figure 4.2 XRD curves of crystallized products and HMT samples. Samples (30%, 40%, and 50% solid contents) crystallized at 90°C, 120°C, and 150°C were further cooled to 25°C (90-25°C, 120-25°C, and 150-25°C), respectively. Spherulites were formed by debranched high-amylose starch and treated by HMT. The moisture contents (MC) of HMT were 20% and 25%, the temperatures of HMT were 140°C and 150°C.

Normal light Polarized light Polarized light and a waveplate

40% solid, 90°C

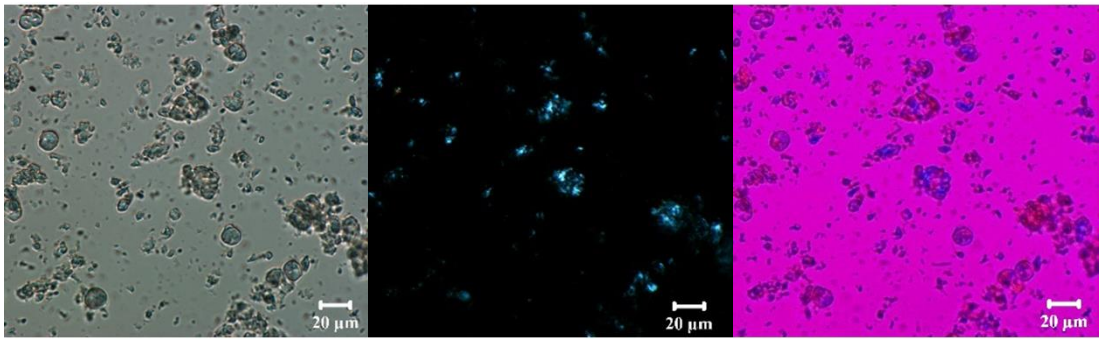

50% solid, 90°C

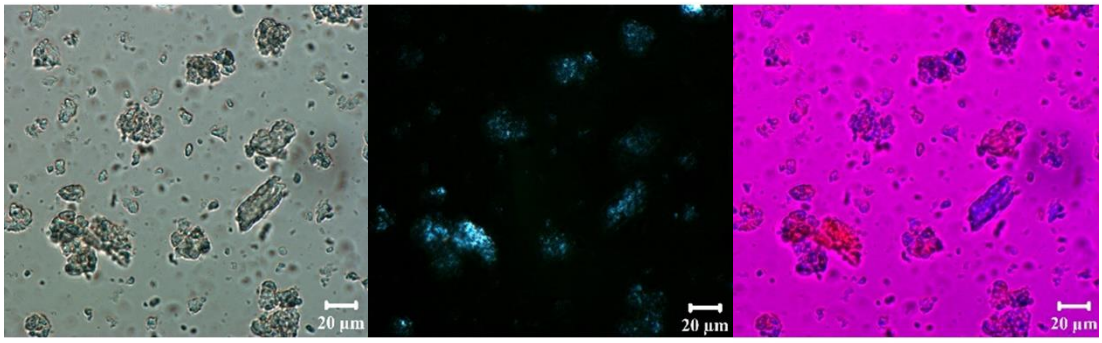

50% solid, 150°C

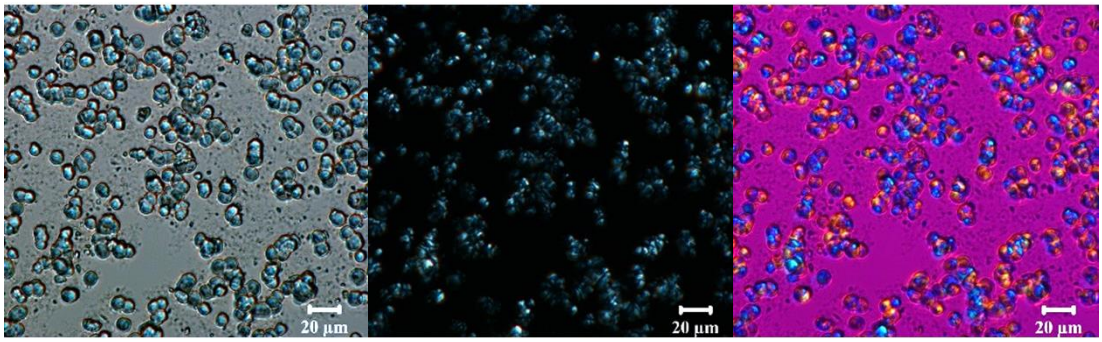

B-type spherulites (25% solid, 25°C)

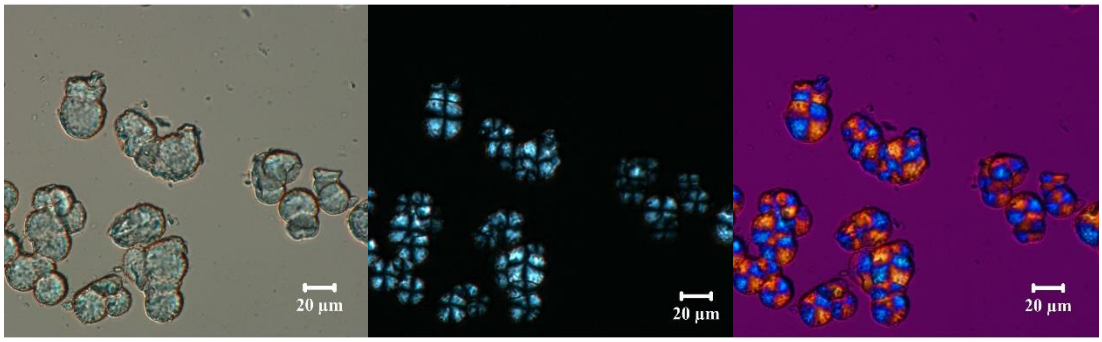

HMT: 150°C, 20% moisture

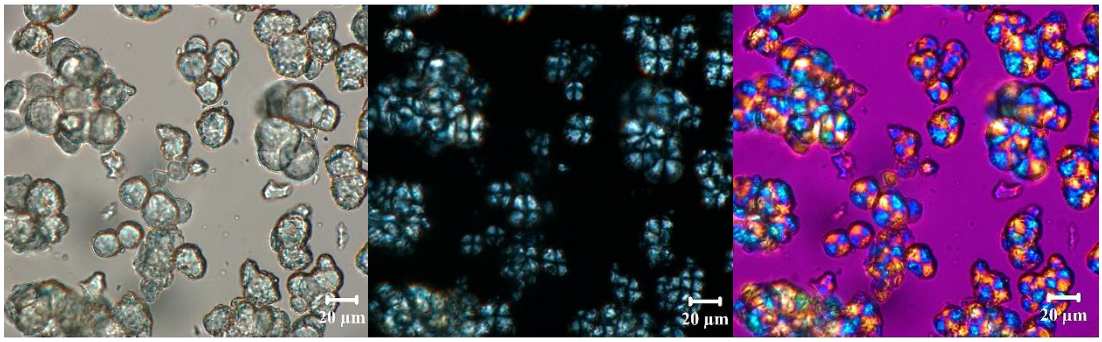

HMT: 150°C, 25% moisture

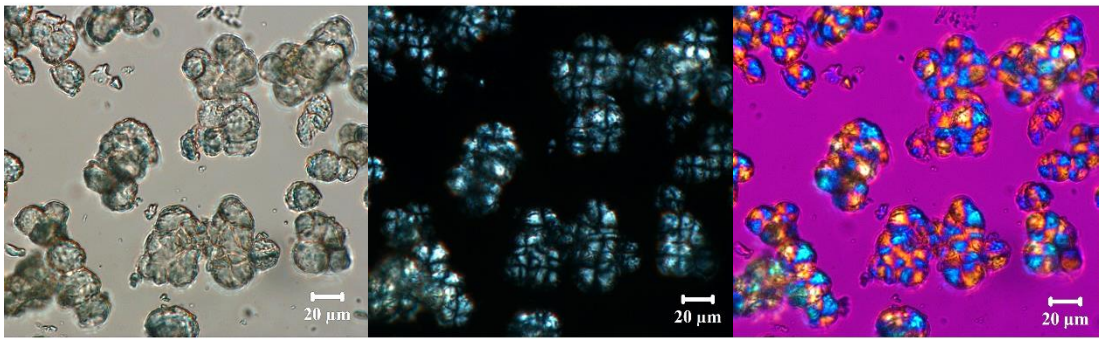

Figure 4.3 The morphology of crystallized products (A-type and C-type crystalline structure), the B-type spherulites, and A-type spherulites formed by the heat-moisture treatment (HMT).

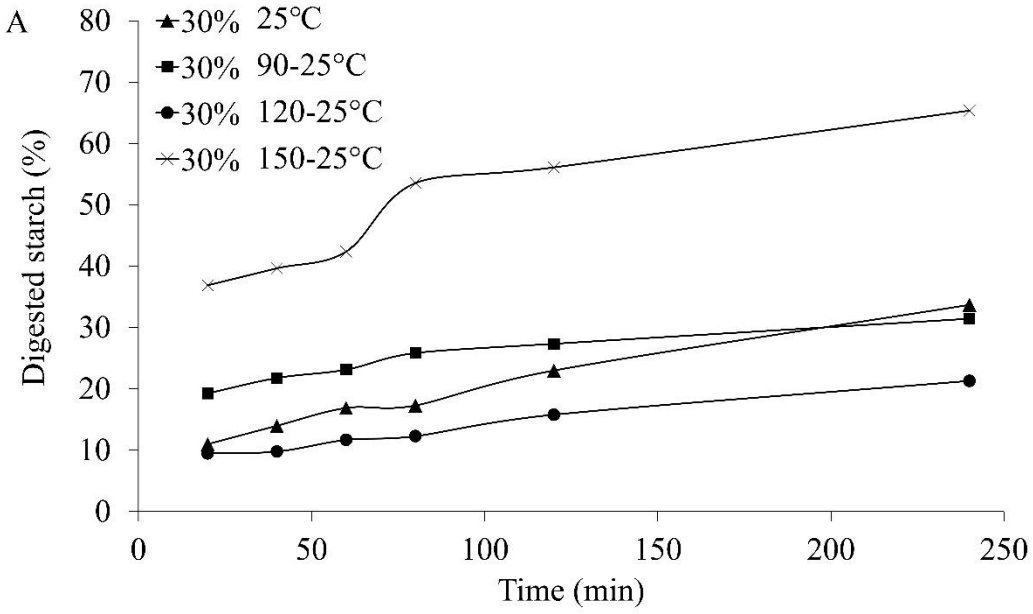
A
30% 25°C
30% 90-25°C
30% 120-25°C
30% 150-25°C
Digested starch (%)
Time (min)
0
10
20
30
40
50
60
70
80
0
50
100
150
200
250

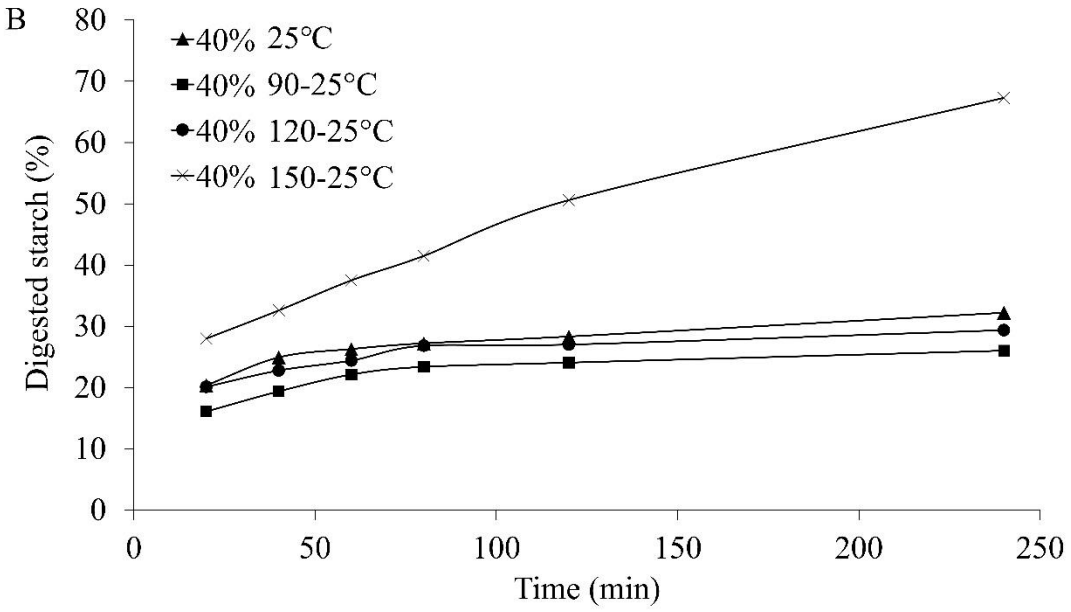
B
40% 25°C
40% 90-25°C
40% 120-25°C
40% 150-25°C
Digested starch (%)
Time (min)
0
10
20
30
40
50
60
70
80
0
50
100
150
200
250

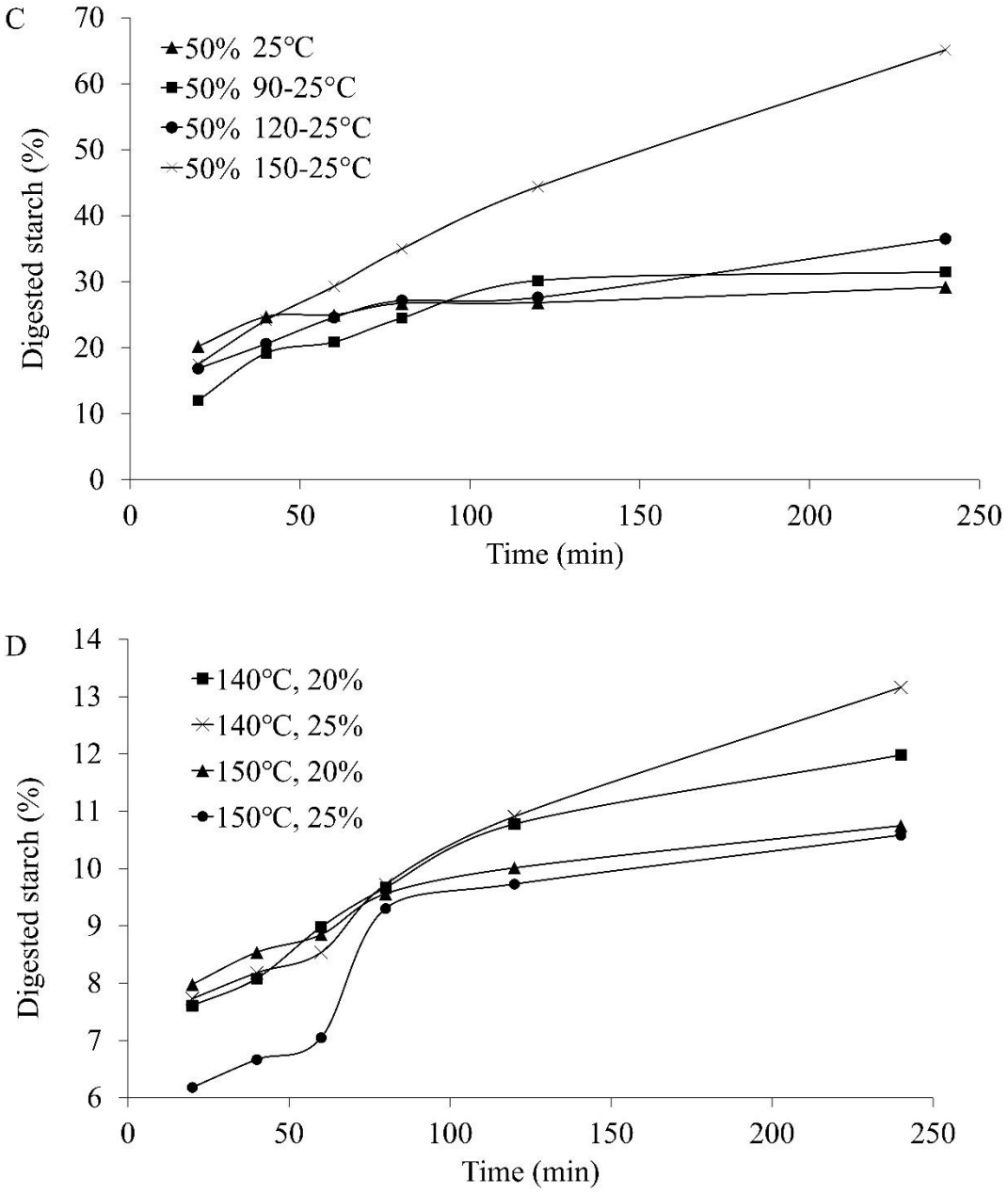

Figure 4.4 Digestion curve of the samples formed by debranched high-amylose starch at different temperatures (25°C, 90°C, 120°C, and 150°C). The solid concentrations were 30% (A), 40% (B), and 50% (C). The digestion curve of heat-moisture treatment (HMT) samples (D) was also included. The temperatures of HMT were 140°C and 150°C, the moisture contents were adjusted to 20% and 25%.

Chapter 5 - Conclusions and Perspectives

In this study, positive and negative spherulites were produced by debranched starches with 25% solid content. Long linear chains were produced by debranching high-amylose maize starch and formed positive spherulites. When crystallization temperature was 150°C, debranched high-amylose maize starch was degraded so that molecular chain length was reduced. In another experiment, short chains molecules were produced by debranching waxy potato starch. These two molecules of short chains formed negative spherulites (Figure 5.1).

When the solid content was 25%, all spherulites showed B-type crystalline structure. By increasing the solid content of debranched high-amylose maize starch to 40%, the products crystallized at 90°C showed A-type allomorphs. When the solid content of debranched high-amylose maize starch was 50%, A-type material was crystallized at 90°C, and C-type material was crystallized at 150°C. However, these A-type and C-type products did not show Maltese cross under a light microscopy. To produce A-type spherulites, heat-moisture treatment (HMT) was applied to the positive and spherulites and negative spherulites. The positive spherulites were from debranched high-amylose maize starch, and the negative spherulites were formed by debranched waxy potato starch. HMT successfully changed the crystalline structure from B-type to A-type, and the birefringence signs were maintained (Figure 5.1).

Positive spherulites formed by debranched high-amylose maize starch had a high resistant starch (RS) content (>89.3%). Negative spherulites formed by the debranched high-amylose maize starch had the lowest RS content (47.9%). After HMT, the RS content of

positive was approximately 90%, and the thermal stability was higher. As a result, the TDF content of HMT samples was 72.1%. But the TDF content of spherulites before HMT was 48.3%.

When negative spherulites were produced by debranched waxy potato starch, the RS contents were between 66.9% and 78.4%. HMT affected the digestibility of the negative spherulites and reduced the RS content from 74.1% to 51.6%, when the temperature and moisture content of HMT were 140°C and 25%, respectively. However, HMT increased the thermal stability of the spherulites formed by debranched waxy potato starch. As a result, the RS content of cooked spherulites only reduced from 61.6% to 33.1%. Whereas the RS content of cooked waxy potato starch was reduced to 1.9%.

The RS contents and thermal properties support the application of spherulites in food products with controlled digestibility as well as desirable texture, quality and shelf life. Spherulites prepared by the authors were analyzed by in-vivo digestion test, and food products containing spherulites were previously designed. In another test, positive and negative spherulites were also applied in bread to study the influence on the bread quality and digestibility. Spherulites mimic both granular morphology and the crystalline types of native starches. Therefore, they are good model systems to study the enzymatic hydrolysis of starch crystallites and provide great insight on enzyme digestion of starch.

Selected A- and B-type starch spherulites were used to partially substitute wheat flour and evaluated in pup-loaf bread application. In addition, human study was conducted to evaluate the glucose and insulin response. Those two studies were not included in this

dissertation. Future work will be to link starch spherulite structure and *in vitro* enzyme digestibility results from this dissertation to human glycemic and insulinemic response.

A

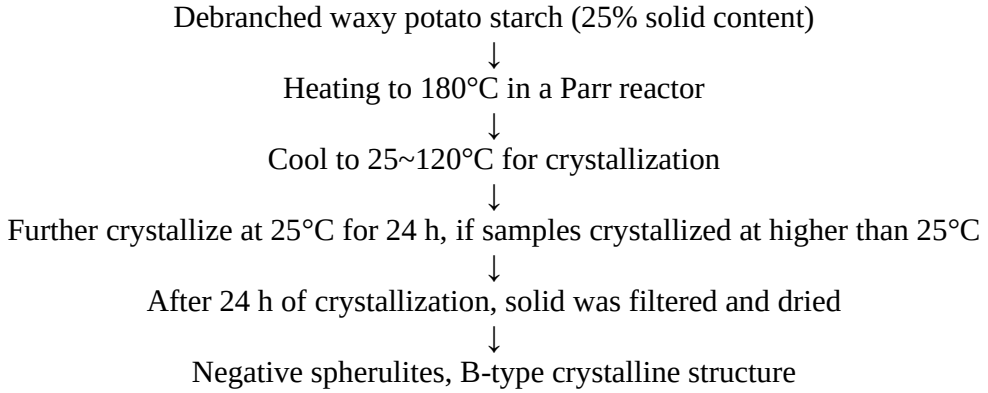
Debranched waxy potato starch (25% solid content)
Heating to 180°C in a Parr reactor
Cool to 25~120°C for crystallization
Further crystallize at 25°C for 24 h, if samples crystallized at higher than 25°C
After 24 h of crystallization, solid was filtered and dried
Negative spherulites, B-type crystalline structure

B

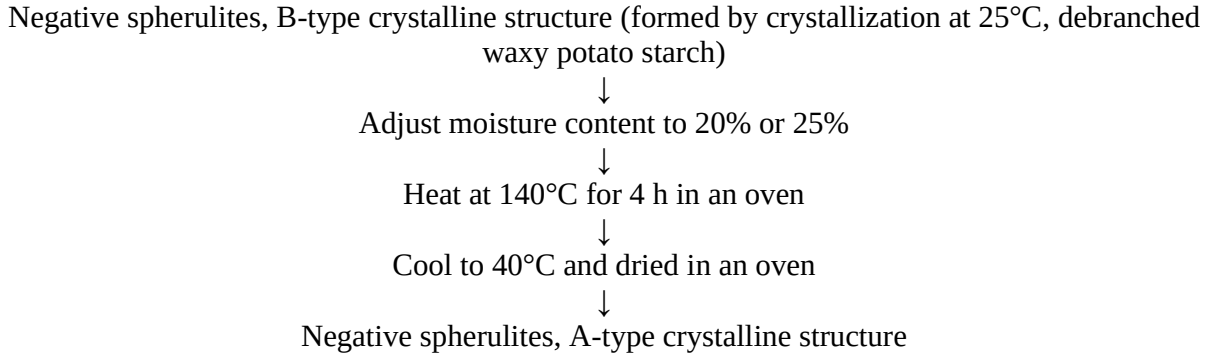
Negative spherulites, B-type crystalline structure (formed by crystallization at 25°C, debranched waxy potato starch)
Adjust moisture content to 20% or 25%
Heat at 140°C for 4 h in an oven
Cool to 40°C and dried in an oven
Negative spherulites, A-type crystalline structure

C

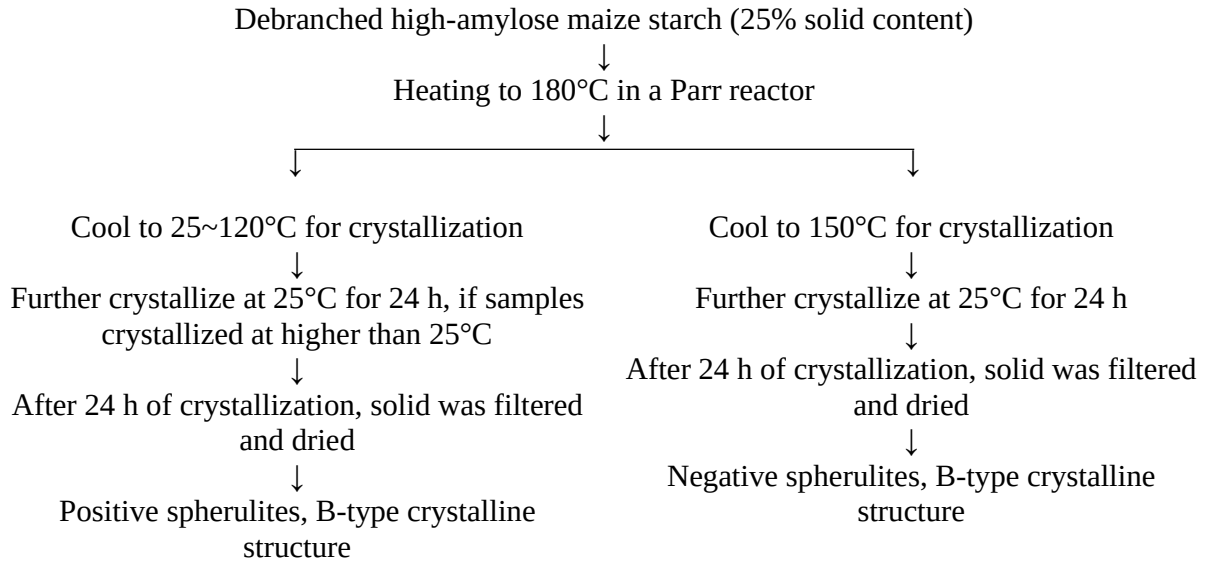
Debranched high-amylose maize starch (25% solid content)
Heating to 180°C in a Parr reactor
Cool to 25~120°C for crystallization
Further crystallize at 25°C for 24 h, if samples crystallized at higher than 25°C
After 24 h of crystallization, solid was filtered and dried
Positive spherulites, B-type crystalline structure
Cool to 150°C for crystallization
Further crystallize at 25°C for 24 h
After 24 h of crystallization, solid was filtered and dried
Negative spherulites, B-type crystalline structure

D

Positive spherulites, B-type crystalline structure (formed by crystallization at 25°C, debranched high-amylose maize starch)

↓

Adjust moisture content to 20% or 25%

↓

Heat at 150°C for 4 h in an oven

↓

Cool to 40°C and dried in an oven

↓

Positive spherulites, A-type crystalline structure

Figure 5.1 Spherulites formation procedure. The spherulites were produced by debranched waxy potato starch (A, B) and debranched high-amylose maize starch (C, D). B-type spherulites were produced by crystallization (A, C). Heat-moisture treatment (HMT) was used to produce A-type spherulites (B, D)

Appendix A – Microscopy images of the crystallized sample.

Normal light Polarized light Polarized light and a waveplate

Figure A. 1. Debranched high-amylose maize starch which was heated in a parr reactor to 170°C. Then samples were crystallized at 25°C.

Normal light Polarized light Polarized light and a waveplate

Native high-amylose starch

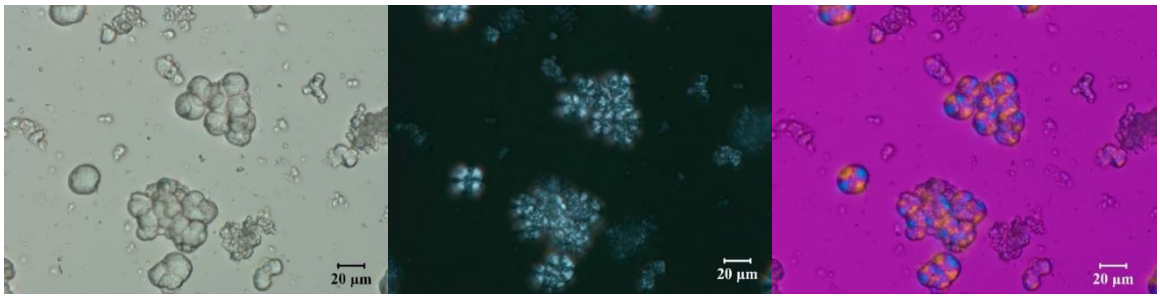

Debranched high-amylose starch

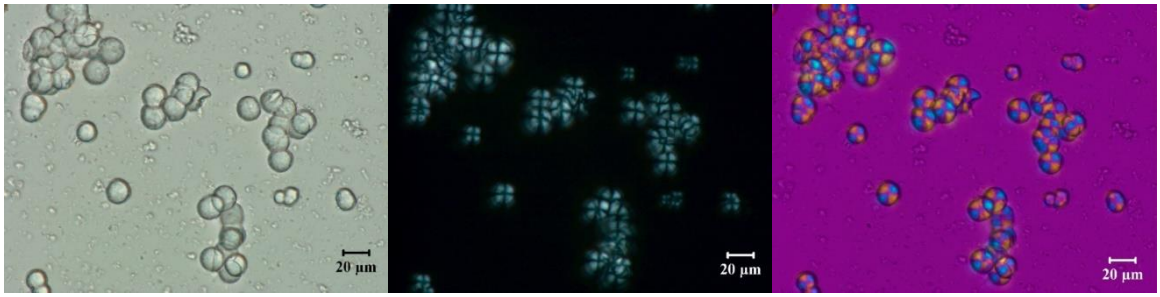

Figure A. 2. The morphology of spherulites formed by native high-amylose starch and debranched high-amylose starch.

Appendix B – Microscopy images of digested spherulites

Normal light Polarized light Polarized light and a waveplate

Digestion time: 20 min

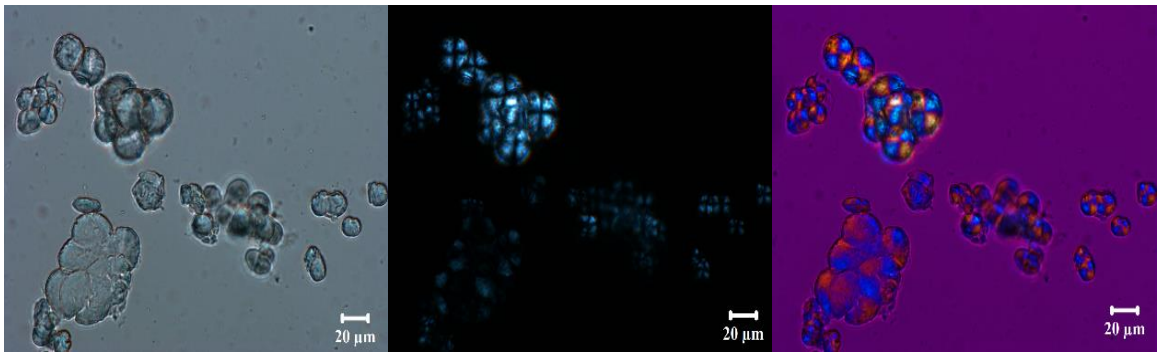

Digestion time: 60 min

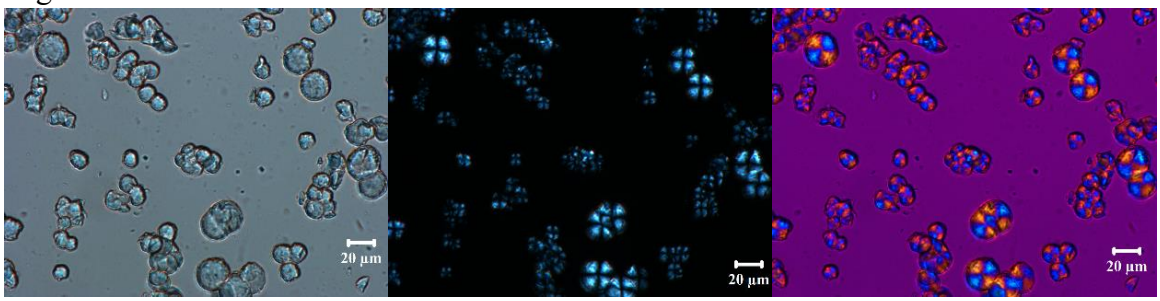

Digestion time: 120 min

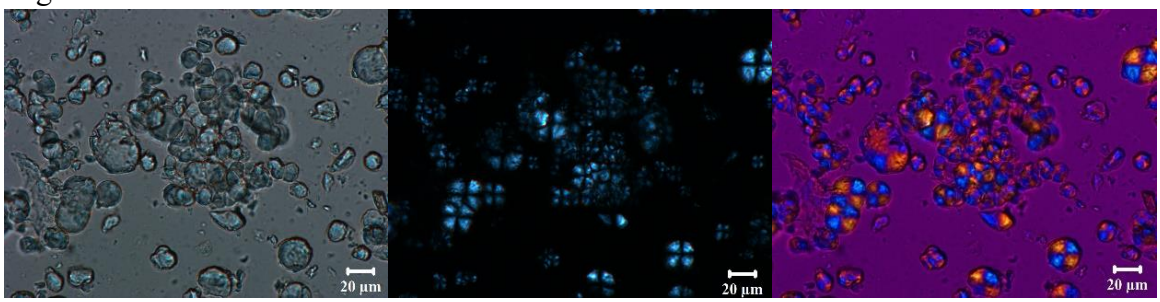

Digestion time: 240 min

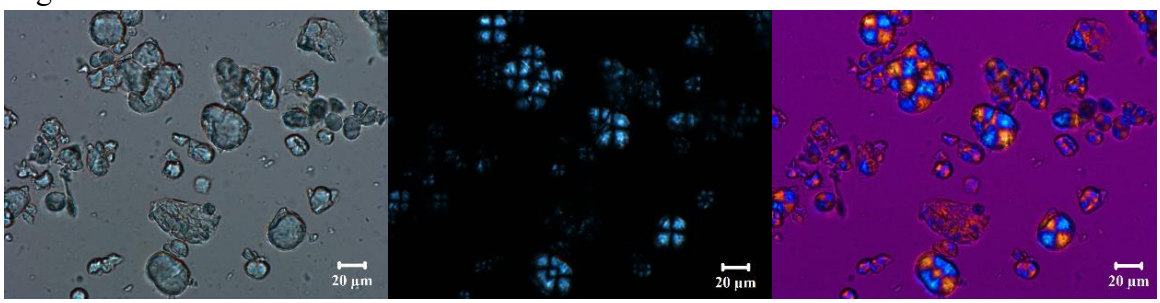

Figure B. 1. The morphology of spherulites during digestion. The spherulites were formed at 50°C with further cooling to 25°C.

Normal light Polarized light Polarized light and a waveplate

Digestion time: 20 min

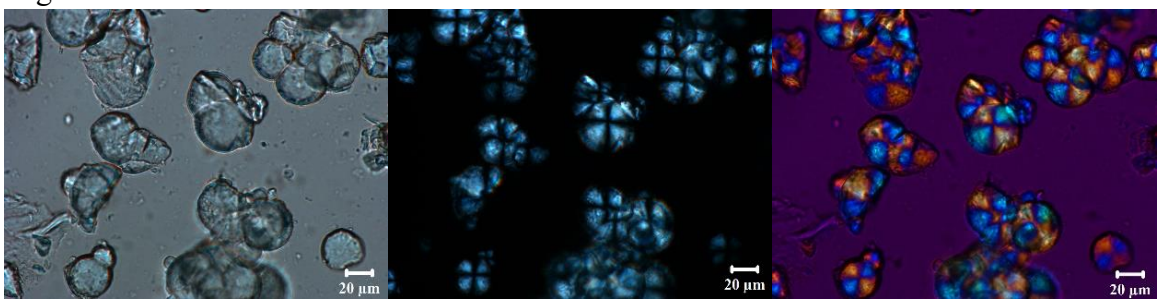

Digestion time: 60 min

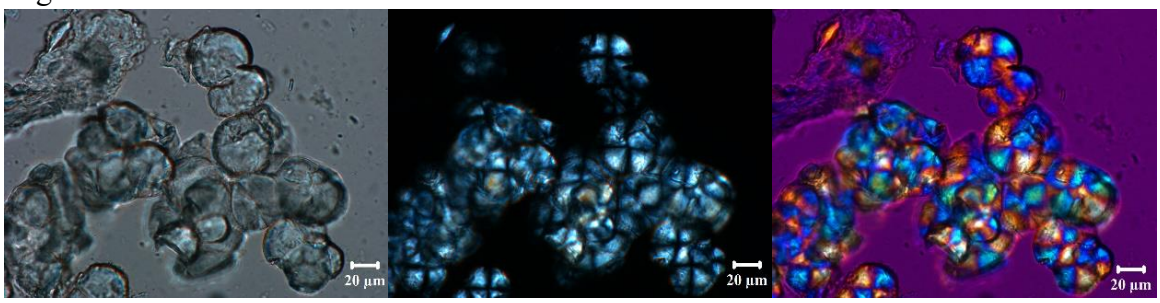

Digestion time: 120 min

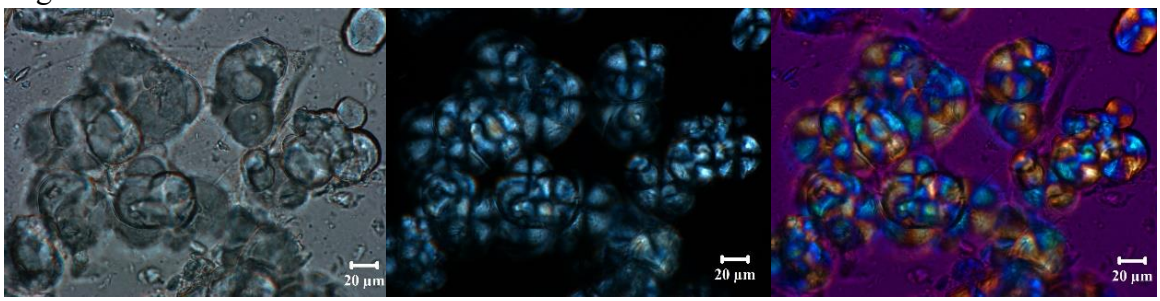

Digestion time: 240 min

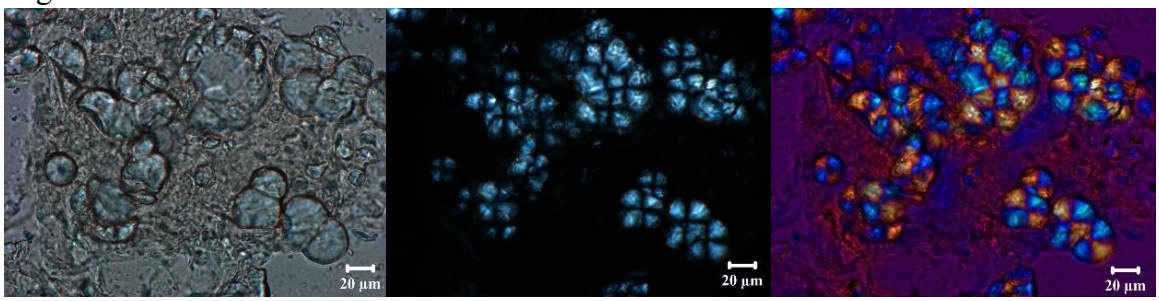

Figure B. 2. The morphology of spherulites during digestion. The spherulites were formed at 70°C with further cooling to 25°C.

Normal light Polarized light Polarized light and a waveplate

Digestion time: 20 min

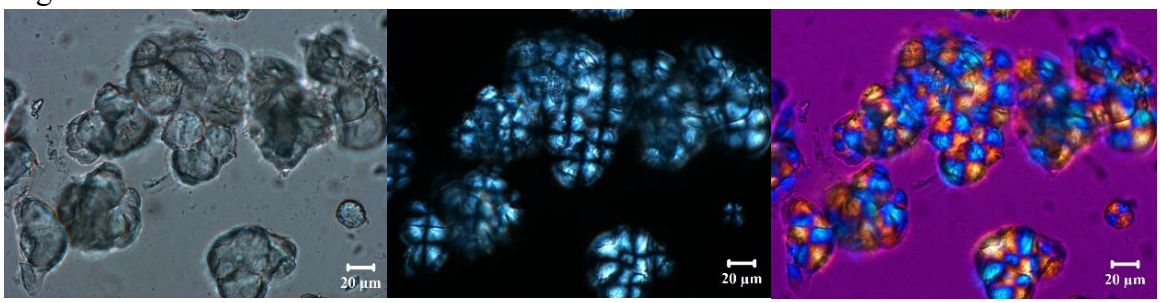

Digestion time: 60 min

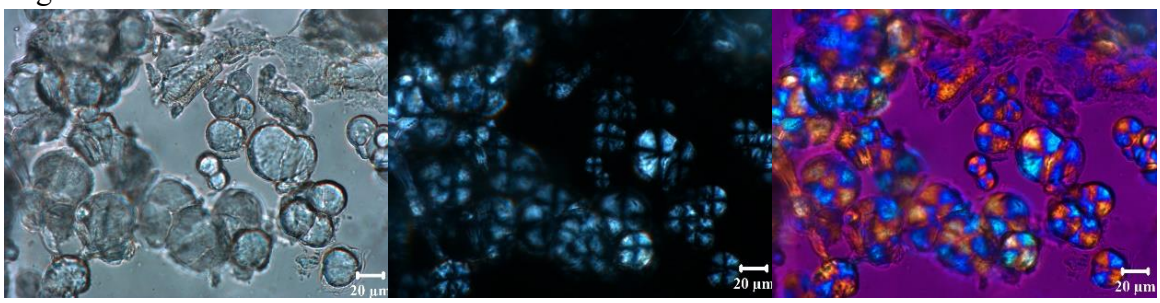

Digestion time: 120 min

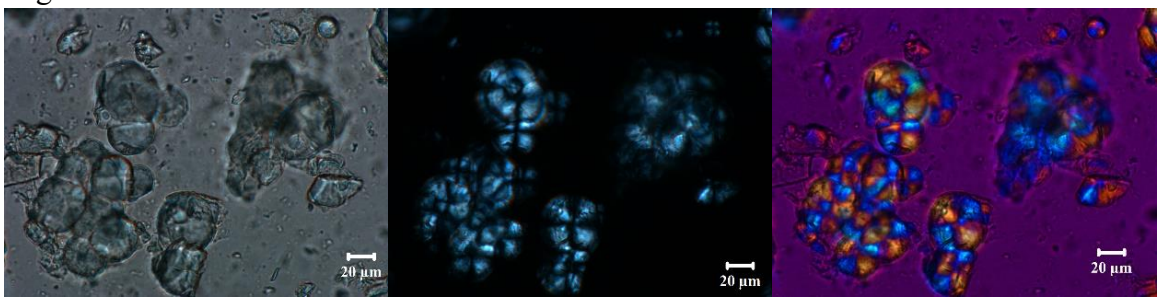

Digestion time: 240 min

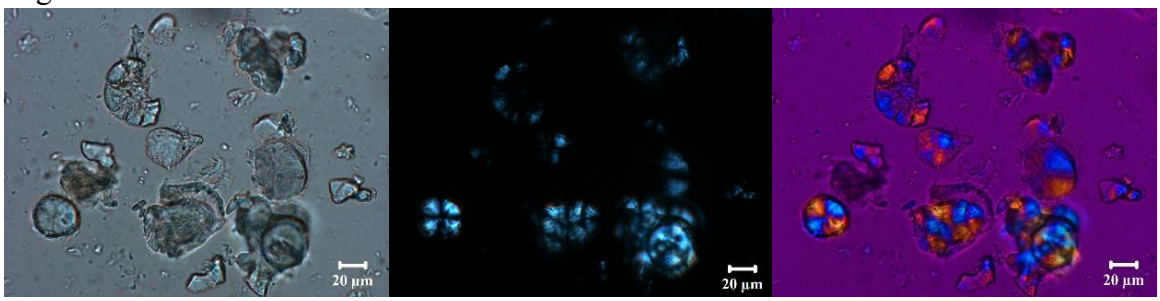

Figure B. 3. The morphology of spherulites during digestion. The spherulites were formed at 90°C with further cooling to 25°C.

Normal light Polarized light Polarized light and a waveplate

Digestion time: 20 min

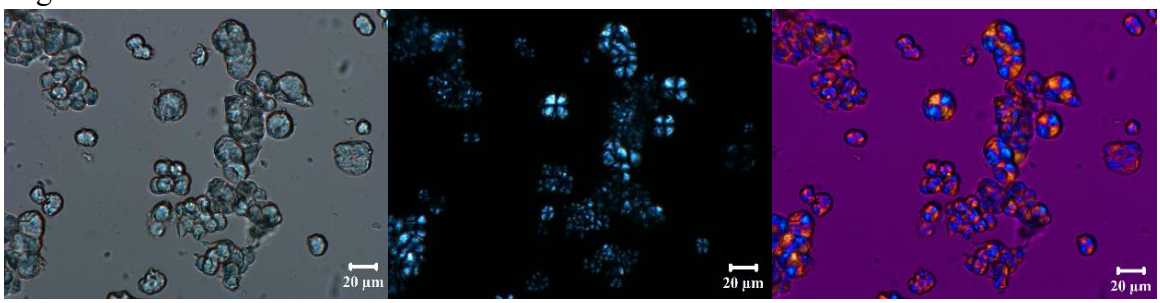

Digestion time: 60 min

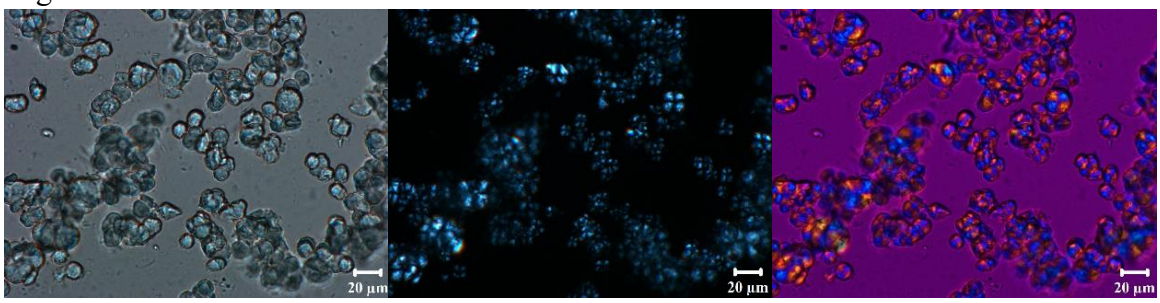

Digestion time: 120 min

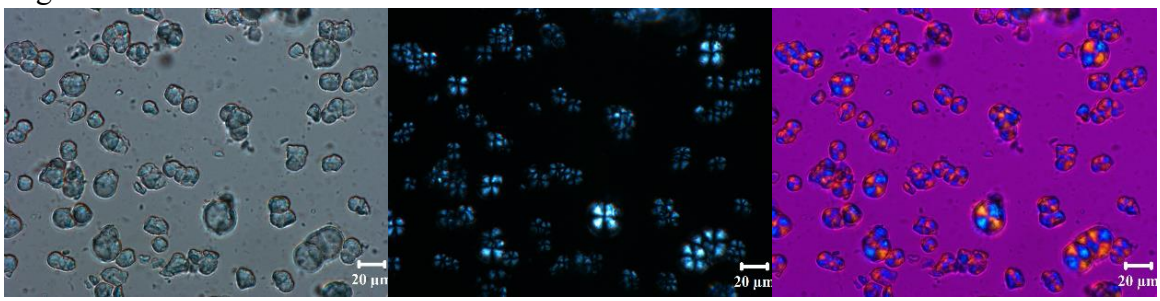

Digestion time: 240 min

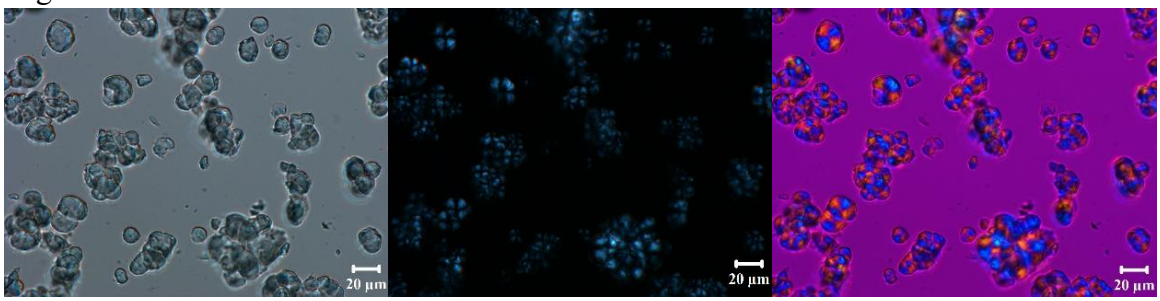

Figure B. 4. The morphology of spherulites during digestion. The spherulites were formed at 120°C with further cooling to 25°C.

Appendix C – Nuclear magnetic resonance (NMR) spectra of positive spherulites

The nuclear magnetic resonance (NMR) spectra showed four signal regions and they were assigned as C1 region (94–105 ppm), C2, C3, C5 region (68–78 ppm), C4 region (80–84 ppm), and C6 region (58–65 ppm). There were two peaks in C1 region (99.9 ppm, 101.1 ppm) and a small peak at C4 region (82.3 ppm). A shoulder was also detected around 103 ppm in C1 region. The number of peaks in C1 region was used to identify the type of crystallinity (Yang et al., 2019; Zou et al., 2020). The two peaks in C1 region indicated a double helix of B-type crystallinity. The C4 peak and the shoulder around 103 pm in C1 region may be due to amorphous or single helix of C-type crystallinity (Morgan et al., 1995; Tan et al., 2007; Yang et al., 2019).

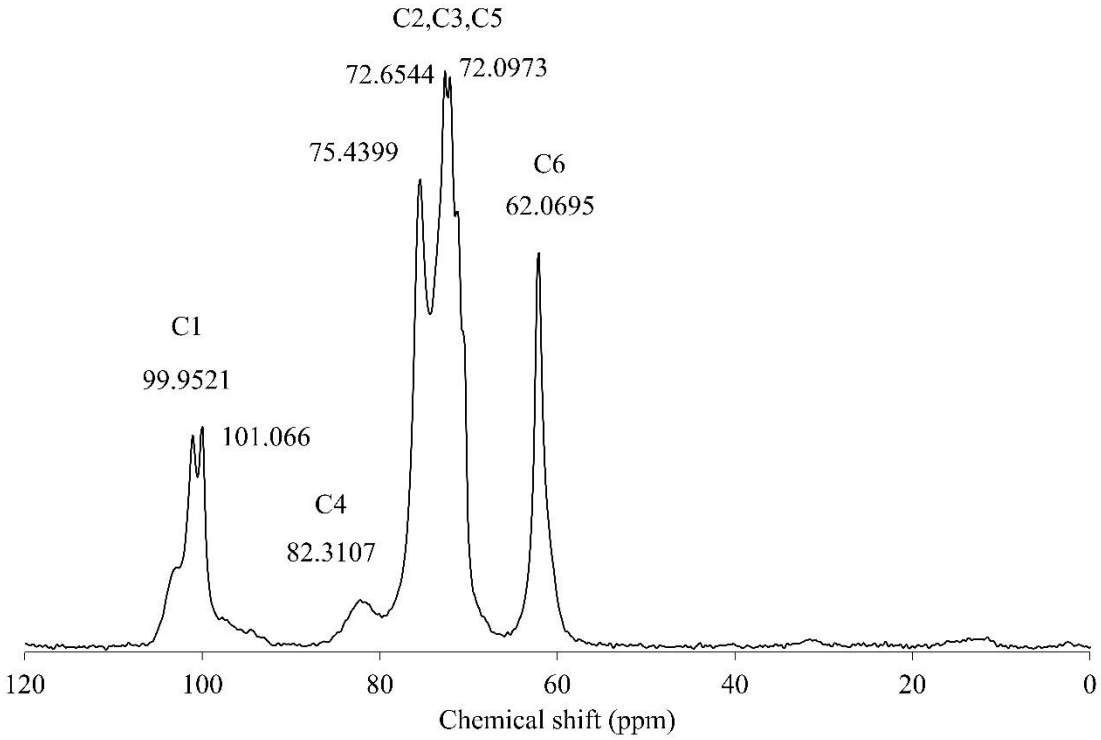

Figure C. 1. ^{13}C NMR spectra of positive spherulites formed by debranched high-amylose maize starch. The crystallization temperature was 25°C, and solid content was 25%.

Appendix reference:

Morgan, K. R., Furneaux, R. H., & Larsen, N. G. (1995). Solid-state NMR studies on the structure of starch granules. *Carbohydrate Research*, *276*(2), 387–399.

Tan, I., Flanagan, B. M., Halley, P. J., Whittaker, A. K., & Gidley, M. J. (2007). A Method for Estimating the Nature and Relative Proportions of Amorphous, Single, and Double-Helical Components in Starch Granules by ^{13} C CP/MAS NMR. *Biomacromolecules*, *8*(3), 885–891.

Yang, Q.-Y., Lu, X.-X., Chen, Y.-Z., Luo, Z.-G., & Xiao, Z.-G. (2019). Fine structure, crystalline and physicochemical properties of waxy corn starch treated by ultrasound irradiation. *Ultrasonics Sonochemistry*, *51*, 350–358.

Zou, J., Xu, M., & Wen, L. (2020). Structure and physicochemical properties of native starch and resistant starch in Chinese yam (Dioscorea opposita Thunb.). *Carbohydrate Polymers,* 237, 1-10